

# MULTIPLE KERNEL LEARNING FROM $U$ -STATISTICS OF EMPIRICAL MEASURES IN THE FEATURE SPACE\*

MASOUD BADIEI KHUZANI<sup>†,‡,◊</sup>, HONGYI REN<sup>‡,◊</sup>, VARUN VASUDEVAN<sup>§,◊</sup>, LEI XING<sup>‡</sup>

<sup>†</sup>DEPARTMENT OF MANAGEMENT SCIENCE

<sup>‡</sup>DEPARTMENT OF RADIATION ONCOLOGY

<sup>§</sup>INSTITUTE FOR COMPUTATIONAL AND MATHEMATICAL ENGINEERING  
STANFORD UNIVERSITY, CA 94043, USA

**ABSTRACT.** We propose a novel data-driven method to learn multiple kernels in kernel methods of statistical machine learning from training samples. The proposed kernel learning algorithm is based on a  $U$ -statistics of the empirical marginal distributions of features in the feature space given their class labels. We prove the consistency of the  $U$ -statistic estimate using the empirical distributions for kernel learning. In particular, we show that the empirical estimate of  $U$ -statistic converges to its population value with respect to all admissible distributions as the number of the training samples increase. We also prove the sample optimality of the estimate by establishing a minimax lower bound via Fano’s method. In addition, we establish the generalization bounds of the proposed kernel learning approach by computing novel upper bounds on the Rademacher and Gaussian complexities using the concentration of measures for the quadratic matrix forms. We apply the proposed kernel learning approach to classification of the real-world data-sets using the kernel SVM and compare the results with 5-fold cross-validation for the kernel model selection problem. We also apply the proposed kernel learning approach to devise novel architectures for the semantic segmentation of biomedical images. The proposed segmentation networks are suited for training on small data-sets and employ new mechanisms to generate representations from input images.

## 1. INTRODUCTION

**K**ERNEL METHODS are one of the most pervasive techniques to capture the non-linear relationship between the representations of input data and labels in statistical machine learning algorithms. The kernel methods circumvent the explicit feature mapping that is required to learn a non-linear function or decision boundary in linear learning algorithms. Instead, the kernel methods only rely on the inner product of feature maps in the feature space, which is often known as the “kernel trick” in the machine learning literature. For large-scale classification problems, however, implicit lifting provided by the kernel trick comes with the cost of prohibitive computational and memory complexities as the kernel Gram matrix must be generated via evaluating the kernel function across all pairs of datapoints. As a result, large training sets incur large computational and storage costs. To alleviate this issue, Rahimi and Recht proposed random Fourier features that aims to approximate the kernel function via *explicit* random feature maps [2, 3].

---

\*Theoretical results of this paper is submitted to the International Conference on Machine Learning (ICML), Long Beach, California 2019. The application of the proposed kernel learning approach to biomedical image segmentation is submitted to the IEEE Transactions on Medical Imaging as a separate paper, where the authors’ names appear in a different order [1].

<sup>◊</sup>These authors contributed equally to this work.

Although the kernel SVMs with random features are typically formulated in terms of convex optimization problems, which have a single global optimum and thus do not require heuristic choices of learning rates, starting configurations, or other hyper-parameters, there are statistical model selection problems within the kernel approach due to the choice of the kernel. In practice, it can be difficult for the practitioner to find prior justification for the use of one kernel instead of another to generate the random feature maps. It would be more desirable to explore data-driven mechanisms that allow kernels to be chosen automatically.

While sophisticated model selection methods such as the cross-validation, jackknife, or their approximate surrogates [4, 5, 6] can address those model selection issues, they often slow down the training process as they repeatedly re-fit the model. Therefore, to facilitate the kernel model selection problem, Sinha and Duchi [7] proposed a novel scheme to learn the kernel from the training samples via robust optimization of the kernel-target alignment [8]. Cortes, *et al.* [9] also presents a kernel learning algorithm based on the notion of centered alignment—a similarity measure between kernels or kernel matrices. In a separate study, [10] have also studied the generalization bounds for learning kernels from a mixture class of base kernels. The same multiple kernel learning scheme have been recently revisited by Shahrampour and Tarokh [11].

An alternative approach to kernel learning is to sample random features from an arbitrary distribution with arbitrary hyper-parameters (*i.e.* no tuning) and then apply a supervised feature screening method to distill random features with high discriminative power from redundant random features. This approach has been adopted by Shahrampour *et al.* [12], where an energy-based exploration of random features is proposed. The feature selection algorithm in [12] employs a score function based on the kernel polarization techniques of [13] to explore the domain of random features and retains samples with the highest score. Therefore, in the context of feature selection, the scoring rule of [12] belongs to the class of *filter methods* [14], *i.e.*, the scoring rule of [12] is based on intrinsic properties of the data, independent of the choice of the classifier (*e.g.* logistic or SVM). In addition, the number of selected random features in [12] is a hyper-parameter of the feature selection algorithm which must be determined by human user or via the cross-validation.

In this paper, we propose a novel method for kernel learning from the mixture class of a set of known base kernels. In contrast to the previous kernel learning approaches that are either use a scoring rule or optimization of the kernel-target alignment, our approach is based on the maximal separation between the empirical marginal distributions of features given their class labels. More specifically, we select the mixing coefficients of the kernel as to maximize the distance between the empirical distributions based on the maximum mean discrepancy (MMD). We analyze the consistency of the MMD for measuring the empirical distributions. In particular, we prove that a biased MMD estimator based on the empirical distributions converges to the MMD of the population measures. We also prove minimax lower bounds for the MMD estimators, *i.e.*, we prove a lower bound on the difference of the population MMD and its estimator for all admissible MMD estimators. In addition, we prove novel generalization bounds based on the notions of Rademacher and Gaussian complexities of the class of functions defined by random features that improves upon previous bounds Cortes, *et al.* [10].

We leverage our kernel learning approach to develop two novel architectures for the semantic segmentation of biomedical images using the kernel SVMs. Specifically, in the first architecture, we leverage the VGG network that is pre-trained on natural images in conjunction with a kernel feature selection method to extract semantic features. In the second

mechanism, we extract features via Mallat’s scattering convolution neural networks (SCNNs) [15]. The scattering network uses a tree-like feature extractor in conjunction with pre-specified wavelet transforms. Each node in the tree is a filter that is obtained by scaling and rotating an atom to construct translation invariant representations from the input images. We then validate our kernel learning algorithm and evaluate the performance of our proposed segmentation networks for Angiodysplasia segmentation from colonoscopy images from the GIANA challenge dataset. Angiodysplasia is an abnormality with the blood vessels in the gastrointestinal (GI) tract. The GI tract includes the mouth, esophagus, small and large intestines, and stomach. This condition causes swollen or enlarged blood vessels, as well as the formation of bleeding lesions in the colon and stomach. Gold-standard examination for angiodysplasia detection and localization in the small bowel is performed using Wireless Capsule Endoscopy (WCE). As a benchmark for comparison, we also evaluate the segmentation performance of fully convolutional network (FCN) [16], a popular architecture for the semantic segmentation of natural images. We compare our segmentation results with that of FCN in terms of *intersection-over-union* (IoU) metric. We show that while FCN over-fit the small dataset, our proposed segmentation architecture provides accurate segmentation results.

**1.1. Prior Works on Kernel Learning Methods.** There exists a copious theoretical literature developed on kernel learning methods [17], [10]. Cortes, *et al.* studied a kernel learning procedure from the class of mixture of base kernels. They have also studied the generalization bounds of the proposed methods via notion of Rademacher complexity. The same authors have also studied a two-stage kernel learning in [18] based on a notion of alignment. The first stage of this technique consists of learning a kernel that is a convex combination of a set of base kernels. The second stage consists of using the learned kernel with a standard kernel-based learning algorithm such as SVMs to select a prediction hypothesis. In [19], the authors have proposed a semi-definite programming for the kernel-target alignment problem. An alternative approach to kernel learning is to sample random features from an arbitrary distribution (without tuning its hyper-parameters) and then apply a supervised feature screening method to distill random features with high discriminative power from redundant random features. This approach has been adopted by Shahrampour *et al.* [12], where an energy-based exploration of random features is proposed. The feature selection algorithm in [12] employs a score function based on the kernel polarization techniques of [13] to explore the domain of random features and retains samples with the highest score.

This paper is closely related to the work of Duchi, *et al.* [7]. Therein, the authors have studied a kernel learning method via maximizing the kernel-target alignment with respect to non-parametric distributions in the ball of a (user-defined) base distribution defined by the  $f$ -divergence distance. Therefore, the proposed kernel alignment in [7] has two hyper-parameters, namely, the radius of the ball determining the size of the distribution class, and the base distribution determining the center of the ball.

The rest of this paper is organized as follows. In Section 2, we present some background on kernel methods in classification and regression problems. In Section 3, we review the notion of the kernel-target alignment. In Section 4, we relate the kernel-target alignment to the notion of two-sample test for discriminating between two distributions. We also provide a kernel selection procedure. In Section 5 we state the main assumptions and provide the generalization bounds and performance guarantees, while deferring the proofs to the appendices. In Section 7, we leverage the kernel learning algorithm to devise novel

architectures for the semantic segmentation. In Section 8 we evaluate the performance of the proposed segmentation networks for localization and delineation of Angiodysplasia from colonoscopy images. In Section 9 we discuss future works and conclude the paper.

## 2. PRELIMINARIES

In this section, we review preliminaries of kernel methods in classification and regression problems.

*Notation and Definitions.* We denote vector by bold small letters, e.g.  $\mathbf{x} = (x_1, \dots, x_n) \in \mathbb{R}^n$ , and matrices by the bold capital letters, e.g.,  $\mathbf{M} = [M_{ij}] \in \mathbb{R}^{n \times m}$ . The unit sphere in  $n$ -dimensions centered at the origin is denoted by  $S^{n-1} = \{\mathbf{x} \in \mathbb{R}^n : \sum_{i=1}^n x_i^2 = 1\}$ . We denote the  $n$ -by- $n$  identity matrix with  $\mathbf{I}_n$ , and the vector of all ones with  $\mathbf{1}_n = (1, 1, \dots, 1) \in \mathbb{R}^n$ . For a symmetric matrix  $\mathbf{M} = [M_{ij}] \in \mathbb{R}^{n \times n}$ , let  $\|\mathbf{M}\|_2 = \sup_{\mathbf{x} \in S^{n-1}} \langle \mathbf{x}, \mathbf{M}\mathbf{x} \rangle$  denotes its spectral norm, and  $\|\mathbf{M}\|_F = \sqrt{\text{Tr}(\mathbf{M}\mathbf{M}^T)} = \sum_{i,j=1}^n |M_{ij}|^2$  denotes its Frobenius norm. The eigenvalues of the matrix  $\mathbf{M}$  are ordered and denoted by  $\lambda_1(\mathbf{M}) \geq \dots \geq \lambda_n(\mathbf{M})$ . We alternatively write  $\lambda_{\min}(\mathbf{M}) = \lambda_n(\mathbf{M})$  and  $\lambda_{\max}(\mathbf{M}) = \lambda_1(\mathbf{M})$  for the minimum and maximum eigenvalues of the matrix  $\mathbf{M}$ , respectively. The empirical spectral measure of the matrix  $\mathbf{M}$  is denoted by

$$(2.1) \quad \widehat{\mu}_{\mathbf{M}}^n = \frac{1}{n} \sum_{i=1}^n \delta_{\lambda_i(\mathbf{M})},$$

where  $\delta_{\lambda_i(\mathbf{M})}$  is Dirac's measure concentrated at  $\lambda_i(\mathbf{M})$ . We denote the limiting spectral distribution of  $\widehat{\mu}_{\mathbf{M}}^n$  by  $\mu_{\mathbf{M}}$ , and its support by  $\text{support}(\mu_{\mathbf{M}})$ .

The Wigner's semi-circle law is denoted by  $\mu_{\text{sc}}$  and is defined as below

$$(2.2) \quad \mu_{\text{sc}}(dx) = \frac{1}{2\pi} \sqrt{4 - \lambda^2} \mathbb{I}_{\{|\lambda| \leq 2\}} dx,$$

where  $\mathbb{I}_{\{\cdot\}}$  is the indicator function. Let  $\mathbf{M} \in \mathbb{R}^{n \times d}$  be a random matrix whose entries are independent identically distributed random variables with the zero mean and the variance  $\sigma^2 < \infty$ . Let  $n, d \rightarrow \infty$  and  $n/d \rightarrow \lambda \in (0, \infty)$ . The limiting distribution of the covariance matrix  $\mathbf{Y}_n = n^{-1} \mathbf{M}\mathbf{M}^T$  is given by the *Marčenko-Pastur* law [20],

$$(2.3) \quad \mu_{\text{MP}, \lambda}(A) = \begin{cases} \nu(A) + (1 - \frac{1}{\lambda}) \mathbb{I}_{\{0 \in A\}} & \text{if } \lambda \geq 1 \\ \nu(A) & \text{if } 0 \leq \lambda \leq 1, \end{cases}$$

where

$$(2.4) \quad \nu(dx) = \frac{1}{2\pi\sigma^2} \frac{\sqrt{(\lambda_+ - x)(x - \lambda_-)}}{\lambda x} \mathbb{I}_{[\lambda_-, \lambda_+]} dx,$$

and  $\lambda_{\pm} \stackrel{\text{def}}{=} \sigma^2(1 \pm \sqrt{\lambda})^2$ . The free additive convolution between two laws  $\mu$  and  $\nu$  in the sense of Voiculescu [21] is denoted by  $\mu \boxplus \nu$ . Similarly, the free multiplicative convolution is denoted by  $\mu \boxtimes \nu$ .

**Definition 2.1.** (ORLICZ NORM) The Young-Orlicz modulus is a convex non-decreasing function  $\psi : \mathbb{R}_+ \rightarrow \mathbb{R}_+$  such that  $\psi(0) = 0$  and  $\psi(x) \rightarrow \infty$  when  $x \rightarrow \infty$ . Accordingly, the Orlicz norm of an integrable random variable  $X$  with respect to the modulus  $\psi$  is defined as

$$(2.5) \quad \|X\|_{\psi} \stackrel{\text{def}}{=} \inf\{\beta > 0 : \mathbb{E}[\psi(|X| - \mathbb{E}[|X|]/\beta)] \leq 1\}.$$

In the sequel, we consider the Orlicz modulus  $\psi_\nu(x) \stackrel{\text{def}}{=} \exp(x^\nu) - 1$ . Accordingly, the cases of  $\|\cdot\|_{\psi_2}$  and  $\|\cdot\|_{\psi_1}$  norms are called the sub-Gaussian and the sub-exponential norms and have the following alternative definitions:

**Definition 2.2.** (SUB-GAUSSIAN NORM) The sub-Gaussian norm of a random variable  $Z$ , denoted by  $\|Z\|_{\psi_2}$ , is defined as

$$(2.6) \quad \|Z\|_{\psi_2} = \sup_{q \geq 1} q^{-1/2} (\mathbb{E}|Z|^q)^{1/q}.$$

For a random vector  $\mathbf{Z} \in \mathbb{R}^n$ , its sub-Gaussian norm is defined as

$$(2.7) \quad \|\mathbf{Z}\|_{\psi_2} = \sup_{\mathbf{x} \in \mathbb{S}^{n-1}} \|\langle \mathbf{x}, \mathbf{Z} \rangle\|_{\psi_2}.$$

**Definition 2.3.** (SUB-EXPONENTIAL NORM) The sub-exponential norm of a random variable  $Z$ , denoted by  $\|Z\|_{\psi_1}$ , is defined as follows

$$(2.8) \quad \|Z\|_{\psi_1} = \sup_{q \geq 1} q^{-1} (\mathbb{E}\|Z|^q)^{1/q}.$$

For a random vector  $\mathbf{Z} \in \mathbb{R}^n$ , its sub-exponential norm is defined as

$$(2.9) \quad \|\mathbf{Z}\|_{\psi_1} = \sup_{\mathbf{x} \in \mathbb{S}^{n-1}} \|\langle \mathbf{Z}, \mathbf{x} \rangle\|_{\psi_1}.$$

For a given convex lower semi-continuous function  $f : (0, \infty) \rightarrow \mathbb{R}$  with  $f(1) = 0$ , the  $f$ -divergence between two Borel probability distributions  $P, Q \in \mathcal{B}(\mathcal{X})$  is defined as follows

$$D_f(P||Q) \stackrel{\text{def}}{=} \begin{cases} \int_{\mathcal{X}} f\left(\frac{dP(\mathbf{x})}{dQ(\mathbf{x})}\right) dQ(\mathbf{x}), & P \ll Q \\ \infty & \text{otherwise.} \end{cases}$$

Here,  $dP/dQ$  is the Radon-Nikodyme derivative of  $P$  with respect to  $Q$ . In the case that  $f(x) = x \log(x)$ , the  $f$ -divergence corresponds to the Kullback-Leibler (KL) divergence  $D_{\text{KL}}(P||Q) = \int_{\mathcal{X}} \log(dP/dQ) dP$ . For  $f(x) = (x - 1)^2$ , the  $f$ -divergence is equivalent to the  $\chi^2$ -divergence  $\chi^2(P||Q)$ . Lastly,  $f(x) = \frac{1}{2}|x - 1|$  corresponds to the total variation distance  $D_{\text{TV}}(P||Q) = \frac{1}{2}\|P - Q\|_1$ .

We use asymptotic notations throughout the paper. We use the standard asymptotic notation for sequences. If  $a_n$  and  $b_n$  are positive sequences, then  $a_n = \mathcal{O}(b_n)$  means that  $\limsup_{n \rightarrow \infty} a_n/b_n < \infty$ , whereas  $a_n = \Omega(b_n)$  means that  $\liminf_{n \rightarrow \infty} a_n/b_n > 0$ . Furthermore,  $a_n = \tilde{\mathcal{O}}(b_n)$  implies  $a_n = \mathcal{O}(b_n \text{poly} \log(b_n))$ . Moreover  $a_n = o(b_n)$  means that  $\lim_{n \rightarrow \infty} a_n/b_n = 0$  and  $a_n = \omega(b_n)$  means that  $\lim_{n \rightarrow \infty} a_n/b_n = \infty$ . Lastly, we have  $a_n = \Theta(b_n)$  if  $a_n = \mathcal{O}(b_n)$  and  $a_n = \Omega(b_n)$ . Finally, for positive  $a, b > 0$ , denote  $a \lesssim b$  if  $a/b$  is at most some universal constant.

### 2.1. Regularized Risk Minimization in Reproducing Kernel Hilbert Spaces.

In this paper we focus on the classical setting of supervised learning, whereby we are given  $n$  feature vectors and their corresponding univariate class labels  $(\mathbf{x}_1, y_1), \dots, (\mathbf{x}_n, y_n) \in \mathcal{X} \times \mathcal{Y} \subset \mathbb{R}^d \times \mathbb{R}$ . In this paper, we are concerned with the binary classification. Therefore, the target spaces is given by  $\mathcal{Y} = \{-1, 1\}$ .

In the following definition, we characterize the notion of kernel functions and reproducing Hilbert spaces:

---

We say  $P$  is absolutely continuous *w.r.t.*  $Q$ , denoted by  $P \ll Q$ , if for all the subsets  $A \subset \mathcal{X}$  satisfying  $Q(A) = 0$ , we have  $P(A) = 0$ .

**Definition 2.4.** (KERNEL FUNCTION [22]) Let  $\mathcal{X}$  be a non-empty set. Then a function  $k_{\mathcal{X}} : \mathcal{X} \times \mathcal{X} \rightarrow \mathbb{R}$  is called a kernel function on  $\mathcal{X}$  if there exists a Hilbert space  $\mathcal{H}_{\mathcal{X}}$  over  $\mathbb{R}$ , and a map  $g : \mathcal{X} \rightarrow \mathcal{H}_{\mathcal{X}}$  such that for all  $\mathbf{x}_1, \mathbf{x}_2 \in \mathcal{X}$ , we have

$$(2.10) \quad k_{\mathcal{X}}(\mathbf{x}_1, \mathbf{x}_2) = \langle g(\mathbf{x}_1), g(\mathbf{x}_2) \rangle_{\mathcal{H}_{\mathcal{X}}},$$

where  $\langle \cdot, \cdot \rangle_{\mathcal{H}_{\mathcal{X}}}$  is the inner product in the Hilbert space  $\mathcal{H}_{\mathcal{X}}$ .

Some examples of reproducing kernels on  $\mathbb{R}^d$  (in fact all these are radial) that appear throughout the paper are:

- *Gaussian*: The Gaussian kernel is given by  $k_{\mathcal{X}}(\mathbf{x}, \mathbf{y}) \stackrel{\text{def}}{=} \exp(-\|\mathbf{x} - \mathbf{y}\|/2\varrho^2)$ .
- *ANOVA*: The ANOVA kernel is defined by  $k_{\mathcal{X}}(\mathbf{x}, \mathbf{y}) \stackrel{\text{def}}{=} \prod_{k=1}^d \exp(-(x_k - y_k)^2/2\varrho^2)$  and performs well in multidimensional regression problems.
- *Laplacian*: The Laplacian kernel is similar to the Gaussian kernel, except that it is less sensitive to the bandwidth parameter. In particular,  $k_{\mathcal{X}}(\mathbf{x}, \mathbf{y}) \stackrel{\text{def}}{=} \exp(-\|\mathbf{x} - \mathbf{y}\|/\varrho)$ .

**Definition 2.5.** (CHARACTERISTIC KERNEL [22]) We say that an RKHS  $(\mathcal{H}_{\mathcal{X}}, k_{\mathcal{X}})$  is *characteristic* if the embedding map  $P \mapsto \mathbb{E}_P[k_{\mathcal{X}}(\cdot, \mathbf{x})] \in \mathcal{H}_{\mathcal{X}}$  is injective.

If the kernel  $k_{\mathcal{X}}$  is bounded, Definition 2.5 is equivalent to saying that  $\mathcal{H}_{\mathcal{X}}$  is dense in  $L_2(P)$  for any Borel probability measure  $P \in \mathcal{B}(\mathcal{X})$  [23]. Two examples of the characteristic kernels are the Gaussian and Laplacian kernels.

Recall that a positive definite kernel is a function  $k_{\mathcal{X}} : \mathcal{X} \times \mathcal{X} \rightarrow \mathbb{R}$  such that for any  $n \geq 1$ , for any finite set of points  $\{\mathbf{x}_i\}_{i=1}^n$  in  $\mathcal{X}$  and real numbers  $\{a_i\}_{i=1}^n$ , we have  $\sum_{i,j=1}^n a_i a_j k_{\mathcal{X}}(\mathbf{x}_i, \mathbf{x}_j) \geq 0$ . For any symmetric and positive semi-definite kernel  $k_{\mathcal{X}}(\cdot, \cdot)$ , by Mercer's theorem [24], there exists: (i) a unique functional Hilbert space  $\mathcal{H}_{\mathcal{X}}$  referred to as the reproducing kernel Hilbert space (see Definition 2.6) on  $\mathcal{X}$  such that  $k_{\mathcal{X}}(\cdot, \cdot)$  is the inner product in the space, and (ii) a map  $g : \mathcal{X} \rightarrow \mathcal{H}_{\mathcal{X}}$  defined as  $g(\mathbf{x}) \stackrel{\text{def}}{=} k_{\mathcal{X}}(\cdot, \mathbf{x})$  that satisfies Definition 2.4. The function  $g$  is called the *feature map* and the Hilbert space  $\mathcal{H}_{\mathcal{X}}$  is often called the *feature space*.

**Definition 2.6.** (REPRODUCING KERNEL HILBERT SPACE [22]) A kernel  $k_{\mathcal{X}}(\cdot, \cdot)$  is a reproducing kernel of a Hilbert space  $\mathcal{H}_{\mathcal{X}}$  if  $\forall f \in \mathcal{H}_{\mathcal{X}}, f(\mathbf{x}) = \langle k_{\mathcal{X}}(\cdot, \mathbf{x}), f(\cdot) \rangle_{\mathcal{H}_{\mathcal{X}}}$ . For a (compact) subset  $\mathcal{X} \subset \mathbb{R}^d$ , and a Hilbert space  $\mathcal{H}_{\mathcal{X}}$  of functions  $f : \mathcal{X} \rightarrow \mathbb{R}$ , we say  $\mathcal{H}_{\mathcal{X}}$  is a Reproducing Kernel Hilbert Space if there exists a kernel  $k_{\mathcal{X}} : \mathcal{X} \times \mathcal{X} \rightarrow \mathbb{R}$  such that  $k_{\mathcal{X}}$  has the reproducing property, and  $k_{\mathcal{X}}$  spans  $\mathcal{H}_{\mathcal{X}} = \overline{\text{span}\{k_{\mathcal{X}}(\cdot, \mathbf{x}) : \mathbf{x} \in \mathcal{X}\}}$ , where  $\overline{\mathcal{A}}$  is the completion of a set  $\mathcal{A}$ .

Given a loss function  $L : \mathcal{Y} \times \mathbb{R} \mapsto \mathbb{R}_+$  (e.g. hinge function for SVM, or quadratic for linear regression), and a reproducing Hilbert kernel space  $(\mathcal{H}_{\mathcal{X}}, k_{\mathcal{X}})$ , a classifier  $f \in \mathcal{H}_{\mathcal{X}} \oplus \{1\}$  is selected by minimizing the empirical risk minimization with a quadratic regularization,

$$(2.11) \quad \inf_{f \in \mathcal{H}_{\mathcal{X}}} \widehat{R}[f] \stackrel{\text{def}}{=} \mathbb{E}_{\widehat{P}_{\mathbf{X}, Y}^n} L(Y, f(\mathbf{X})) + \frac{\lambda}{2} \|f\|_{\text{HS}}^2,$$

where  $\|\cdot\|_{\text{HS}}$  is the RKHS norm,  $\lambda > 0$  is a regularization parameter, and  $\widehat{P}_{\mathbf{X}, Y}^n$  is the joint empirical measure, i.e.,

$$(2.12) \quad \widehat{P}_{\mathbf{X}, Y}^n = \frac{1}{n} \sum_{i=1}^n \delta(\mathbf{X} - \mathbf{x}_i, Y - y_i),$$

where  $\delta(\cdot)$  is Dirac's delta function. The Representer Theorem due to Wahba [25] for quadratic loss functions, and its generalization due to Schlkopf, Herbrich, and Smola [26] for general losses states that the optimal solution  $f^*$  of the empirical loss minimization in Eq. (2.11) admits the following representation

$$(2.13) \quad f^*(\mathbf{x}) = \omega_0 + \sum_{k=1}^n \omega_k k_{\mathcal{X}}(\mathbf{x}, \mathbf{x}_k),$$

where  $\omega_i \in \mathbb{R}$ , for all  $1 \leq i \leq n$ , where  $\omega_0$  is an offset term. Moreover, we have that  $\|f\|_{\text{HS}}^2 = \langle \omega, \mathbf{K}_n \omega \rangle$ , where  $\mathbf{K}_n \stackrel{\text{def}}{=} [\mathbf{k}_1, \dots, \mathbf{k}_n] \in \mathbb{R}^{n \times n}$  is the kernel matrix with columns  $\mathbf{k}_i \stackrel{\text{def}}{=} (k_{\mathcal{X}}(\mathbf{x}_i, \mathbf{x}_j))_{1 \leq j \leq n}$ . The key insight provided by the Representer Theorem is that even when the Hilbert space  $\mathcal{H}_{\mathcal{X}}$  is high-dimensional or infinite dimensional, we can solve (2.11) in polynomial time via reducing the empirical loss minimization in Eq. (2.11) to a finite dimensional optimization over the spanning vector  $\omega$ , namely,

$$(2.14) \quad \min_{\omega \in \mathbb{R}^d} \frac{1}{n} \sum_{i=1}^n L(y_i, \langle \mathbf{k}_i, \omega \rangle) + \frac{\lambda}{2} \langle \omega, \mathbf{K}_n \omega \rangle.$$

For small training data-sets, the optimization problem in Eq. (2.14) is solvable in polynomial time using stochastic or batch gradient descent. However, for large training data-sets, solving the empirical risk minimization in Eq. (2.14) is cumbersome since evaluating the kernel expansion (2.13) at a test point requires  $\mathcal{O}(nd)$  operations. Moreover, the computational complexity of preparing the kernel matrix  $\mathbf{K}_n$  during training phase increases quadratically with the sample size  $n$ .

To address this problem, Rahimi and Rechet proposed random Fourier features [2] to generate low-dimensional embedding of shift invariant kernels  $k_{\mathcal{X}}(\mathbf{x}, \mathbf{y}) = k_{\mathcal{X}}(\mathbf{x} - \mathbf{y})$  using explicit feature maps. In particular, let  $\varphi : \mathcal{X} \times \Xi \rightarrow \mathbb{R}$  be the explicit feature map, where  $\Xi$  is the support set of random features. Then, the kernel  $k_{\mathcal{X}}(\mathbf{x} - \mathbf{y})$  has the following

$$(2.15) \quad k_{\mathcal{X}}(\mathbf{x}, \mathbf{y}) = \int_{\Xi} \varphi(\mathbf{x}, \xi) \varphi(\mathbf{y}, \xi) \mu_{\Xi}(\mathrm{d}\xi)$$

$$(2.16) \quad = \mathbb{E}_{\mu_{\Xi}}[\varphi(\mathbf{x}; \xi) \varphi(\mathbf{y}; \xi)],$$

where  $\mu_{\Xi} \in \mathcal{P}(\Xi)$  is a probability measure, and  $\mathcal{P}(\Xi)$  is the set of Borel measures with the support set  $\Xi$ . In the standard framework of random fourier feature proposed by Rahimi and Rechet [2],  $\varphi(\mathbf{x}, \xi) = \sqrt{2} \cos(\langle \mathbf{x}, \xi \rangle + b)$ , where  $b \sim \text{Uni}[0, 2\pi]$ , and  $\xi \sim \mu_{\Xi}(\cdot)$ . In this case, by Bochner's Theorem [28],  $\mu_{\Xi}(\cdot)$  is indeed the Fourier transform of the shift invariant kernel  $k_{\mathcal{X}}(\mathbf{x}, \mathbf{y}) = k_{\mathcal{X}}(\mathbf{x} - \mathbf{y})$ .

For training purposes, the expression in Eq. (2.15) is approximated using the Monte Carlo sampling method. In particular, let  $\xi_1, \dots, \xi_N \sim_{\text{i.i.d.}} \mu_{\Xi}$  be the *i.i.d.* samples. Then, the kernel function  $k_{\mathcal{X}}(\mathbf{x}, \mathbf{y})$  can be approximated by the sample average of the expectation

---

An alternative approach to develop scalable kernel methods is the so-called Nyström approximation [27] which aims to construct a small sketch of the kernel matrix  $\mathbf{K}_n$  and use it in lieu of the full matrix to solve Problem (2.14).

in Eq. (2.16). Specifically, the following point-wise estimate has been shown in [2]:

$$(2.17) \quad \mathbb{P} \left[ \sup_{\mathbf{x}, \mathbf{y} \in \mathcal{R}} \left| k_{\mathcal{X}}(\mathbf{x}, \mathbf{y}) - \frac{1}{D} \sum_{j=1}^D \varphi(\mathbf{x}; \boldsymbol{\xi}_j) \varphi(\mathbf{y}; \boldsymbol{\xi}_j) \right| \geq \varepsilon \right] \leq 2^8 \left( \frac{\sigma_p \text{diam}(\mathcal{X})}{\varepsilon} \right)^2 \exp \left( -\frac{D\varepsilon^2}{4(d+2)} \right),$$

where typically  $D \ll n$ . In the preceding inequality,  $\mathcal{X} \subset \mathbb{R}^d$  is assumed to be a compact subset with the diameter of  $\text{diam}(\mathcal{X})$ , and  $\sigma_p^2 = \mathbb{E}_{\mu_{\Xi}}[\boldsymbol{\xi}\boldsymbol{\xi}^T]$ .

Using the random Fourier features  $\{\varphi(\mathbf{x}_i; \boldsymbol{\xi}_j)\}_{j=1}^n$ , the following empirical loss minimization is solved:

$$(2.18a) \quad \boldsymbol{\beta}^* = \arg \min_{\boldsymbol{\beta} \in \mathbb{R}^N} \frac{1}{n} \sum_{i=1}^n L \left( y_i, \frac{1}{\sqrt{N}} \boldsymbol{\beta}^T \boldsymbol{\varphi}(\mathbf{x}_i) \right),$$

$$(2.18b) \quad \text{s.t.}: \|\boldsymbol{\beta}\|_{\infty} \leq R/N,$$

for some constant  $R > 0$ , where  $\boldsymbol{\varphi}(\mathbf{x}) \stackrel{\text{def}}{=} (\varphi(\mathbf{x}, \boldsymbol{\xi}_1), \dots, \varphi(\mathbf{x}, \boldsymbol{\xi}_m))$ , and  $\boldsymbol{\beta} \stackrel{\text{def}}{=} (\beta_1, \dots, \beta_D)$ . The approach of Rahimi and Recht [2] is appealing due to its computational tractability. In particular, preparing the feature matrix during training requires  $\mathcal{O}(nD)$  computations, while evaluating a test sample needs  $\mathcal{O}(D)$  computations, which significantly outperforms the complexity of traditional kernel methods.

### 3. DATA-DEPENDENT KERNEL SELECTION VIA KERNEL-TARGET ALIGNMENT

In this paper, we focus on a hinge loss function associated with the support vector machines (SVMs) for classification problems. To describe a kernel selection strategy for SVMs, we recall the definition of the margin based classifiers. Given a training dataset of  $n$  points of the form  $(\mathbf{x}_1, y_1), \dots, (\mathbf{x}_n, y_n) \in \mathcal{X} \times \{-1, 1\}$ , and a feature map  $g(\mathbf{x})$ , the margin based classifier is given by

$$(3.1a) \quad \min_{\boldsymbol{\beta}} \frac{1}{2} \|\boldsymbol{\beta}\|_2^2$$

$$(3.1b) \quad \text{s.t.}: y_i (\langle \boldsymbol{\beta}, g(\mathbf{x}_i) \rangle + b) \geq 1, \quad i = 1, 2, \dots, n.$$

Soft-margin SVMs corresponds to the penalty function method for the optimization in Eq. (3.1), namely

$$(3.2) \quad \min_{(b, \boldsymbol{\beta}) \in \mathbb{R} \times \mathbb{R}^n} \frac{1}{n} \sum_{i=1}^n [1 - y_i (\langle \boldsymbol{\beta}, g(\mathbf{x}_i) \rangle + b)]_+ + \frac{\lambda}{2} \|\boldsymbol{\beta}\|_2^2,$$

where  $[x]_+ \stackrel{\text{def}}{=} \max\{0, x\}$ . Alternatively, by transforming Eq. (3.1) into its corresponding Lagrangian dual problem, the solution is given by

$$(3.3a) \quad \max_{\boldsymbol{\alpha}} \langle \boldsymbol{\alpha}, \mathbf{e} \rangle - \boldsymbol{\alpha}^T \mathbf{G}_{k_{\mathcal{X}}} \boldsymbol{\alpha}$$

$$(3.3b) \quad \text{s.t.}: \mathbf{0} \preceq \boldsymbol{\alpha}, \quad \langle \boldsymbol{\alpha}, \mathbf{y} \rangle = 0,$$

where  $\mathbf{G}_{k_{\mathcal{X}}} = [G_{ij}]_{i,j \in [n]}$  is a  $n$ -by- $n$  with elements  $G_{ij} = y_i y_j \langle g(\mathbf{x}_i), g(\mathbf{x}_j) \rangle_{\mathcal{H}_{\mathcal{X}}} = y_i y_j k_{\mathcal{X}}(\mathbf{x}_i, \mathbf{x}_j)$ . Moreover, there is the following connection between primal and dual variables

$$(3.4) \quad \boldsymbol{\beta} = \sum_{i=1}^n \alpha_i y_i g(\mathbf{x}_i).$$



Therefore, the optimal margin of the classifier is related to the matrix  $\mathbf{G}_{k_{\mathcal{X}}}$  via

$$(3.5) \quad \frac{1}{2} \|\boldsymbol{\beta}_*\|_2^2 = \frac{1}{2} \sum_{i,j=1}^n \alpha_{*,i} \alpha_{*,j} y_i y_j \langle g(\mathbf{x}_i), g(\mathbf{x}_j) \rangle$$

$$(3.6) \quad = \boldsymbol{\alpha}_*^T \mathbf{G}_{k_{\mathcal{X}}} \boldsymbol{\alpha}_*.$$

To gain further insight about the matrix  $\mathbf{G}_{k_{\mathcal{X}}}$ , we need to define the notion of the kernel alignment as a similarity measure between two kernel functions over a set of data-points:

**Definition 3.1.** (KERNEL ALIGNMENT, CORTES, *et al.* [9]) The empirical alignment of a kernel  $k_1(\cdot, \cdot)$  with a kernel  $k_2(\cdot, \cdot)$  with respect to the (unlabeled) samples  $\mathcal{S} = \{\mathbf{x}_1, \dots, \mathbf{x}_n\}$  is defined by

$$(3.7) \quad \rho_{\mathcal{S}}(k_1, k_2) \stackrel{\text{def}}{=} \frac{\langle \mathbf{K}_1, \mathbf{K}_2 \rangle}{\sqrt{\langle \mathbf{K}_1, \mathbf{K}_1 \rangle \langle \mathbf{K}_2, \mathbf{K}_2 \rangle}},$$

where  $\mathbf{K}_1 \stackrel{\text{def}}{=} [k_1(\mathbf{x}_i, \mathbf{x}_j)]_{i,j \in [n]}$ ,  $\mathbf{K}_2 \stackrel{\text{def}}{=} [k_2(\mathbf{x}_i, \mathbf{x}_j)]_{i,j \in [n]}$ , and  $\langle \mathbf{K}_1, \mathbf{K}_2 \rangle \stackrel{\text{def}}{=} \text{Tr}(\mathbf{K}_1 \mathbf{K}_2^T)$ .

Define the kernel  $\mathbf{K}_* \stackrel{\text{def}}{=} [k_*(\mathbf{x}_i, \mathbf{x}_j)]_{i,j \in [n]} = \mathbf{y}\mathbf{y}^T$ , defined by the labels  $\mathbf{y} \stackrel{\text{def}}{=} (y_1, \dots, y_n)^T$ . Notice that the kernel  $\mathbf{K}_*$  is optimal since it creates optimal separation between feature vectors, *i.e.*,  $k_*(\mathbf{x}_i, \mathbf{x}_j) = 1$  when  $y_i = y_j$ , and  $k_*(\mathbf{x}_i, \mathbf{x}_j) = -1$  when  $y_i \neq y_j$ . From Definition 3.1, we now observe that the matrix  $\mathbf{G}_{k_{\mathcal{X}}}$  captures the alignment between the kernel matrix  $\mathbf{K}_n \stackrel{\text{def}}{=} [k_{\mathcal{X}}(\mathbf{x}_i, \mathbf{x}_j)]_{i,j \in [n]}$  and the optimal kernel  $\mathbf{K}_*$ . More specifically, since  $\langle \mathbf{K}_*, \mathbf{K}_* \rangle = \langle \mathbf{y}\mathbf{y}^T, \mathbf{y}\mathbf{y}^T \rangle = n^2$ , the kernel alignment metric in Eq. (3.7) can be expressed in terms of the matrix  $\mathbf{G}_{k_{\mathcal{X}}}$  as follows

$$(3.8) \quad p_{\mathcal{S}}(k_{\mathcal{X}}, k_*) = \frac{\langle \mathbf{K}_n, \mathbf{y}\mathbf{y}^T \rangle}{n \|\mathbf{K}_n\|_F} = \frac{1}{n \|\mathbf{K}_n\|_F} \mathbf{e}_n^T \mathbf{G}_{k_{\mathcal{X}}} \mathbf{e}_n,$$

where  $\|\cdot\|_F$  is the Frobenious norm, and  $\mathbf{e}_n = (1, 1, \dots, 1) \in \mathbb{R}^n$  is the vector of all ones. Therefore, the matrix  $\mathbf{G}_{k_{\mathcal{X}}}$  captures the alignment of the kernel  $k_{\mathcal{X}}$  with the optimal kernel  $k_*$ .

#### 4. KERNEL ALIGNMENT AS AN UNBIASED TWO-SAMPLE TEST

In this section, we propose a scoring rule method for selection of random features. To specify the proposed method, we first review the notion of the Maximum Mean Discrepancy (MMD):

**Definition 4.1.** (MAXIMUM MEAN DISCREPANCY [29]) Let  $(\mathcal{X}, d)$  be a metric space. Let  $\mathcal{F}$  be a class of functions  $f: \mathcal{X} \rightarrow \mathbb{R}$ . Let  $P, Q \in \mathcal{B}(\mathcal{X})$  be two Borel probability measures from the set of Borel probability measures  $\mathcal{B}(\mathcal{X})$  on  $\mathcal{X}$ . We define the maximum mean discrepancy (MMD) between two distributions  $P$  and  $Q$  with respect to the function class  $\mathcal{F}$  as follows

$$(4.1) \quad D_{\mathcal{F}}^{\text{MMD}}[P, Q] \stackrel{\text{def}}{=} \sup_{f \in \mathcal{F}} \int_{\mathcal{X}} f(\mathbf{x}) d(P - Q)(\mathbf{x}).$$

As shown by Zhang, *et al.* [30], the kernel-target alignment in Eq. (3.7) is closely related to the notion of the Maximum Mean Discrepancy (MMD) between the distribution of two classes, measured by functions from RHKS, *i.e.*, when  $\mathcal{F} = \mathcal{H}_{\mathcal{X}}$  in Definition 4.1. To see this, define the modified labels as  $\hat{y}_i = 1/n_+$  for  $y_i = 1$ , and  $\hat{y}_i = -1/n_-$  when  $y_i = -1$  each  $i = 1, 2, \dots, n$ . Here,  $n_+$  and  $n_-$  denotes the number of positive and negative labels, such

that  $n_+ + n_- = n$ . Let  $\widehat{\mathbf{y}} = (\widehat{y}_1, \dots, \widehat{y}_n)$ . Then, the kernel alignment can be reformulated as follows

$$(4.2) \quad \langle \mathbf{K}_n, \widehat{\mathbf{y}}\widehat{\mathbf{y}}^T \rangle = \left\| \sum_{i \in [n]} \widehat{y}_i k_{\mathcal{X}}(\cdot, \mathbf{x}_i) \right\|_{\text{HS}}^2.$$

The formula in Eq. (4.2) is an *unbiased* estimator of the MMD between distributions with respect to functions from RHKS,

$$(4.3) \quad \begin{aligned} D_{k_{\mathcal{X}}}^{\text{MMD}}[P_0, Q_0] &= \left\| \int_{\mathcal{X}} k_{\mathcal{X}}(\cdot; \mathbf{x}) d(P_0 - Q_0)(\mathbf{x}) \right\|_{\text{HS}} \\ &= \left[ \mathbb{E}_{\mathbf{z}, \mathbf{z}' \sim P_0} [k_{\mathcal{X}}(\mathbf{z}; \mathbf{z}')] + \mathbb{E}_{\mathbf{s}, \mathbf{s}' \sim Q_0} [k_{\mathcal{X}}(\mathbf{s}; \mathbf{s}')] - 2\mathbb{E}_{\mathbf{z} \sim P_0, \mathbf{s} \sim Q_0} [k_{\mathcal{X}}(\mathbf{z}; \mathbf{s})] \right]^{1/2}, \end{aligned}$$

equality follows by the reproducing property  $\langle k_{\mathcal{X}}(\cdot; \mathbf{x}), k_{\mathcal{X}}(\cdot; \mathbf{x}') \rangle_{\mathcal{H}_{\mathcal{X}}} = k_{\mathcal{X}}(\mathbf{x}; \mathbf{x}')$ . Here,  $P_0 \stackrel{\text{def}}{=} P_{\mathbf{X}|Y=+1}$  and  $Q_0 \stackrel{\text{def}}{=} P_{\mathbf{X}|Y=-1}$  are the marginal distributions, whereby features with the positive and negative labels are drawn, respectively.

For characteristic kernels  $k_{\mathcal{X}}$  (cf. Definition 2.5), the discrepancy  $D_{\mathcal{H}_{\mathcal{X}}}^{\text{MMD}}[\cdot, \cdot]$  indeed defines a valid metric on the space of Borel probability measures  $\mathcal{B}(\mathcal{X})$  in the sense that for any  $P_0, Q_0 \in \mathcal{B}(\mathcal{X})$ ,  $D_{\mathcal{H}_{\mathcal{X}}}^{\text{MMD}}[P_0, Q_0] = 0$  if and only if  $P_0 = Q_0$ , see [31].

Let  $\mathcal{Y}_+$  and  $\mathcal{Y}_-$  denote the set of samples with positive  $y_i = 1$  and negative  $y_i = -1$  labels, respectively. We define the empirical marginal distributions corresponding to the observed samples  $\mathbf{x}_1, \dots, \mathbf{x}_n$

$$(4.4a) \quad \widehat{P}_0^{n+} \stackrel{\text{def}}{=} \frac{1}{n_+} \sum_{i \in \mathcal{Y}_+} \delta(\mathbf{x} - \mathbf{x}_i),$$

$$(4.4b) \quad \widehat{Q}_0^{n-} \stackrel{\text{def}}{=} \frac{1}{n_-} \sum_{i \in \mathcal{Y}_-} \delta(\mathbf{x} - \mathbf{x}_i).$$

Instead of unbiased estimator in Eq. (4.2), we leverage the following *biased* empirical estimate of Eq. (4.3) is the sum of two  $U$ -statistics and a sample average as below (see [29])

$$(4.5) \quad \begin{aligned} D_{k_{\mathcal{X}}}^{\text{MMD}}[\widehat{P}_0^{n+}, \widehat{Q}_0^{n-}] &= \left( \frac{1}{n_+(n_+ - 1)} \sum_{\substack{i, j \in \mathcal{Y}_+ \\ i \neq j}} k_{\mathcal{X}}(\mathbf{x}_i, \mathbf{x}_j) + \frac{1}{n_-(n_- - 1)} \sum_{\substack{i, j \in \mathcal{Y}_- \\ i \neq j}} k_{\mathcal{X}}(\mathbf{x}_i, \mathbf{x}_j) - \frac{2}{n_+ n_-} \sum_{i \in \mathcal{Y}_+} \sum_{j \in \mathcal{Y}_-} k_{\mathcal{X}}(\mathbf{x}_i, \mathbf{x}_j) \right)^{1/2}. \end{aligned}$$

For a balanced training data-set,  $n_+ = n_- = n_0$ , an unbiased empirical estimate of Eq. (4.3) can be computed as one  $U$ -statistic

$$(4.6) \quad D_{k_{\mathcal{X}}}^{\text{MMD}}[\widehat{P}_0^{n+}, \widehat{Q}_0^{n-}] = \left( \frac{1}{n_0(n_0 - 1)} \sum_{\substack{i, j \in \mathcal{Y}_+ \\ i \neq j}} \widehat{k}_{\mathcal{X}}(\mathbf{z}_i, \mathbf{z}_j) \right)^{1/2},$$

where  $\mathbf{z}_i = (\mathbf{x}_i, \mathbf{y}_i)$ , and  $\mathbf{z}_1, \dots, \mathbf{z}_{n_0} \sim_{\text{i.i.d.}} P_0 \otimes Q_0$ , and

$$\widehat{k}_{\mathcal{X}}(\mathbf{z}_i, \mathbf{z}_j) = k_{\mathcal{X}}(\mathbf{x}_i, \mathbf{x}_j) + k_{\mathcal{X}}(\mathbf{y}_i, \mathbf{y}_j) - k_{\mathcal{X}}(\mathbf{x}_i, \mathbf{y}_j) - k_{\mathcal{X}}(\mathbf{x}_j, \mathbf{y}_i).$$

To simplify the analysis, we assume  $n_+ = n_- = n_0$  and consider the  $U$ -statistics in Eq. (4.6). We also consider a class of mixture kernels of a set of known base kernels  $k_{\mathcal{X}}^{\ell} : \mathcal{X} \times \mathcal{X} \rightarrow \mathbb{R}$ , *i.e.*, we consider

$$(4.7) \quad k_{\mathcal{X}}^{\mathbf{w}}(\mathbf{x}, \mathbf{y}) \stackrel{\text{def}}{=} \sum_{\ell=1}^m w_{\ell} k_{\mathcal{X}}^{\ell}(\mathbf{x}, \mathbf{y}),$$

where the mixing coefficients  $\mathbf{w} \stackrel{\text{def}}{=} (w_1, \dots, w_m)$  are determined based on the MMD scores

$$(4.8) \quad w_{\ell} \stackrel{\text{def}}{=} w_{\ell}(\widehat{P}_0^{n_+}, \widehat{Q}_0^{n_-}) = \frac{D_{k_{\mathcal{X}}^{\ell}}(\widehat{P}_0^{n_+}, \widehat{Q}_0^{n_-})}{\sum_{\ell=0}^m D_{k_{\mathcal{X}}^{\ell}}(\widehat{P}_0^{n_+}, \widehat{Q}_0^{n_-})}.$$

Computing efficient mixture coefficients  $\{w_{\ell}\}_{\ell=1}^m$  for multiple kernel learning has been studied extensively over the past few years [32]. However, those approaches propose to solve an optimization problem to maximize the kernel alignment which can be computationally prohibitive when the number of base kernels is very large.

Associated with the mixture model of Eq. (4.7), we consider the following class of functions parameterized by  $R > 0$ :

$$(4.9) \quad \mathcal{F}_m(R) \stackrel{\text{def}}{=} \left\{ f(\mathbf{x}) = \frac{\boldsymbol{\beta}^T \boldsymbol{\varphi}^{\mathbf{w}}(\mathbf{x})}{\sqrt{D}} : \|\boldsymbol{\beta}\|_2 \leq \frac{R}{\sqrt{mD}}, \mathbf{w} \in \Delta_m \right\},$$

where  $\boldsymbol{\beta} \in \mathbb{R}^{Dm}$  and the vector  $\boldsymbol{\varphi}^{\mathbf{w}}(\mathbf{x}) \in \mathbb{R}^{mD}$  is defined via concatenation of random features associated with each base kernel, *i.e.*,

$$(4.10) \quad \boldsymbol{\varphi}^{\mathbf{w}}(\mathbf{x}) \stackrel{\text{def}}{=} (\sqrt{w_1} \varphi^1(\mathbf{x}, \boldsymbol{\xi}_1^1), \dots, \sqrt{w_1} \varphi^1(\mathbf{x}, \boldsymbol{\xi}_D^1), \dots, \sqrt{w_m} \varphi^m(\mathbf{x}, \boldsymbol{\xi}_1^m), \dots, \sqrt{w_m} \varphi^m(\mathbf{x}, \boldsymbol{\xi}_D^m)).$$

Furthermore,  $\Delta_m \stackrel{\text{def}}{=} \{\mathbf{w} : \mathbf{w} \geq 0, \sum_{i=1}^m w_i = 1\}$  is the simplex of probability distributions with  $m$  mass functions. Algorithm 1 outlines the procedure for SVMs with the multiple kernel learning algorithm proposed in this paper.

*Remark 4.2.* Alternatively, the statistic in Eq. (4.5) can be rewritten in terms of random Fourier features. In particular, due to the bijection between the kernel and the generative distribution of random features, we can write

$$(4.11) \quad D_{\mu_{\Xi}}^{\text{MMD}}[\widehat{P}_0^{n_+}, \widehat{Q}_0^{n_-}] = \left[ \frac{1}{n_+(n_+ - 1)} \sum_{\substack{i, j \in \mathcal{Y}_+ \\ i \neq j}} \mathbb{E}_{\mu_{\Xi}}[\varphi(\mathbf{x}_i; \boldsymbol{\xi}) \varphi(\mathbf{x}_j; \boldsymbol{\xi})] \right. \\ \left. + \frac{1}{n_-(n_- - 1)} \sum_{\substack{i, j \in \mathcal{Y}_- \\ i \neq j}} \mathbb{E}_{\mu_{\Xi}}[\varphi(\mathbf{x}_i; \boldsymbol{\xi}) \varphi(\mathbf{x}_j; \boldsymbol{\xi})] \right. \\ \left. - \frac{2}{n_+ n_-} \sum_{i \in \mathcal{Y}_+} \sum_{j \in \mathcal{Y}_-} \mathbb{E}_{\mu_{\Xi}}[\varphi(\mathbf{x}_i; \boldsymbol{\xi}) \varphi(\mathbf{x}_j; \boldsymbol{\xi})] \right]^{1/2}.$$

The correspondence between the base kernel  $k_{\mathcal{X}}^{\ell}$  and its generative distributions  $\mu_{\Xi}^{\ell}$ , provides the following alternative mixture model for the distribution of random features instead of

---

**Algorithm 1** SVMs WITH MULTIPLE KERNELS LEARNING.
 

---

- 1: **Input:** Training samples  $(\mathbf{x}_1, y_1), \dots, (\mathbf{x}_n, y_n) \in \mathcal{X} \times \mathcal{Y}$ . A set of base kernels  $\{k_{\mathcal{X}}^{\ell}\}_{\ell=1}^m$ . Integers  $D$  and  $m$ .
- 2: Compute the empirical marginal measures  $\widehat{P}_0^{n+}$  and  $\widehat{Q}_0^{n-}$  from Eq. (4.4).
- 3: Compute the MMD score of each kernel  $D_{k_{\mathcal{X}}^{\ell}}^{\text{MMD}}[\widehat{P}_0^{n+}, \widehat{Q}_0^{n-}]$  from Eq. (4.6) (if  $n_+ = n_-$ ) or Eq. (4.5).
- 4: Associated with each base kernel  $k_{\mathcal{X}}^{\ell}$ , draw  $D$  samples  $\xi_1^{\ell}, \dots, \xi_D^{\ell} \sim_{\text{i.i.d.}} \mu_{\Xi}^{\ell}$ .
- 5: Compute the random feature vector  $\varphi^{\mathbf{w}}(\mathbf{x})$  in Eq. (4.10) using the mixing coefficients  $\mathbf{w} = (w_{\ell})_{1 \leq \ell \leq m}$  given in Eq. (4.8).
- 6: **Output:** The solution of the following optimization problem

$$\beta^* = \arg \min_{\beta \in \mathbb{R}^{mD}: \|\beta\|_2 \leq \frac{R}{\sqrt{mD}}} \frac{1}{n} \sum_{i=1}^n L\left(y_i, \frac{1}{\sqrt{D}} \beta^T \varphi^{\mathbf{w}}(\mathbf{x}_i)\right),$$


---

kernels,

$$(4.12) \quad \mu_{\Xi}^{\mathbf{w}} \stackrel{\text{def}}{=} \sum_{\ell=1}^m w_{\ell} \mu_{\Xi}^{\ell}.$$

Using the mixture model in Eq. (4.12), we draw  $mD$  random feature maps  $\varphi(\mathbf{x}, \xi_k)$ , where  $\xi_1, \dots, \xi_{mD} \sim_{\text{i.i.d.}} \mu_{\Xi}^{\mathbf{w}}$ , and let  $\varphi^{\mathbf{w}}(\mathbf{x}) = (\varphi(\mathbf{x}, \xi_k))_{1 \leq k \leq mD}$ . In this paper, we only analyze the mixture kernel model in Eq. (4.7).

## 5. THEORETICAL RESULTS: CONSISTENCY, MINIMAX RATE, AND GENERALIZATION BOUNDS

In this section, we state our main theoretical results regarding the performance guarantees of the proposed kernel learning procedure in Section 4. The proof of theoretical results is presented in Appendix.

**5.1. Technical Assumptions.** To state our theoretical results, we first state the technical assumptions under which we prove our theoretical results:

- (A.1) The kernel is Hilbert-Schmidt, *i.e.*,  $\sup_{\mathbf{x}, \mathbf{y} \in \mathcal{X}} |k_{\mathcal{X}}(\mathbf{x}, \mathbf{y})| \leq M$ .
- (A.2) The base kernels are shift invariant, *i.e.*,  $k_{\mathcal{X}}^{\ell}(\mathbf{x}, \mathbf{y}) = k_{\mathcal{X}}^{\ell}(\mathbf{x} - \mathbf{y})$  for all  $\ell = 1, 2, \dots, m$ .
- (A.3) Given a loss function  $L: \mathcal{Y} \times \mathcal{S} \rightarrow \mathbb{R}$ , we assume there exists a function  $\ell: \mathcal{Y} \times \mathcal{S} \rightarrow \mathbb{R}$  dominating  $L$  in the sense that for all  $y \in \mathcal{Y}$  and  $x \in \mathcal{S}$ ,  $\ell(y, x) \geq L(y, x)$ . Further, we suppose  $\ell(y, \cdot)$  is a Lipschitz function with respect to Euclidean distance  $\|\cdot\|_{\mathcal{S}}$  on  $\mathcal{S}$  with constant  $K$ , *i.e.*,  $|\ell(y, \mathbf{x}_1) - \ell(y, \mathbf{x}_2)| \leq K \|\mathbf{x}_1 - \mathbf{x}_2\|_{\mathcal{S}}$ . Moreover, we assume  $\ell(y, \cdot)$  passes through the origin and is uniformly bounded, *i.e.*,  $\ell(y, 0) = 0$  for all  $y \in \mathcal{Y}$ .
- (A.4) The feature space  $\mathcal{X} \subset \mathbb{R}^d$  is compact with a finite diameter  $\text{diam}(\mathcal{X}) < \infty$ .

**5.2. Consistency, MinMax Lower Bound, and Asymptotic Distribution.** The first result of this paper is concerned with the consistency of biased MMD estimator in Eq. (4.3) with respects to the sampling data distributions:

**Theorem 5.1.** (CONSISTENCY AND ASYMPTOTIC DISTRIBUTION) *Suppose the conditions in (A.1) hold. Let  $P, Q$  be two arbitrary Borel probability measures from the set  $\mathcal{P}_{\alpha}(\mathcal{X}) \stackrel{\text{def}}{=} \{(P, Q) \in \mathcal{B}(\mathcal{X}) : D_{\text{TV}}(P||Q) \leq \alpha\}$ . Let  $\widehat{P}_0^{n+}$  and  $\widehat{Q}_0^{n+}$  denote the empirical measures corresponding to the samples  $X_1, \dots, X_{n_+} \sim_{\text{i.i.d.}} P$  and  $X_1, \dots, X_{n_-} \sim_{\text{i.i.d.}} Q$ , respectively. Then, for a fixed distribution  $\mu_{\Xi}^{\theta} \in \Xi_m$  of random features we have that*

- With the probability of (at least)  $1 - \rho$ , we have

$$(5.1) \quad \sup_{(P,Q) \in \mathcal{P}_\alpha(\mathcal{X})} |D_{k_{\mathcal{X}}}^{\text{MMD}}[P, Q] - D_{k_{\mathcal{X}}}^{\text{MMD}}[\hat{P}^n, \hat{Q}^n]| \leq \sqrt{\frac{6M \log(en/3)}{n}} + 2\sqrt{\frac{M}{2n} \log\left(\frac{2}{\rho}\right)}.$$

In particular,

$$(5.2) \quad \text{p-lim}_{n \rightarrow \infty} \sup_{(P,Q) \in \mathcal{P}_\alpha(\mathcal{X})} D_{k_{\mathcal{X}}}^{\text{MMD}}[\hat{P}^n, \hat{Q}^n] = D_{k_{\mathcal{X}}}^{\text{MMD}}[P, Q].$$

- For the special case of the Gaussian RBF kernel  $k_{\mathcal{X}}(\mathbf{x}, \mathbf{y}) = \exp\left(-\frac{\|\mathbf{x} - \mathbf{y}\|_2^2}{2\sigma^2}\right)$ , the following lower bound holds with the probability of (at least)  $1/5$ ,

$$(5.3) \quad \sup_{(P,Q) \in \mathcal{P}_\alpha(\mathcal{X})} \left| D_{k_{\mathcal{X}}}^{\text{MMD}}[P, Q] - D_{k_{\mathcal{X}}}^{\text{MMD}}[\hat{P}^{n_+}, \hat{Q}^{n_-}] \right| \geq \frac{1}{8} \frac{1}{\sqrt{3(d+1)Mn}}.$$

- Consider a balanced data-set  $n_+ = n_- = n_0$ . For all the Borel probability measures  $(P, Q) \in \mathcal{B}^{\otimes 2}(\mathcal{X})$ , the asymptotic distribution is given by

$$(5.4) \quad \sqrt{n_0}(D_{k_{\mathcal{X}}}^{\text{MMD}}[\hat{P}^n, \hat{Q}^n]) \stackrel{d}{\rightsquigarrow} \mathbf{N}(0, \sigma^2),$$

where  $\sigma^2 = 2(\mathbb{E}_{\mathbf{z} \sim P_0, \mathbf{s} \sim Q_0}[k_{\mathcal{X}}^2(\mathbf{z}; \mathbf{s})] - [\mathbb{E}_{\mathbf{z} \sim P_0, \mathbf{s} \sim Q_0}[k_{\mathcal{X}}(\mathbf{z}; \mathbf{s})]]^2)$ .

*Proof.* The proof is presented in Section A.1 of the supplementary materials.  $\square$

The upper bound in Eq. (5.1) shows that the MMD estimator converges to its population value at the rate of  $\tilde{\mathcal{O}}(1/\sqrt{n})$ . The lower bound in Eq. (5.3) also proves a rate of  $\Omega(1/\sqrt{n})$ , and hence  $\tilde{\Theta}(1/\sqrt{n})$ .

We remark that a similar upper bound is established in [29], albeit using a different approach. Specifically, our proof relies the convergence rate of the empirical measures to their population value under the total variation distance. In addition, the upper bound in Eq. (5.1) includes the additional supremum term. Note that both the upper bound (5.1) and the lower bound (5.3) are uniform and are independent of the radius  $\alpha$  of the distribution set  $\mathcal{P}_\alpha(\mathcal{X})$ . However, from our proofs in Section A.1 of the supplementary material, it is apparent that the uniform convergence property is exclusive to the total variation distance, and does not extend to the parameteric set  $\mathcal{P}_\alpha(\mathcal{X})$  defined by different  $f$ -divergences.

In addition, the lower bound provided in Eq. (5.3) is proved via Fano's method which is a standard technique to compute the minimax rate via reducing the estimation problem to a multi-way hypothesis testing problem. We remark that our method improves upon [33] that uses Le Cadram's two point method to establish the minimax rate.

The proof of the asymptotic distribution in Eq. (5.4) is due to Gretton, *et al.* [29] and shows that the fluctuations of the estimator is asymptotically zero-mean Gaussian, with a variance related to the variance of the random variables  $k_{\mathcal{X}}(\mathbf{z}, \mathbf{s})$ ,  $\mathbf{z} \sim P$ ,  $\mathbf{s} \sim Q$ . The additional factor 2 in the variance term  $\sigma^2$  is due to the averaging over  $\lfloor n_0/2 \rfloor$  terms.

The following corollary is an immediate result of Theorem 5.1 and establishes the convergence in probability of the mixing coefficients defined in Eq. (4.8) to their population versions:

**Corollary 5.1.1.** For all  $(P, Q) \in \mathcal{P}_\alpha(\mathcal{X})$  and for every  $\ell = 1, 2, \dots, m$ ,

$$(5.5) \quad \text{p-lim}_{n \rightarrow \infty} w_\ell(\hat{P}^{n_+}, \hat{Q}^{n_+}) = w_\ell(P, Q).$$

**5.3. Generalization Bounds.** To upper bound the out-of-sample error in terms of the training error, we require the following notions of complexities of a function class:

**Definition 5.2.** (RADEMACHER AND GAUSSIAN COMPLEXITIES) Given a finite-sample set  $S = (\mathbf{X}_1, \dots, \mathbf{X}_n)$ , and function class  $\mathcal{F}$  consider the following random variable

$$(5.6) \quad \widehat{\mathfrak{R}}_S^n(\mathcal{F}) \stackrel{\text{def}}{=} \mathbb{E}_{P_\epsilon} \left[ \sup_{f \in \mathcal{F}} \frac{1}{n} \sum_{i=1}^n \epsilon_i f(\mathbf{X}_i) \middle| \mathbf{X}_1, \dots, \mathbf{X}_n \right].$$

where  $\epsilon \stackrel{\text{def}}{=} (\epsilon_1, \dots, \epsilon_n)$  are *i.i.d.* Rademacher random variables, *i.e.*,  $(\epsilon_1, \dots, \epsilon_n) \sim_{i.i.d.} P_\epsilon = \text{Uni}\{-1, 1\}$ , and  $P_\epsilon = P_\epsilon^{\otimes n}$ . The *Rademacher complexity* is then defined as the expected value of  $\widehat{\mathfrak{R}}_S^n(\mathcal{F})$  with respect to the observed samples, *i.e.*,

$$(5.7) \quad \mathfrak{R}^n(\mathcal{F}) \stackrel{\text{def}}{=} \mathbb{E}_{P_{\mathbf{X}}} [\widehat{\mathfrak{R}}_S^n(\mathcal{F})].$$

Similarly, the *Gaussian complexities*  $\mathfrak{G}_S^n(\mathcal{F})$  and  $\mathfrak{G}^n(\mathcal{F})$  is defined by letting  $P_\epsilon = \mathbf{N}(0, 1)$  in Eqs. (5.6)-(5.7), respectively.

In the following proposition, we establish novel upper bounds on the Rademacher and Gaussian complexities of the class of functions based on the mixture kernel (4.7).

**Proposition 5.1.** (UPPER BOUNDS ON THE FUNCTION CLASS COMPLEXITIES) *Consider the class of functions  $\mathcal{F}_m(R)$  defined in Eqs. (4.9)-(4.10). Then,*

(i) *The Rademacher complexity of the class  $\mathcal{F}_m(R)$  is*

$$(5.8) \quad \mathfrak{R}^n(\mathcal{F}_m(R)) \leq \frac{R}{nD} \sqrt{\frac{\pi}{192}} \|\Phi\|_2 \cdot \text{erfc}(\sqrt{192D}).$$

(ii) *The Gaussian complexity of the class  $\mathcal{F}_m(R)$  is given by*

$$(5.9) \quad \mathfrak{G}^n(\mathcal{F}_m(R)) \leq \frac{R}{nD} \left( 2 \frac{\sqrt{\pi \text{Tr}((\Phi \Phi^T)^2)}}{\|\Phi\|_F} + \frac{\|\Phi\|_F}{2\|\Phi\|_2^2} e^{-\frac{\|\Phi\|_F^4}{4\text{Tr}((\Phi \Phi^T)^2)}} \right).$$

Here,  $\Phi \stackrel{\text{def}}{=} [\varphi^{\mathbf{w}}(\mathbf{x}_i, \boldsymbol{\xi}_j)]_{(i,j) \in [n] \times [mD]}$ .

*Proof.* The proof is presented in Section A.2 of the supplementary material. □

Let us make some remarks about the implications of Proposition 5.1.

The proof techniques we used to establish the upper bound on the Rademacher complexity are novel and based on concentration inequalities for quadratic matrix forms. In particular, our proofs does *not* use the Khintchin-Kahane type inequality that is standard in computation of the upper bounds on the Rademacher complexity; see, *e.g.*, [10],[11]. In particular, the Khintchin-Kahane type inequality yields the following upper bound on the Rademacher complexity (See Section A.2 of the supplementary materials):

$$(5.10) \quad \mathfrak{R}^n(\mathcal{F}_m(R)) \leq \frac{R}{nD\sqrt{m}} \sqrt{\frac{23}{44}} \|\Phi\|_F.$$

Since  $0 < \text{erfc}(x) \leq 1$  for  $0 < x$ , and  $\|\Phi\|_2 \leq \|\Phi\|_F$  for any feature matrix  $\Phi \in \mathbb{R}^{n \times mD}$ , the upper bound we established in Eq. (5.8) is sharper than that of Eq. (5.10). Similarly, the proof of the upper bound on the Gaussian complexity is based on the concentration of measure for  $\chi^2$  random variables.

To compute explicit bounds from the Rademacher and Gaussian complexities, we require upper and lower bounds on the matrix norms of the feature matrix  $\Phi = [\varphi^{\mathbf{w}}(\mathbf{x}_i, \boldsymbol{\xi}_j)]_{(i,j) \in [n] \times [D]}$ .

The following lemma shows that the spectra of the random matrix  $\Phi$  concentrates around the kernel matrix  $\mathbf{K}_n^{\mathbf{w}} \stackrel{\text{def}}{=} [k_{\mathcal{X}}^{\mathbf{w}}(\mathbf{x}_i, \mathbf{x}_j)]_{(i,j) \in [n] \times [n]}$  scaled by the factor  $D$ :

**Lemma 5.3.** (CONCENTRATION OF THE SPECTRA OF FEATURE MATRICES) *Suppose (A.6) holds. Consider the feature matrix  $\Phi = [\varphi^{\mathbf{w}}(\mathbf{x}_i; \boldsymbol{\xi}_j)]_{(i,j) \in [n] \times [D]} \in \mathbb{R}^{n \times D}$  and the associated kernel matrix  $\mathbf{K}_n^{\mathbf{w}} \stackrel{\text{def}}{=} [k_{\mathcal{X}}^{\mathbf{w}}(\mathbf{x}_i, \mathbf{x}_j)]_{(i,j) \in [n] \times [n]}$ . The Frobenious norm of the matrix  $\Phi$  satisfies the following concentration bound*

$$(5.11) \quad \mathbb{P} \left[ \left| \|\Phi\|_F^2 - D \cdot \text{Tr}(\mathbf{K}_n^{\mathbf{w}}) \right| \geq \delta \right] \leq 2^8 m \left( \frac{\sigma_p D n \|\mathbf{w}\|_2 \text{diam}(\mathcal{X})}{\delta} \right)^2 e^{-\frac{\delta^2}{4 D n^2 \|\mathbf{w}\|_2 (d+2)}}.$$

Furthermore, the spectral norm of the matrix  $\|\Phi\|_2$  satisfies

$$(5.12) \quad \mathbb{P} \left[ \left| \|\Phi\|_2^2 - D \cdot \|\mathbf{K}_n^{\mathbf{w}}\|_2 \right| \geq \delta \right] \leq e^{3n \log 3} 2^8 m \left( \frac{2 \sigma_p D n^2 \|\mathbf{w}\|_2 \text{diam}(\mathcal{X})}{\delta} \right)^2 e^{-\frac{\delta^2}{16 D n^2 \|\mathbf{w}\|_2 (d+2)}}.$$

*Proof.* The proof is presented in Section A.3 of the supplementary materials.  $\square$

Lemma 5.3 suggests that the spectra of the feature matrix  $\Phi$  concentrates around the spectra of the kernel matrix  $\mathbf{K}_n^{\mathbf{w}}$ . The concentration bounds in Eqs. (5.11)-(5.12) naturally follows from the point-wise estimate in Eq. (2.17) and using the standard  $\varepsilon$ -net argument.

The asymptotic analysis of the spectrum of the kernel matrices has been studied extensively in the random matrix literature; see, *e.g.*, [34] for locally smooth kernel functions, and [35], [36] for non-smooth kernel functions. Those asymptotic results are universal and consequently do not impose any conditions on the distribution of feature vectors. In the sequel, we are concerned with the non-asymptotic results for the spectrum of the Gram matrices of the mixture kernels. Naturally, the proof of non-asymptotic results require tail conditions on the feature vectors.

**Lemma 5.4.** (NON-ASYMPTOTIC BOUNDS ON THE SPECTRUM OF RADIAL KERNELS) *Suppose (A.1) and (A.2) hold.*

$$(5.13) \quad \|\mathbf{K}_n^{\mathbf{w}}\|_2 \leq \sum_{\ell=1}^m w_{\ell} \|\mathbf{K}_n^{\ell}\|_2,$$

where  $\mathbf{K}_n^{\ell} \stackrel{\text{def}}{=} [k_{\mathcal{X}}^{\ell}(\mathbf{x}_i, \mathbf{x}_j)]_{(i,j) \in [n]^2}$ . Furthermore,

- If the feature vectors  $\mathbf{X}_1, \dots, \mathbf{X}_n \sim_{i.i.d.} \mathbf{N}(0, \mathbf{I}_{d \times d})$  are independent Gaussian random variables. Then, with the probability of at least  $1 - \rho$ , the spectral norm of the mixture kernel matrix is bounded from above by

$$(5.14) \quad \|\mathbf{K}_n^{\ell}\|_2 \leq 2k_{\mathcal{X}}^{\ell}(0) + \frac{e^{2n \log 3}}{c\sqrt{2}} \max \left\{ 3n \times 2^{10} \mathbb{E}_{\mu_{\Xi}^{\ell}} \left[ \frac{1}{\|\boldsymbol{\xi}\|_2} \right] \sqrt{\ln \left( \frac{1}{\rho} \right)}, 2^8 \sqrt{\frac{n}{2}} \mathbb{E}_{\mu_{\Xi}^{\ell}} \left[ \frac{1}{\|\boldsymbol{\xi}\|_2^2} \right] \ln \left( \frac{1}{\rho} \right) \right\}.$$

In Equation (5.14),  $c > 0$  is a universal constant, and  $\mu_{\Xi}^{\ell}$  is the distribution associated with the kernel  $k_{\mathcal{X}}^{\ell}$ .

- If the feature vectors  $\mathbf{X}_1, \dots, \mathbf{X}_n$  are independent with bounded independent components  $|X_{ij}| \leq K$ ,  $i = 1, 2, \dots, n$ ,  $j = 1, 2, \dots, d$ , for some  $K > 0$ . Then, with the probability of at least  $1 - \rho$ , the spectral norm of the mixture kernel matrix is bounded from above by

**Table 1.** Summary of the benchmark data-sets from ASU data-base [39] for our empirical evaluation.

	BASEHOCK	ISOLET	ORL	PCMAC	ARCENE	warpPIE10P
Samples	1,993	1,560	400	1,943	200	210
Features	4,862	617	1,024	3,289	10,000	2,420
Classes	2	26	40	2	2	10

(5.15)

$$\left\| \mathbf{K}_n^\ell \right\|_2 \leq 2k_{\mathcal{X}}^\ell(0) + \frac{e^{2n \log 3}}{c\sqrt{2}} \max \left\{ 3n \times 2^{10} \mathbb{E}_{\mu_\Xi} \left[ \frac{1}{K \|\xi\|_2} \right] \sqrt{\ln \left( \frac{1}{\rho} \right)}, 2^8 \sqrt{\frac{n}{2}} \mathbb{E}_{\mu_\Xi} \left[ \frac{1}{K^2 \|\xi\|_2^2} \right] \ln \left( \frac{1}{\rho} \right) \right\}.$$

*Proof.* The proof is deferred to Section A.4 of the supplementary materials.  $\square$

We remark that our non-asymptotic analysis of the spectrum of kernel matrices in Lemma 5.4 generalizes those of [37] that are established for the special cases of the Gaussian and polynomial kernels. More specifically, the proof we present employs the *decoupling* technique from the random matrix theory [38] as well as a concentration of measure for Lipschitz functions of the Gaussian random variables.

We now are in position to state the main result of this section which is a generalization bound for the risk function based on the Rademacher complexity of the class of function  $\mathcal{F}_m(R)$  established by Bartlett, *et al.* [40]. Due to the space limitation, we state our results using the Rademacher complexity  $\mathfrak{R}_n(\mathcal{F}_m(R))$ . A similar generalization bound can be stated using the Gaussian complexity:

**Theorem 5.5.** (GENERALIZATION BOUNDS, [40]) *Consider a loss function  $L : \mathcal{Y} \times \mathbb{R} \rightarrow \mathbb{R}_+$  and a dominating cost function  $\ell$  in (A.3). Let  $\mathcal{F}_m(R)$  be the class of functions in Eq. (4.9)-(4.10) and let  $\{(\mathbf{X}_i, Y_i)\}_{i=1}^n$  be independently selected from the joint distribution  $P_{\mathbf{X}, Y}$ . Then, for any integer  $n$  and any  $0 < \delta < 1$ , with probability at least  $1 - \delta$  over samples of length  $n$ , every  $f$  in  $\mathcal{F}_R$  satisfies*

$$(5.16) \quad \mathbb{E}_{P_{\mathbf{X}, Y}}[L(f(\mathbf{X}), Y)] \leq \mathbb{E}_{\tilde{P}_{\mathbf{X}, Y}^n}[\ell(f(\mathbf{X}), Y)] + K\mathfrak{R}_n(\mathcal{F}_m(R)) + \sqrt{8 \ln(2/\delta)/n}.$$

where the Rademacher complexity of the class  $\mathcal{F}_m(\mathcal{R})$  is given by

$$\mathfrak{R}_n(\mathcal{F}_m(R)) \leq \frac{R}{n\sqrt{D}} \sqrt{\frac{\pi}{192}} \operatorname{erfc}(\sqrt{192D}) \|\mathbf{K}_n^w\|_2^{1/2} + \varepsilon_n,$$

with the probability of (at least)  $1 - e^{-3n \log 3} 2^8 m \left( \frac{2\sigma_p D n^2 \|\mathbf{w}\|_2 \operatorname{diam}(\mathcal{X})}{\varepsilon_n} \right)^2 e^{-\frac{\varepsilon_n^2}{16 D n^2 \|\mathbf{w}\|_2^{(d+2)}}$ , where  $\|\mathbf{K}_n^w\|_2^{1/2}$  is upper bounded by the expressions in Eqs. (5.13)-(5.15) of Lemma 5.4.  $\square$

## 6. EXPERIMENTAL EVALUATION FOR CLASSIFICATION OF REAL-WORLD DATASETS

**6.1. Evaluation Data-Set.** In this section, we carry out experiments on 12 standard benchmark tasks from the ASU feature selection website [39]. Table 1 summarizes the benchmark data sets we use for our empirical evaluation. The data sets are drawn from several domains including gene data, image data, and voice data, and span both the low-dimensional and high-dimensional regimes.



**6.2. Feature Selection.** For each classification task, we select a subset of features of size  $m$ . Performance is then measured by training a kernel SVM on the top  $m$  features. In our numerical experiments, the top  $m$  features are selected using the kernel feature selection scheme of [41]. This is done for  $m \in \{5, 10, \dots, 100\}$ .

**6.3. Implementation Details.** We implement the SVM classification and RBF sampler using Python `Sklearn` library [42], and the MMD metric using Python `Shogun` library [43]. For multi-class datasets, we use the one-versus-all rule. We implement our codes on Python 3.7 and train our models on NVIDIA Titan V100 32GB graphics processing units (GPU). In all experiments, we fix the regularization constant of the SVM to  $\lambda = 1$ .

**6.4. Numerical Results.** In the first set of experiments, we first fix the number of features to  $m = 100$ , and compute the best value for the bandwidth  $\gamma$  of the Gaussian RBF kernel  $k_{\mathcal{X}}(\mathbf{x}, \mathbf{y}) = \exp(-\gamma\|\mathbf{x} - \mathbf{y}\|_2^2)$  from the set of base values ranging from  $10^{-20}$  to  $10^3$ .

In Figure 1, we demonstrate the bandwidth selection using the 5-fold cross validation, and the two-sample test via  $U$ -statistics as defined in Eq. (4.6). The blue curves in Figure 1 are associated with the 5-fold cross validation (CV), averaged over 20 different validation sets. More specifically, for each blue curve, we compute the accuracy of the SVM classifier for 20-trials on different validation sets and average the result. Accordingly, the blue hulls around each blue curve in Figure 1 shows the 95% confidence intervals. Moreover, the red curves denote MMD values in conjunction with the empirical conditional measures defined in Eq. (4.4), using the  $U$ -statistics in Eq. (4.6).

From Figures 1 (a)-(b)-(d), we observe a good agreement in the selected bandwidth using the 5-fold cross-validation and the MMD attained via the  $U$ -statistic in Eq. (4.6). However, evaluating  $U$ -statistics is significantly faster than the cross-validation as it is independent of the SVM classifier and thus does not involve training. Figures 1 (a)-(b)-(d) corresponding have a small number of features and/or a small number of classes. However, for high-dimensional data-sets with a large number of features or classes, such as `ORL`, `ARCENE`, and `wrapPIE10P` in Figures 1 (c)-(e)-(f), there are discrepancies between the bandwidth selected using the cross-validation and the MMD scores.

Nevertheless, the accuracies of the kernel SVM attained on the associated test data-sets are comparable as demonstrated in Figures 2 (c)-(e)-(f). In Figure 2, both the blue and the red curves correspond to the kernel SVM with a single Gaussian RBF kernel, where the bandwidth of the kernel is selected based on the cross-validation, and the highest MMD score, respectively. The green curves in Figure 2 correspond to the kernel SVM using multiple kernels as characterized in Eq. (4.7). We also note that for easier data-sets such as `PCMAC`, our proposed multiple kernel learning approach outperforms the cross-validation as demonstrated in Figure 2-(b).

## 7. APPLICATION TO THE SEMANTIC SEGMENTATION OF BIOMEDICAL IMAGES

Equipped with the theoretical framework for kernel learning in Section 3, here we propose a new architecture for the semantic segmentation of biomedical images.

**7.1. Background on the Semantic Segmentation.** Semantic Segmentation refers to the process of associating each pixel of an image with a class label, and has extensive applications in precision medicine for the development of computer-aided diagnosis based on radiological images with different modalities such as magnetic resonance imaging (MRI), computed tomography (CT), or colonoscopy images. Semantic segmentation is also crucial

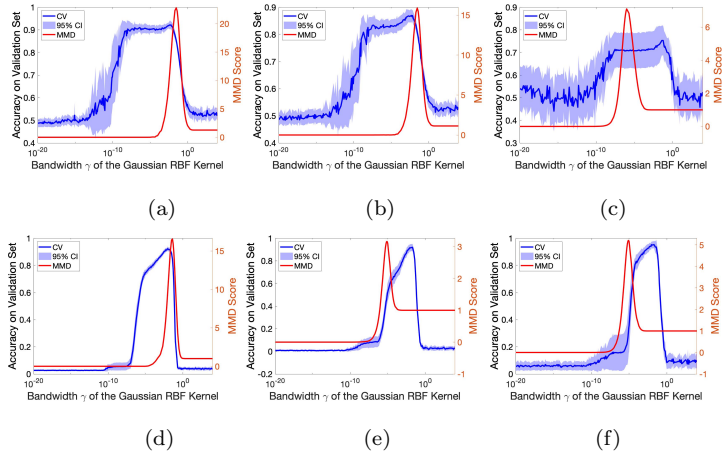


**Figure 1.** Model Selection for the bandwidth parameter  $\gamma = 1/2\varrho^2$  of the Gaussian RBF kernels  $k_{\mathcal{X}}(\mathbf{x}, \mathbf{y}) = \exp(-\gamma\|\mathbf{x} - \mathbf{y}\|_2^2)$  using the 5-fold cross-validation and the two-sample test. Blue hulls around each curve shows the 95% confidence intervals from 20 trials of the cross-validation on different validation sets. Panel (a): BASEHOCK, Panel (b): PCMAC, Panel (c): ARCENE, Panel (d): ISOLET, Panel (e): ORL, Panel (f):warpPIE10P.

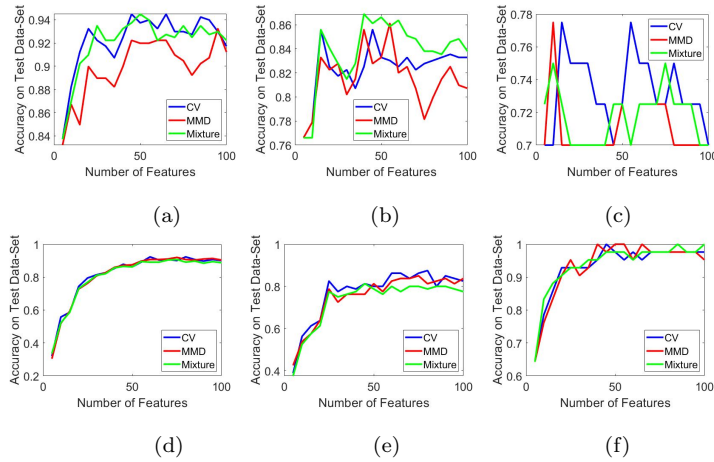


**Figure 2.** Classification accuracy of the kernel SVMs on the test data-set using the the Gaussian RBF kernel  $k_{\mathcal{X}}(\mathbf{x}, \mathbf{y}) = \exp(-\gamma\|\mathbf{x} - \mathbf{y}\|_2^2)$ . The bandwidth  $\gamma$  of the trained SVM classifier is selected using the cross-validation (blue), MMD score (red), and the mixture model in Eq. (4.7) (green). Panel (a): BASEHOCK, Panel (b): PCMAC, Panel (c): ARCENE, Panel (d): ISOLET, Panel (e): ORL, Panel (f):warpPIE10P.

for complete scene understanding and to infer knowledge from imagery which is the principal objective of the field of the computer vision.

In recent years, deep artificial neural networks (ANNs) and, in particular, deep convolutional neural networks (CNNs) have achieved the state-of-the-art performance for the semantic segmentation of natural images; see, *e.g.*, [44, 45, 46]. This success is largely due

to the paradigm shift from manual to automatic feature extraction enabled by large representational capacity of deep learning networks. Such automatic feature extraction is guided by a large amount of training data accessible in public datasets, the archetype of which are *CIFAR-10*, *CIFAR-100*, and *ImageNet*. These datasets collectively contain millions of annotated samples from natural images. In contrast, extracting, harvesting, and building large-scale annotated data-sets in medical imaging is extremely challenging as it requires extensive clinical expertise. Therefore, training deep networks on clinical images can often be cumbersome due to the lack of databases that are adequately sized to satisfy the needs of the deep learning models. Without sufficient training samples, deep architectures with the expressiveness of *ResNet* [46], *AlexNet* [47], *VGGNet* [48], and *GoogLeNet* [49], often dramatically overfit the dataset, even with generic regularization strategies such as dropout [50], sparse regularization of the network [51], and model averaging [52]. In addition, deep learning networks trained on a small dataset often fail to extract salient features that are crucial for pattern classification due to presence of noisy or irrelevant features.

In contrast, the kernel support vector machines (SVMs) are sample efficient learning algorithms in which representations are generated using a set of pre-specified filters. Contrary to deep learning models, the kernel SVMs are transparent learning models whose theoretical foundations are grounded in the extensive statistical machine learning literature; see [53] and references therein for a survey of theoretical results. However, to improve the accuracy of the kernel-based learning algorithms, the following two challenges must be addressed:

First, although the kernel SVMs are typically formulated in terms of convex optimization problems, which have a single global optimum and thus do not require heuristic choices of learning rates, starting configurations, or other hyper-parameters, there are statistical model selection problems within the kernel approach arising from the choice of the kernel. In practice, it can be difficult for the practitioner to find prior justification for the use of one kernel instead of another. It would be more desirable to explore data-driven mechanisms that allow kernels to be chosen automatically.

Second, the kernel SVMs have been traditionally employed in conjunction with the hand-crafted features such as SIFT or Daisy type descriptors [54, 55]. Such hand crafted descriptors are unable to capture semantic representations and are less powerful in extracting semantic features compared to their deep learning counterparts [56]. In addition, the manual design of such hand crafted feature maps requires extensive prior knowledge about the underlying imaging domain.

To address the first challenge, we leverage the kernel learning approach we proposed in Section 4. To circumvent the second challenge, we consider two mechanisms for generating representations from input images. In the first mechanism, we use the VGG network that is pre-trained on natural images from CAIFAR data-set as a generic feature extractor in conjunction with a kernel feature selection method. In the second mechanism, we use a scattering convolution network [15] to generate feature maps. Figure 6 shows the proposed segmentation network. In the sequel, we provide detailed description of each component of this network.

**7.2. Feature Extraction via Pre-trained VGG Net and Scattering Convolution Networks (SCN).** We consider two feature extraction mechanisms, namely one based on ensemble of filters generated by a pre-trained VGG-net on natural images, and another based on scattering convolution neural networks due to Bruna and Mallat [15]. In the sequel, we describe both feature extractors in details.

7.2.1. *Pre-trained VGG-Net.* We use a pre-trained VGG-Net as a generic feature extractor. Specifically, we extract the filters of a pre-trained VGG net from all of its layers (thirteen layers) to build a filter bank consisting of 4224 filters.

It is important to differentiate our approach from domain adaptation [57] and transfer learning [58] paradigms. In those approaches, a deep learning network such as the VGG Net or AlexNet is trained on a different dataset such as natural images. Then, the *entire* network is employed to classify images on a different dataset such as medical imaging.

In contrast, in our approach we only use the convolutional filters of a pre-trained VGG network to extract representation from our data. From this perspective, the VGG network can be thought of as a generic filter bank. As depicted in Figure 6, the extracted representations from the filter bank is further processed before supplying them to the linear SVM for classification.

7.2.2. *Scattering Convolution Networks (SCNs).* The scattering convolution networks (SCNs) were proposed by and further generalized by Wiatowski and Bolcskei [59]. Scattering convolution network computes a translation invariant image representation, which is stable to deformations and preserves high frequency information for classification. It cascades wavelet transform convolutions with non-linear modulus and averaging operators. The first network layer outputs SIFT-type descriptors, whereas the next layers provide complementary invariant information which improves classification.

The basic building blocks of the feature extractor we described in this section consists of a convolutional transforms with a set of pre-specified structured filters, non-linearity, and pooling operation. In what follows, we first review each building block. We then describe the architecture of the network.

- *Convolutional Transform:* The network we consider consist of  $d$  convolutional layers. Each layer applies a convolutional transform that is made up of a set of pre-specified structured filters  $\Psi_{\Lambda_n} = \{g_{\lambda_n}\}_{\lambda_n \in \Lambda_n}, n = 1, 2, \dots, d$  to generate different representations of input image. The finite index set  $\Lambda_n$  is a collection of scales, directions, or frequency-shifts, and  $g_{\lambda_n}$  are the corresponding atoms of the filters that can be different in each layer.

As an example, consider the two dimensional Gabor wavelet filters. Let  $j \in \mathbb{Z}$  denotes an integer,  $R_\vartheta \in \text{SO}(2)$  a rotation element from the rotation group  $\text{SO}(2)$ , represented by the matrix

$$(7.1) \quad R_\vartheta = \begin{bmatrix} \cos \vartheta & \sin \vartheta \\ -\sin \vartheta & \cos \vartheta \end{bmatrix},$$

where  $\vartheta = k\pi/K$ , and  $K$  is the total number of orientations.

Then,  $\lambda = mk \in \Lambda \stackrel{\text{def}}{=} \mathbb{Z} \times \{0, 1, 2, \dots, K-1\}$ , and the wavelet filters are specified by

$$(7.2) \quad \psi_{mn}(x, y) = 2^{-j} \psi(\tilde{x}, \tilde{y}),$$

where  $\tilde{x} = 2^{-j}(x \cos(\vartheta) + y \sin(\vartheta))$ ,  $\tilde{y} = 2^{-j}(-x \cos(\vartheta) + y \sin(\vartheta))$ , and the scale factor  $2^{-j}$  ensures that the energy is independent of  $j$ .

Moreover,  $\psi$  is the mother wavelet. We consider two types of wavelet frameworks:

(i) *Garbor Filters:* The atom of the Garbor filter is specified on 2D spatial domain by the following equation

$$(7.3) \quad \psi(x, y) = \frac{1}{2\pi\sigma_x\sigma_y} \exp\left(-\frac{1}{2}\left(\frac{x^2}{\sigma_x^2} + \frac{y^2}{\sigma_y^2}\right) + 2\pi j W x\right),$$

with the following Fourier transform

$$(7.4) \quad \widehat{\psi}(u, v) = \exp\left(-\frac{1}{2} \left[ \frac{(u - W)^2}{\sigma_u^2} + \frac{v^2}{\sigma_v^2} \right]\right).$$

Figure 4 depicts the constructed Garbor wavelet filters  $\psi_{mn}(x, y)$  by scaling and rotating the mother wavelet  $\psi$  specified in Eq. (7.3). It is known that the continuous Garbor transform has the ability to identify the singularities of a signal. In fact, if a function  $f \in L^2(\mathbb{R}^2)$  is smooth apart from a discontinuity at a point, say  $(x_0, y_0)$ , then the continuous Garbor transform  $\langle \psi, f \rangle_{L^2(\mathbb{R})}$  decays rapidly except near  $(x_0, y_0)$  [60]. This property is useful to identify the set of points where  $f$  is not regular, and explains the ability of the continuous Garbor transform to detect edges.

(ii) *Shearlets*: In most multivariate problems, important features of the considered data are concentrated on lower dimensional manifolds. For example, in image processing an edge is an 1D curve that follows a path of rapid change in image intensity. Shearlets provide efficient tools for analyzing the intrinsic geometrical features of a signal using anisotropic and directional window functions [61]. Classical Shearlets are defined as follows. Let  $\psi \in L^2(\mathbb{R}^2)$  be defined by

$$(7.5) \quad \psi(x, y) = \psi_1(x)\psi_2(y/x),$$

where  $\psi_1 \in L^2(\mathbb{R})$  is a discrete wavelet in the sense that it satisfies the discrete Calderón condition, given by

$$(7.6) \quad \sum_{j \in \mathbb{Z}} |\psi_1(2^{-j}x)|^2 = 1,$$

almost everywhere  $x \in \mathbb{R}$ , and  $\psi_1 \in C^\infty(\mathbb{R})$  and  $\text{supp}\psi_1 \in [-\frac{1}{2}, -\frac{1}{16}] \cup [-\frac{1}{16}, \frac{1}{2}]$ . Furthermore,  $\psi_2 \in L^2(\mathbb{R})$  is a *bump* function in the sense that

$$(7.7) \quad \sum_{k=-1}^1 |\psi_2(y+k)|^2 = 1,$$

almost everywhere  $y \in [-1, 1]$ , satisfying  $\psi_2 \in C^2(\mathbb{R})$  and  $\text{supp}(\psi_2) \subset [-1, 1]$ .

Figure 5 demonstrates the constructed Shearlets from the prescribed atom in Eq. (7.5).

Now, we have the following definition:

**Definition 7.1.** (CONVOLUTIONAL SET) Let  $\Lambda$  denotes a finite set. The collection  $\Psi_\Lambda = \{g_\lambda\}_{\lambda \in \Lambda}$  is called a convolutional set with Bessle bound  $B \geq 0$  if

$$(7.8) \quad \sum_{\lambda_d \in \Lambda_d} \|f \star g_{\lambda_d}\|_2^2 \leq B \|f\|_2^2.$$

- *Non-Linearity*: A pointwise non-linearity  $\rho_n : \mathbb{R} \rightarrow \mathbb{R}$  that is Lipschitz  $|\rho(x) - \rho(y)| \leq L|x - y|, \forall x, y \in \mathbb{R}$  is applied after each convolution layer. Some examples of non-linearities are as follows:

- (1) *Hyperbolic Tangent*: The non-linearity is defined as  $\rho(x) = \frac{e^x - e^{-x}}{e^x + e^{-x}}$ , and has the Lipschitz constant  $L = 2$ .
- (2) *Rectified Linear Unit*: The non-linearity is defined by  $\rho(x) = \max\{0, x\}$  with Lipschitz constant  $L = 1$ .
- (3) *Modulus*: The non-linearity is defined as  $\rho(x) = |x|$ , and has the Lipschitz constant  $L = 1$ .



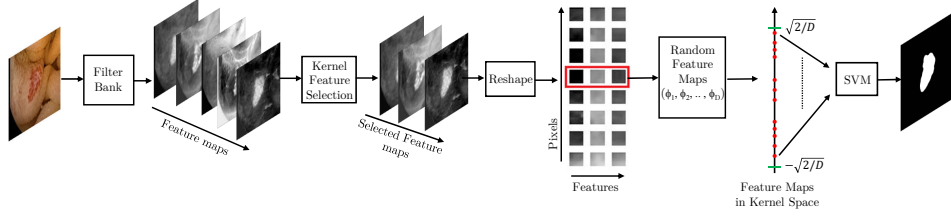


**Figure 6.** The architecture of the proposed kernel-based segmentation network, using a filter bank (either the VGG or the SCN filters) in conjunction with the kernel feature selection to generate semantic representations. Random feature maps  $\varphi_1, \dots, \varphi_D$  are sampled from a distribution that is learned in a data-driven manner from the input training images.

for  $n \in \{0, 1, 2, \dots, N_{d+1}\}$ .

We now have all the ingredients to formally define the notion of a module sequence:

**Definition 7.2.** (MODULE SEQUENCE) For network layers  $n$ ,  $1 \leq n \leq d$ , let  $\Psi_n = \{g_{\lambda_n}\}_{\lambda_n \in \Lambda_n}$  be a convolutional set,  $\rho_n : \mathbb{R} \rightarrow \mathbb{R}$  a point-wise Lipschitz-continuous non-linearity, and  $P_n : \mathbb{R}^{N_n} \rightarrow \mathbb{R}^{N_{n+1}}$  a Lipschitz-continuous pooling operator with  $N_{n+1} = N_n/S_n$ , where  $S_n \in \mathbb{N}$  denotes the pooling factor  $S_n$  in the  $n$ -th layer. Then, the sequence of triplets  $\Omega \stackrel{\text{def}}{=} (\Psi_n, \rho_n, P_n)_{1 \leq n \leq d}$  is called a *module-sequence*.

Consider the module  $\Omega = (\Psi_n, \rho_n, P_n)_{1 \leq n \leq d}$ , and a path of index  $p_n \stackrel{\text{def}}{=} (\lambda_1, \dots, \lambda_n) \in \Lambda_1^n \stackrel{\text{def}}{=} \prod_{i=1}^n \Lambda_i$  of length  $n$ . The output of the  $n$ -th layer is computed according to

$$(7.9) \quad U[p_n](f) \stackrel{\text{def}}{=} U[\lambda_n] \cdots U[\lambda_2] U[\lambda_1](f),$$

where the scattering propagators are defined as below

$$(7.10) \quad U[\lambda_i]f \stackrel{\text{def}}{=} P_i(\rho_i(f \star g_{\lambda_i})), \quad i = 1, 2, \dots, n.$$

For the empty path  $e \stackrel{\text{def}}{=} \emptyset$  we let  $U[e]f \stackrel{\text{def}}{=} f$ . The feature map of the  $n$ -th layer is computed by

$$(7.11) \quad S_n[p_n](f) = U[p_n](f) \star \chi_n,$$

where  $\chi_n$  is the output generating atom. In particular, when  $\chi_n = \delta_n$  is Dirac's delta function concentrated at zero, the feature map is the same as the output of each layer, *i.e.*,  $S_n[p_n] = U[p_n]$ . Moreover, by letting  $\chi_n = 0$ , a particular feature map can be eliminated  $S_n[p_n] = 0$ . See Figure 3 for the diagram of the scattering propagator, and Figures 4 and 5 for some examples of the Garbor filters generated by the scattering network.

**Definition 7.3.** (FEATURE EXTRACTOR) Let  $\Omega \stackrel{\text{def}}{=} (\Psi_d, \rho_n, P_n)_{1 \leq n \leq d}$  be a given module sequence. The feature extractor  $T_\Omega$  based on the map  $\Omega$  is a map from  $L^2(\mathbb{R})$  to its feature vector, defined by

$$(7.12) \quad T_\Omega(f) \stackrel{\text{def}}{=} \cup_{k=0}^d T_\Omega^k(f),$$

where  $T_\Omega^k(f) \stackrel{\text{def}}{=} \{U[p_n] \star \chi_n\}_{p_n \in \Lambda_1^k}$ .

Let  $f = (f_{ij}) \in \mathbb{R}^{n \times m}$  denotes the input image, where  $f_{ij}$  denotes the  $(i, j)$ -th pixel of the input image. The feature vector  $\mathbf{x}_{ij} \in \mathbb{R}^D$  associated with the pixel  $f_{ij}$  can be obtained by stacking the feature maps generated in each layer of the scattering network. Formally, we define

$$(7.13) \quad \mathbf{x}_{ij} \stackrel{\text{def}}{=} (T_\Omega(f))_{ij}.$$

Stacking features from different layers of the scattering network is similar to the *skip architecture* in CNNs that is often used to overcome the loss of locality caused by sub-sampling and pooling operations, see [44] for details.

**7.3. Kernel Feature Selection in the Feature Space.** Although the deep layers of VGG network generates random features that are generic and independent of the segmentation task, the lower layers generate representations that are potentially dependent on the training dataset (here natural images), and are unsuitable for segmentation of colonoscopy images. In addition, VGG networks produces

Kernel feature selection proposed by Chen *et al.* [41] select a subset of generated representations. In particular, it employs kernel-based measures of independence to find a subset of covariates that is maximally predictive of the response. Let  $\boldsymbol{\omega} \in \{0, 1\}^d$  denotes a vector that indicates which feature is active. Let  $k_{\mathcal{X}}(\cdot, \cdot)$  denotes the kernel that is learned from data using Algorithm of . The algorithm in [41] proposes to minimize the following integer programming optimization problem

$$(7.14a) \quad \min_{\boldsymbol{\omega}} \mathbf{y}^T (G_{\boldsymbol{\omega} \odot \mathbf{X}} + d\varepsilon_d \mathbf{I}_d)^{-1} \mathbf{y}$$

$$(7.14b) \quad \text{s.t. : } \omega_i \in \{0, 1\}, \quad i = 1, 2, \dots, d,$$

$$(7.14c) \quad \mathbf{1}_d^T \boldsymbol{\omega} = m,$$

where  $G_{\boldsymbol{\omega} \odot \mathbf{X}}$  is the centralized version of the kernel matrix  $\mathbf{K}_{\boldsymbol{\omega} \odot \mathbf{X}}$  with  $(K_{\boldsymbol{\omega} \odot \mathbf{X}_{ij}}) = k_{\mathcal{X}}(\boldsymbol{\omega} \odot \mathbf{x}_i, \boldsymbol{\omega} \odot \mathbf{x}_j)$ .

We then approximate the problem (7.15) by relaxing the domain of  $\boldsymbol{\omega}$  to the unit hypercube  $[0, 1]^d$  and replacing the equality constraint with an inequality constraint, *i.e.*,

$$(7.15a) \quad \min_{\boldsymbol{\omega}} \mathbf{y}^T (G_{\boldsymbol{\omega} \odot \mathbf{X}} + d\varepsilon_d \mathbf{I}_d)^{-1} \mathbf{y}$$

$$(7.15b) \quad \text{s.t. : } 0 \leq \omega_i \leq 1, \quad i = 1, 2, \dots, d,$$

$$(7.15c) \quad \mathbf{1}_d^T \boldsymbol{\omega} \leq m.$$

The optimization problem in Eq. (7.15) can be solved efficiently via gradient descent. A solution to the relaxed problem is then converted back into a solution for the original problem by setting the  $m$  largest values of  $\boldsymbol{\omega}$  to 1 and remaining values to 0.

Since we employ random features, we use the following approximation in [41],

$$(G_{\boldsymbol{\omega} \odot \mathbf{X}} + d\varepsilon_d \mathbf{I}_d)^{-1} \approx \frac{1}{\varepsilon_n n} (\mathbf{I} - \mathbf{V}_{\boldsymbol{\omega}} (\mathbf{V}_{\boldsymbol{\omega}}^T \mathbf{V}_{\boldsymbol{\omega}} + \varepsilon_n n \mathbf{I}_D)^{-1} \mathbf{V}_{\boldsymbol{\omega}}^T),$$

where  $\mathbf{V}_{\boldsymbol{\omega}} = (\mathbf{I} - \mathbb{I}^T/n) \boldsymbol{\varphi}^T$ , where  $\boldsymbol{\varphi} \in \mathbb{R}^{n \times D}$ .

**7.4. Random Fourier Features with Kernel-Target Alignment.** To approximate the RBF kernel, we use the setup of random Fourier features of Rahimi and Recht [2]. In particular, let  $\boldsymbol{\xi}_k = (\mathbf{v}_k, w_k) \sim \mathbf{N}(\mathbf{0}, \mathbf{I}_d) \times \text{Uni}[0, 2\pi]$ , and consider the feature vector  $\boldsymbol{\varphi}(\mathbf{x}_{ij}) \stackrel{\text{def}}{=} (\varphi_1(\mathbf{x}_{ij}), \dots, \varphi_D(\mathbf{x}_{ij}))$ , where  $\varphi_k(\mathbf{x}_{ij}) \stackrel{\text{def}}{=} \varphi(\mathbf{x}_{ij}, \boldsymbol{\xi}_k)$ ,  $k = 1, 2, \dots, D$ .



Each element of the random feature vector is generated according to

$$(7.16) \quad \varphi(\mathbf{x}_{ij}; \boldsymbol{\xi}_k) \stackrel{\text{def}}{=} \sqrt{\frac{2}{D}} \cos\left(\frac{1}{2\varrho^2} \langle \mathbf{x}_{ij}, \mathbf{v}_k \rangle + w_k\right),$$

for all  $k = 1, 2, \dots, n$ . To determine the value of the bandwidth  $\gamma = \frac{1}{2\varrho^2}$ , we use a set of base RBF kernels  $k_{\chi^i}(\mathbf{x}_i, \mathbf{x}_j) = \exp(-\gamma_i \|\mathbf{x}_i - \mathbf{x}_j\|_2^2)$ , where  $\gamma_i = 10^{2i-2}$ ,  $i = -4, \dots, 4$ . We then invoke the procedure in Section 4 to compute the best set of mixtures and compute the optimal parameter  $\boldsymbol{\theta}$  of the mixture class.

In Figure 7, we illustrate the three dimensional visualization of the random feature maps in the kernel space, using the  $t$ -SNE plot [62]. To enhance the visualization, we have cropped the selected image and retained a balanced numbers of pixels from each class label. From Figure 7, we clearly observe the effect of the bandwidth parameter  $\gamma = \frac{1}{2\varrho^2}$  on the accuracy of the kernel-based segmentation architecture.

In particular, as we observe from Figures 7 (c) – (d), choosing an unsuitable bandwidth parameters of  $\gamma = 0.1$  and  $\gamma = 1$  significantly degrades the classification accuracy, and results in a mixture of two classes that can not be separated by the downstream linear SVMs. The sensitivity of classification accuracy to the value of the bandwidth  $\gamma$  also highlights the importance of our kernel selection approach, as outlined in Section 4, to automating the kernel selection process.

**7.5. The Linear SVM Classifier.** In the last layer of our proposed network, we train a linear SVM classifier. Specifically, we solve the following optimization problem over all the training samples  $(y_{ij}, f_{ij})_{(i,j) \in [I] \times [J]}$ ,

$$(7.17) \quad \min_{(b, \boldsymbol{\beta}) \in \mathbb{R} \times \mathbb{R}^n} \frac{1}{n} \sum_{i,j} \left[ 1 - y_{ij} \left( \sum_{k=1}^D \beta_k \varphi((T_{\Omega}(f))_{ij}, \boldsymbol{\xi}_k) + b \right) \right]_+ + \frac{\lambda}{2} \|\boldsymbol{\beta}\|_2^2,$$

where  $b$  is an offset term. Let  $(b^*, \boldsymbol{\beta}^*)$  denotes the optimal solution of the optimization problem in Eq. (7.17).

For a new input image  $\tilde{f} = (\tilde{f}_{ij})_{(i,j) \in [I] \times [J]}$ , we generate a class label  $\tilde{y}_{ij} \in \{-1, +1\}$  using

$$(7.18) \quad \tilde{y}_{ij} = \text{sgn} \left[ \sum_{k=1}^D \beta_k^* \varphi((T_{\Omega}(\tilde{f}))_{ij}, \boldsymbol{\xi}_k) + b^* \right],$$

where  $\text{sgn}$  is the sign function.

## 8. EVALUATION OF SEGMENTATION ARCHITECTURES FOR ANGIODYSPLASIA SEGMENTATION

In this section, we present the segmentation results for Angiodysplasia segmentation from colonoscopy images obtained by the architectures described in the previous section.

**8.1. Data Set and Pre-processing Steps.** We use GIANA challenge data-set for Angiodysplasia detection. The annotated data-set consists of 600 images for training and 600 hundreds for testing. Each set is composed of 300 images presenting with Angiodysplasia and an other set of 300 without pathology.

To demonstrate the performance of our architectures for a small datasets, we limit our experiments to 300 images with Angiodysplasia for training and testing. To accelerate the training phase, we cropped the images of size  $576 \times 576$  to the size  $240 \times 320$  while preserving the pathologic regions of each image.

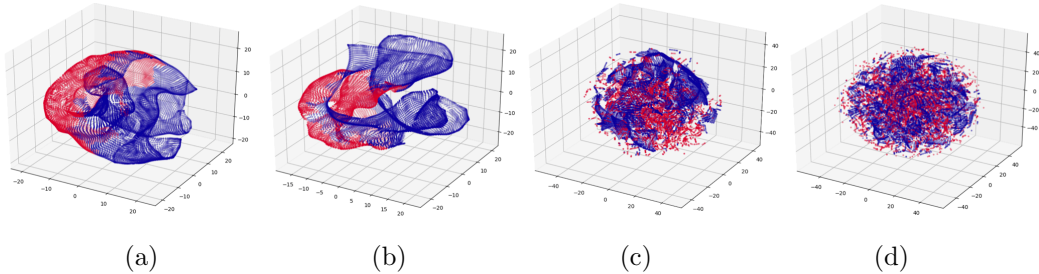


**Figure 7.** Visualization of the random feature maps in three dimensions, using the  $t$ -SNE plot [62], and for different bandwidth parameters  $\gamma \stackrel{\text{def}}{=} 1/2\sigma^2$  of the Gaussian RBF kernel. To generate the feature maps, the pre-trained VGG network is used. The red and blue regions correspond to the random feature maps generated by the pixels from each class label in a sampled colonoscopy image, respectively. Panel (a):  $\gamma = 10^{-6}$ , Panel (b):  $\gamma = 10^{-3}$ , and Panel (c):  $\gamma = 0.1$ , Panel (d):  $\gamma = 1$ .

**8.2. Training and Testing Implementations.** To demonstrate the effect of the size of training samples on the performance of our proposed networks, we divide our dataset of 300 images to various portions for testing and training. In particular, we consider the

We implement our codes on Python 3.7 and train our models on NVIDIA Titan V100 32GB graphics processing units (GPUs). To train the deep learning model described in the sequel, the Adam optimizer [63] is used with the momentum parameter  $\beta_1 = 0.9$  and  $\beta_2 = 0.999$ , mini-batch sizes of  $L_b = 4$  image for small training data-set. The initial learning rate is  $\mu = 10^{-4}$ . We implement the SVM classification and RBF sampler using Python Sklearn library [42], and the MMD metric using Python Shogun library [43].

**8.3. Comparison Benchmark.** FCN [16] is a popular convolutional type network for the image segmentation. The network architecture of FCN is

We compare our networks with FCN for Angiodysplasia segmentation and evaluate their performances. To quantify the foregoing performance comparison, we define the mean *Intersection-over-Union* (IoU) score as follows: consider an input image with  $\mathcal{S}$  pixels. Let  $n_{ij}$  be the number of pixels of class  $i$  predicted to belong to class  $j$ . The mean IoU score for semantic segmentation is defined as follows (see [16])

$$(8.1) \quad M_{\text{IoU}} \stackrel{\text{def}}{=} \frac{1}{2} \frac{n_{11}}{n_{12} + n_{21} + n_{11}} + \frac{1}{2} \frac{n_{22}}{n_{12} + n_{21} + n_{22}}.$$

**8.4. Segmentation Results.** In Figures 8 and 9, we illustrate the segmentation results for four sampled images from the GIANA challenge data-set, using FCN and our proposed architecture in Figure 6. We train both networks on one percent of the data-set to showcase the ability of our proposed architecture in coping with small training sample sizes.

Figure 8 shows the segmentation results, using the FCN architecture [16]. The middle row corresponds to the heat map generated from the soft-max output of the FCN. In addition, the bottom row shows the the heat map of the residual image, computed as the absolute difference between the generated segmentation map and the ground truth. From Figure 8 (a)-(c), we observe that while FCN correctly locates the swollen blood vessels from the surrounding tissues, the segmentation results is rather poor as can be seen in the bottom

---

The Python codes of the experiments in this section can be found on our Github repository.

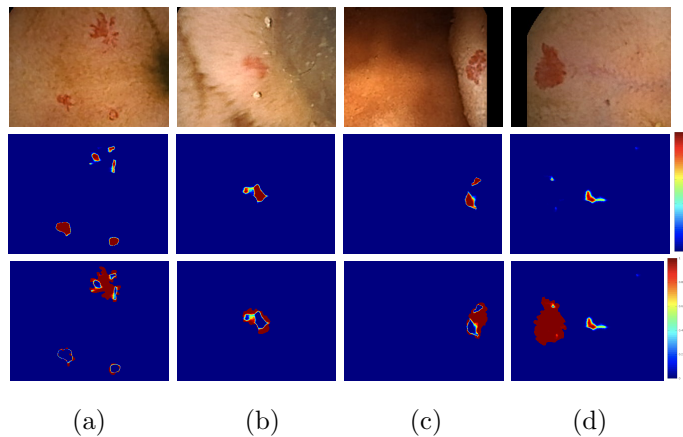


**Figure 8.** Segmentation of Angiodysplasia colonoscopy images generated by FCN [16] on sampled test images from the GIANA challenge dataset. Top: the colonoscopy images obtained using Wireless Capsule Endoscopy (WCE), Middle: the heat maps depicting the soft-max output of FCN, Bottom: the heat map of the residual image computed as the absolute difference between the proposed segmentation and the ground truth. Due to training on a small data-set, FCN tends to overfit and does not generalize well to the test dataset.

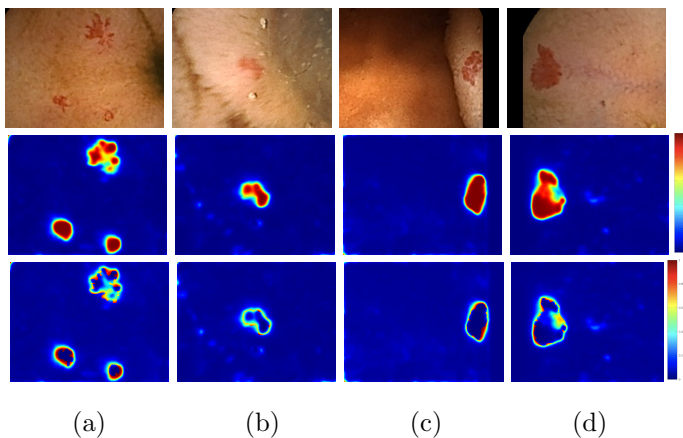


**Figure 9.** Segmentation of Angiodysplasia colonoscopy images on sampled test images from the GIANA challenge dataset, generated via the kernel SVM using the VGG filter bank with the kernel feature selection. The bandwidth of RBF kernel  $1/2\sigma^2$  is selected via maximum mean discrepancy optimization. Top: the colonoscopy images obtained using Wireless Capsule Endoscopy (WCE), Middle: the heat maps depicting the soft-max of SVM kernel classifier, Bottom: the heat map of the residual image computed as the absolute difference between the proposed segmentation and the ground truth. Despite training on a small data-set, the kernel SVM performs well on the test data set.

row of Figure 8. In the case of Figure 8 (d), the FCN almost entirely misses the swollen blood vessels.

Figure 8 illustrates the segmentation results for the same images using kernel SVM architecture. Here, the heat maps are generated via the soft-max function (*a.k.a.* the inverse

**Table 2.** Comparison between the cross-validation (CV) and the statistical two-sample test for model selection associated with the choice of bandwidth in Gaussian RBF kernels.

Bandwidth	Cross-Validation		Two Sample Test	
	$M_{\text{IoU}}$ (VGG)	$M_{\text{IoU}}$ (SCN)	$D_{k_{\chi}}^{\text{MMD}}$ (VGG)	$D_{k_{\chi}}^{\text{MMD}}$ (SCN)
$\gamma = 10^{-8}$	0.686	0.436	8.068	$3.830 \times 10^{-4}$
$\gamma = 10^{-6}$	<b>0.697</b>	0.542	<b>127.106</b>	11.114
$\gamma = 10^{-4}$	0.667	<b>0.618</b>	9.796	<b>26.880</b>
$\gamma = 10^{-2}$	0.584	0.514	1.996	5.518
$\gamma = 1$	0.293	0.299	1.0596	1.000
$\gamma = 10^2$	0.298	0.297	1.000	1.000
$\gamma = 10^4$	0.300	0.298	1.000	1.000
$\gamma = 10^6$	0.301	0.299	1.000	1.000

logit function) of the kernel SVM classifier, *i.e.*, for each pixel, we generate the output

$$(8.2) \quad \text{logit}^{-1} \left( \frac{1}{\sqrt{D}} \boldsymbol{\beta}^T \boldsymbol{\varphi}(\mathbf{x}) \right) \stackrel{\text{def}}{=} \frac{\exp \left( \frac{1}{\sqrt{D}} \boldsymbol{\beta}^T \boldsymbol{\varphi}(\mathbf{x}) \right)}{1 + \exp \left( \frac{1}{\sqrt{D}} \boldsymbol{\beta}^T \boldsymbol{\varphi}(\mathbf{x}) \right)}.$$

We observe from Figure 8 that the segmentation results from the kernel SVM outperforms those of FCN. Moreover, while FCN misses the bleeding region in Figure 8-(d), the SVM network produces a correct segmentation.

In Figure 10, we illustrate the jitter plots as well as box plots for the mean IoU scores defined in Eq. (8.1) for the kernel SVM network as well as FCN on the test data-set. We use different training sample sizes for each plot as reported in Section 8.2 to evaluate the performance of each network. We observe that on a small training data-set, the kernel SVM achieves higher IoU scores than the deep learning network. This due to the fact that fewer hyper-parameters are need to be determined during the training phase of the kernel SVM. In contrast, due to the a large number of hyper-parameters that must be determined in FCN from a small training sample size, the network is prone to over-fitting, even with regularization techniques such as drop-out.

From Figure 10, we also observe that increasing the training sample size does not change the performance of kernel SVMs significantly as the hyper-parameters of the classifiers converge to their optimal values very quickly with a few training samples. In contrast, due to the large representational capacity of deep learning network and due to a large number of hyper-parameters in the network, increasing the number of training samples significantly improves the performance of FCN.

In Table 2, we compare the performance of the 5-fold cross-validation and the two-sample test for the bandwidth selection for the Gaussian RBF kernels. We observe that both model selection methods choose the same bandwidth parameter, namely,  $\gamma = 10^{-6}$  for the VGG filter bank, and  $\gamma = 10^{-4}$  for the SCN filter bank. Nevertheless, the proposed two-sample test can be computed independent of the SVM classifier and as such it can be carried out quickly and efficiently. Furthermore, in contrast to the cross-validation method, the two-sample test does not require.

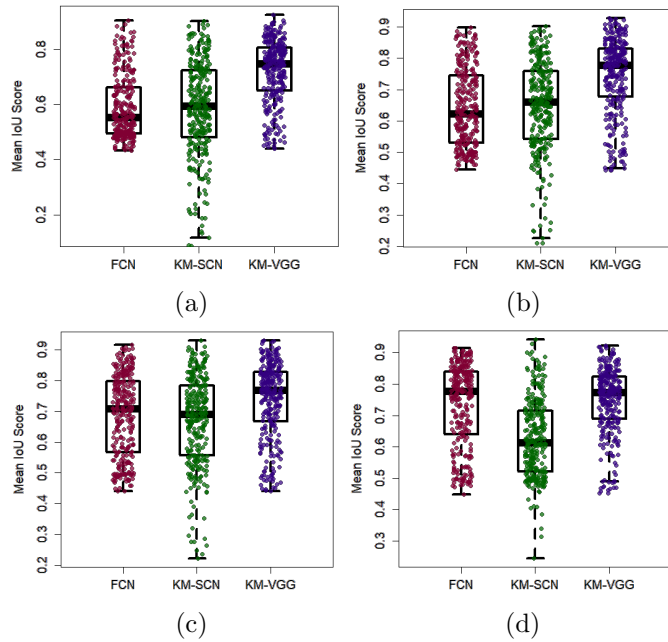


**Figure 10.** Comparison of the mean IoU score  $M_{IoU}$  for FCN [16] (the red color), the kernel SVM with SCN filter bank (the green color), and the kernel SVM with VGG filter bank (the blue color) on the test dataset. To tune the parameters of the Gaussian RBF kernel, the two-sample test is performed. Each plot correspond to the performance of networks that are trained on different sample sizes. Panel (a): 76800 Pixels (1 image), Panel (b): 153600 Pixels (two images), Panel (c): Trained on 1% of the data-set (3 images), (d): Trained on 5% of the data-set (15 images).

## 9. DISCUSSION AND CONCLUDING REMARKS

In this paper, we proposed novel kernel-based architectures for localization and segmentation of Angiodysplasia from colonoscopy images. In the first architecture, features are generated via a VGG network pre-trained on natural images combined with a kernel feature selection. In the second network, we used an invariant scattering convolution neural network to generate features that are stable with respect to deformations and rotations.

We compared the performance of the proposed segmentation networks with FCN -a popular convolutional neural network for segmentation of natural images-and showed that the proposed segmentation networks in this paper outperforms FCN in terms of the mean IoU score when the size of training samples is small. However, as the size of training samples increase, the FCN achieve better segmentation results due to its large representational capacity. Therefore, the proposed segmentation networks are particularly suited for medical imaging applications, where extracting and annotating large scale data-sets is difficult. The main issue in applying kernel-based segmentation networks is to select a good kernel function to achieve good generalization performance. To automate the process of kernel selection, we proposed an optimization problem based on the notion of maximum mean discrepancy between two probability distributions.

The performance of kernel-based networks significantly depends on the quality of generated representations. A pre-trained VGG network used as a generic feature extractor

is capable of generating diverse representations from input data. Nevertheless, the key to achieve a good generalization performance is to select the best discriminating representations from the pool of representations produced by VGG filter bank. Consequently, devising better feature selection schemes in the feature space is the research direction that we pursue in future works.

#### ACKNOWLEDGEMENT

M.B.K. would like to thank PROF. SHAHIN SHAHRAMPOUR of University of Texas A&M, and DR. AHMAD BEIRAMI of EA Digital Platform for introducing him to the kernel learning problem during his Ph.D. studies at Harvard University.

This research is partially supported by NIH under the grant 1R01 CA176553 and R01E0116777. The content of this article are solely the responsibility of the authors and do not necessarily reflect the official NIH views.

#### REFERENCES

- [1] H. Ren, M. Badii Khuzani, V. Vasudevan, J. Xiao, and L. Xing, “A two-sample test for learning mixture kernels with application to the semantic segmentation,” *submitted to IEEE Transactions on Medical Imaging*, 2018.
- [2] A. Rahimi and B. Recht, “Random features for large-scale kernel machines,” in *Advances in neural information processing systems*, 2008, pp. 1177–1184.
- [3] —, “Weighted sums of random kitchen sinks: Replacing minimization with randomization in learning,” in *Advances in neural information processing systems*, 2009, pp. 1313–1320.
- [4] A. Beirami, M. Razaviyayn, S. Shahrampour, and V. Tarokh, “On optimal generalizability in parametric learning,” in *Advances in Neural Information Processing Systems*, 2017, pp. 3455–3465.
- [5] S. Wang, W. Zhou, H. Lu, A. Maleki, and V. Mirrokni, “Approximate leave-one-out for fast parameter tuning in high dimensions,” *arXiv preprint arXiv:1807.02694*, 2018.
- [6] R. Giordano, W. Stephenson, R. Liu, M. I. Jordan, and T. Broderick, “Return of the infinitesimal Jackknife,” *arXiv preprint arXiv:1806.00550*, 2018.
- [7] A. Sinha and J. C. Duchi, “Learning kernels with random features,” in *Advances in Neural Information Processing Systems*, 2016, pp. 1298–1306.
- [8] N. Cristianini, J. Shawe-Taylor, A. Elisseeff, and J. S. Kandola, “On kernel-target alignment,” in *Advances in neural information processing systems*, 2002, pp. 367–373.
- [9] C. Cortes, M. Mohri, and A. Rostamizadeh, “Algorithms for learning kernels based on centered alignment,” *Journal of Machine Learning Research*, vol. 13, no. Mar, pp. 795–828, 2012.
- [10] —, “New generalization bounds for learning kernels,” *arXiv preprint arXiv:0912.3309*, 2009.
- [11] S. Shahrampour and V. Tarokh, “Learning bounds for greedy approximation with explicit feature maps from multiple kernels.”
- [12] S. Shahrampour, A. Beirami, and V. Tarokh, “On data-dependent random features for improved generalization in supervised learning,” *arXiv preprint arXiv:1712.07102*, 2017.
- [13] Y. Baram, “Learning by kernel polarization,” *Neural Computation*, vol. 17, no. 6, pp. 1264–1275, 2005.
- [14] I. Guyon and A. Elisseeff, “An introduction to variable and feature selection,” *Journal of machine learning research*, vol. 3, no. Mar, pp. 1157–1182, 2003.
- [15] J. Bruna and S. Mallat, “Invariant scattering convolution networks,” *IEEE transactions on pattern analysis and machine intelligence*, vol. 35, no. 8, pp. 1872–1886, 2013.
- [16] E. Shelhamer, J. Long, and T. Darrell, “Fully convolutional networks for semantic segmentation,” *arXiv preprint arXiv:1605.06211*, 2016.
- [17] F. R. Bach, G. R. Lanckriet, and M. I. Jordan, “Multiple kernel learning, conic duality, and the SMO algorithm,” in *Proceedings of the twenty-first international conference on Machine learning*. ACM, 2004, p. 6.
- [18] C. Cortes, M. Mohri, and A. Rostamizadeh, “Two-stage learning kernel algorithms.” in *ICML*, 2010, pp. 239–246.
- [19] G. R. Lanckriet, N. Cristianini, P. Bartlett, L. E. Ghaoui, and M. I. Jordan, “Learning the kernel matrix with semidefinite programming,” *Journal of Machine learning research*, vol. 5, no. Jan, pp. 27–72, 2004.

- [20] V. A. Marčenko and L. A. Pastur, “Distribution of eigenvalues for some sets of random matrices,” *Mathematics of the USSR-Sbornik*, vol. 1, no. 4, p. 457, 1967.
- [21] D. Voiculescu, “Addition of certain non-commuting random variables,” *Journal of functional analysis*, vol. 66, no. 3, pp. 323–346, 1986.
- [22] T. Hofmann, B. Schölkopf, and A. J. Smola, “Kernel methods in machine learning,” *The annals of statistics*, pp. 1171–1220, 2008.
- [23] K. Fukumizu, F. R. Bach, M. I. Jordan *et al.*, “Kernel dimension reduction in regression,” *The Annals of Statistics*, vol. 37, no. 4, pp. 1871–1905, 2009.
- [24] H. Q. Minh, P. Niyogi, and Y. Yao, “Mercers theorem, feature maps, and smoothing,” in *International Conference on Computational Learning Theory*. Springer, 2006, pp. 154–168.
- [25] G. Wahba, *Spline models for observational data*. Siam, 1990, vol. 59.
- [26] B. Schölkopf, R. Herbrich, and A. J. Smola, “A generalized representer theorem,” in *International conference on computational learning theory*. Springer, 2001, pp. 416–426.
- [27] P. Drineas and M. W. Mahoney, “On the Nyström method for approximating a Gram matrix for improved kernel-based learning,” *journal of machine learning research*, vol. 6, no. Dec, pp. 2153–2175, 2005.
- [28] S. Bochner, *Harmonic analysis and the theory of probability*. Courier Corporation, 2005.
- [29] A. Gretton, K. M. Borgwardt, M. J. Rasch, B. Schölkopf, and A. Smola, “A kernel two-sample test,” *Journal of Machine Learning Research*, vol. 13, no. Mar, pp. 723–773, 2012.
- [30] X. Zhang and S. Liao, “Online kernel selection via incremental sketched kernel alignment.” in *IJCAI*, 2018, pp. 3118–3124.
- [31] K. Muandet, K. Fukumizu, B. Sriperumbudur, B. Schölkopf *et al.*, “Kernel mean embedding of distributions: A review and beyond,” *Foundations and Trends® in Machine Learning*, vol. 10, no. 1-2, pp. 1–141, 2017.
- [32] M. Gönen and E. Alpaydın, “Multiple kernel learning algorithms,” *Journal of machine learning research*, vol. 12, no. Jul, pp. 2211–2268, 2011.
- [33] I. O. Tolstikhin, B. K. Sriperumbudur, and B. Schölkopf, “Minimax estimation of maximum mean discrepancy with radial kernels,” in *Advances in Neural Information Processing Systems*, 2016, pp. 1930–1938.
- [34] N. El Karoui *et al.*, “The spectrum of kernel random matrices,” *The Annals of Statistics*, vol. 38, no. 1, pp. 1–50, 2010.
- [35] Z. Fan and A. Montanari, “The spectral norm of random inner-product kernel matrices,” *Probability Theory and Related Fields*, pp. 1–59, 2015.
- [36] X. Cheng and A. Singer, “The spectrum of random inner-product kernel matrices,” *Random Matrices: Theory and Applications*, vol. 2, no. 04, p. 1350010, 2013.
- [37] S. P. Kasiviswanathan and M. Rudelson, “Spectral norm of random kernel matrices with applications to privacy,” *arXiv preprint arXiv:1504.05880*, 2015.
- [38] R. Vershynin, “Introduction to the non-asymptotic analysis of random matrices,” *arXiv preprint arXiv:1011.3027*, 2010.
- [39] [Online]. Available: <http://featureselection.asu.edu/datasets.php>
- [40] P. L. Bartlett and S. Mendelson, “Rademacher and gaussian complexities: Risk bounds and structural results,” *Journal of Machine Learning Research*, vol. 3, no. Nov, pp. 463–482, 2002.
- [41] J. Chen, M. Stern, M. J. Wainwright, and M. I. Jordan, “Kernel feature selection via conditional covariance minimization,” in *Advances in Neural Information Processing Systems*, 2017, pp. 6946–6955.
- [42] [Online]. Available: <https://scikit-learn.org>.
- [43] [Online]. Available: <http://shogun-toolbox.org>.
- [44] J. Long, E. Shelhamer, and T. Darrell, “Fully convolutional networks for semantic segmentation,” in *Proceedings of the IEEE conference on computer vision and pattern recognition*, 2015, pp. 3431–3440.
- [45] O. Ronneberger, P. Fischer, and T. Brox, “U-net: Convolutional networks for biomedical image segmentation,” in *International Conference on Medical image computing and computer-assisted intervention*. Springer, 2015, pp. 234–241.
- [46] K. He, X. Zhang, S. Ren, and J. Sun, “Deep residual learning for image recognition,” in *Proceedings of the IEEE conference on computer vision and pattern recognition*, 2016, pp. 770–778.
- [47] A. Krizhevsky, I. Sutskever, and G. E. Hinton, “Imagenet classification with deep convolutional neural networks,” in *Advances in neural information processing systems*, 2012, pp. 1097–1105.

- [48] K. Simonyan and A. Zisserman, “Very deep convolutional networks for large-scale image recognition,” *arXiv preprint arXiv:1409.1556*, 2014.
- [49] C. Szegedy, W. Liu, Y. Jia, P. Sermanet, S. Reed, D. Anguelov, D. Erhan, V. Vanhoucke, and A. Rabinovich, “Going deeper with convolutions,” in *Proceedings of the IEEE conference on computer vision and pattern recognition*, 2015, pp. 1–9.
- [50] N. Srivastava, G. Hinton, A. Krizhevsky, I. Sutskever, and R. Salakhutdinov, “Dropout: a simple way to prevent neural networks from overfitting,” *The Journal of Machine Learning Research*, vol. 15, no. 1, pp. 1929–1958, 2014.
- [51] S. Scardapane, D. Comminiello, A. Hussain, and A. Uncini, “Group sparse regularization for deep neural networks,” *Neurocomputing*, vol. 241, pp. 81–89, 2017.
- [52] I. J. Goodfellow, D. Warde-Farley, M. Mirza, A. Courville, and Y. Bengio, “Maxout networks,” *arXiv preprint arXiv:1302.4389*, 2013.
- [53] B. Scholkopf and A. J. Smola, *Learning with kernels: support vector machines, regularization, optimization, and beyond*. MIT press, 2001.
- [54] D. G. Lowe, “Distinctive image features from scale-invariant keypoints,” *International journal of computer vision*, vol. 60, no. 2, pp. 91–110, 2004.
- [55] E. Tola, V. Lepetit, and P. Fua, “DAISY: An efficient dense descriptor applied to wide-baseline stereo,” *IEEE transactions on pattern analysis and machine intelligence*, vol. 32, no. 5, pp. 815–830, 2010.
- [56] S. Khan and S.-P. Yong, “A comparison of deep learning and hand crafted features in medical image modality classification,” in *Computer and Information Sciences (ICCOINS), 2016 3rd International Conference on*. IEEE, 2016, pp. 633–638.
- [57] S. Ben-David, J. Blitzer, K. Crammer, A. Kulesza, F. Pereira, and J. W. Vaughan, “A theory of learning from different domains,” *Machine learning*, vol. 79, no. 1-2, pp. 151–175, 2010.
- [58] M. Xie, N. Jean, M. Burke, D. Lobell, and S. Ermon, “Transfer learning from deep features for remote sensing and poverty mapping,” *arXiv preprint arXiv:1510.00098*, 2015.
- [59] T. Wiatowski and H. Bölcskei, “A mathematical theory of deep convolutional neural networks for feature extraction,” *IEEE Transactions on Information Theory*, vol. 64, no. 3, pp. 1845–1866, 2018.
- [60] M. Holschneider, “Wavelets,” *An analysis tool*, 1995.
- [61] G. Kutyniok and D. Labate, “Introduction to shearlets,” in *Shearlets*. Springer, 2012, pp. 1–38.
- [62] L. v. d. Maaten and G. Hinton, “Visualizing data using t-SNE,” *Journal of machine learning research*, vol. 9, no. Nov, pp. 2579–2605, 2008.
- [63] D. P. Kingma and J. Ba, “Adam: A method for stochastic optimization,” *arXiv preprint arXiv:1412.6980*, 2014.
- [64] T. Tao, *Topics in random matrix theory*. American Mathematical Soc., 2012, vol. 132.
- [65] J. Duchi. Chapter 2: Minimax lower bounds: the Fano and Lé Cam methods. [Online]. Available: <https://web.stanford.edu/class/stats311/Lectures/lec-03.pdf>
- [66] M. S. Pinsker, “Information and information stability of random variables and processes,” 1960.
- [67] I. Tolstikhin, B. K. Sriperumbudur, and K. Muandet, “Minimax estimation of kernel mean embeddings,” *The Journal of Machine Learning Research*, vol. 18, no. 1, pp. 3002–3048, 2017.
- [68] P. Bellec, “Concentration of quadratic forms under a Bernstein moment assumption,” 2014.
- [69] M. Rudelson, R. Vershynin *et al.*, “Hanson-wright inequality and sub-gaussian concentration,” *Electronic Communications in Probability*, vol. 18, 2013.
- [70] B. Laurent and P. Massart, “Adaptive estimation of a quadratic functional by model selection,” *Annals of Statistics*, pp. 1302–1338, 2000.
- [71] R. Bhatia, “Matrix analysis graduate texts in mathematics, 169,” 1997.
- [72] D. Pollard, *Convergence of stochastic processes*. Springer Science & Business Media, 2012.
- [73] T. M. Cover and J. A. Thomas, *Elements of information theory*. John Wiley and Sons, 2012.
- [74] X. Nguyen, M. J. Wainwright, and M. I. Jordan, “Estimating divergence functionals and the likelihood ratio by convex risk minimization,” *IEEE Transactions on Information Theory*, vol. 56, no. 11, pp. 5847–5861, 2010.
- [75] C. McDiarmid, “On the method of bounded differences,” *Surveys in combinatorics*, vol. 141, no. 1, pp. 148–188, 1989.
- [76] A. W. Van Der Vaart and J. A. Wellner, “Weak convergence,” in *Weak convergence and empirical processes*. Springer, 1996, pp. 16–28.
- [77] A. Ben-Tal, D. Den Hertog, A. De Waegenare, B. Melenberg, and G. Rennen, “Robust solutions of optimization problems affected by uncertain probabilities,” *Management Science*, vol. 59, no. 2, pp. 341–357, 2013.



- [78] V. N. Vapnik and A. Y. Chervonenkis, “On the uniform convergence of relative frequencies of events to their probabilities,” in *Measures of complexity*. Springer, 2015, pp. 11–30.
- [79] D. Pollard, “Empirical processes: theory and applications,” in *NSF-CBMS regional conference series in probability and statistics*. JSTOR, 1990, pp. i–86.
- [80] N. Sauer, “On the density of families of sets,” *Journal of Combinatorial Theory, Series A*, vol. 13, no. 1, pp. 145–147, 1972.

## APPENDIX A.

**A.1. Proof of Theorem 5.1.** In the sequel, we separately present the proofs of the upper and lower bounds.

**A.1.1. The Upper Bound.** To prove the upper bound, we leverage the elementary inequality  $|\sqrt{x} - \sqrt{y}| \leq \sqrt{|x - y|}$ ,  $x, y \geq 0$ . We then have that

$$\begin{aligned}
 |D_{k_{\mathcal{X}}}^{\text{MMD}}[P, Q] - D_{k_{\mathcal{X}}}^{\text{MMD}}[\hat{P}^n, \hat{Q}^n]| &\leq \sqrt{|(D_{k_{\mathcal{X}}}^{\text{MMD}}[P, Q])^2 - (D_{k_{\mathcal{X}}}^{\text{MMD}}[\hat{P}^n, \hat{Q}^n])^2|} \\
 &= \sqrt{|T_1(P) + T_2(Q) + T_3(P, Q)|} \\
 \text{(A.1)} \qquad \qquad \qquad &\leq \sqrt{|T_1(P)| + |T_2(Q)| + |T_3(P, Q)|},
 \end{aligned}$$

where  $T_1(P)$ ,  $T_2(Q)$ , and  $T_3(P, Q)$  are defined as follows

$$\begin{aligned}
 T_1(P) &\stackrel{\text{def}}{=} \iint k_{\mathcal{X}}(\mathbf{x}, \mathbf{x}') d(P - \hat{P}^n)^{\otimes 2}(\mathbf{x}, \mathbf{x}') \\
 T_2(Q) &\stackrel{\text{def}}{=} \iint k_{\mathcal{X}}(\mathbf{x}, \mathbf{x}') d(Q - \hat{Q}^n)^{\otimes 2}(\mathbf{x}, \mathbf{x}') \\
 T_3(P, Q) &\stackrel{\text{def}}{=} \iint k_{\mathcal{X}}(\mathbf{x}, \mathbf{y}) d(P - \hat{P}^n)(\mathbf{x}) d(Q - \hat{Q}^n)(\mathbf{y})
 \end{aligned}$$

Then, due to (A.2), the following inequalities hold

$$\text{(A.3a)} \qquad |T_1(P)| \leq 4MD_{\text{TV}}^2(P||\hat{P}^n)$$

$$\text{(A.3b)} \qquad |T_2(Q)| \leq 4MD_{\text{TV}}^2(Q||\hat{Q}^n)$$

$$\text{(A.3c)} \qquad |T_3(P, Q)| \leq 4MD_{\text{TV}}(P||\hat{P}^n)D_{\text{TV}}(Q||\hat{Q}^n).$$

Substituting the upper bounds in Eqs. (A.3) into Eq. (A.1) and some algebraic manipulations yields

$$|D_{k_{\mathcal{X}}}^{\text{MMD}}[P, Q] - D_{k_{\mathcal{X}}}^{\text{MMD}}[\hat{P}^n, \hat{Q}^n]| \leq 2\sqrt{M}(D_{\text{TV}}(Q||\hat{Q}^n) + D_{\text{TV}}(P||\hat{P}^n)).$$

Fix  $Q$  and take the supremum with respect to  $P$  from both sides of the preceding inequality

$$\text{(A.4)} \qquad \sup_{P: D_f(P||Q) \leq \alpha} |D_{k_{\mathcal{X}}}^{\text{MMD}}[P, Q] - D_{k_{\mathcal{X}}}^{\text{MMD}}[\hat{P}^n, \hat{Q}^n]| \leq 2\sqrt{M}D_{\text{TV}}(Q||\hat{Q}^n) + 2\sqrt{M} \sup_{P: D_f(P||Q) \leq \alpha} D_{\text{TV}}(P||\hat{P}^n).$$

non-asymptotic convergence rate of the empirical measure to the population distribution with respect to the  $f$ -divergence:

**Proposition A.1.** (WEAK CONVERGENCE OF EMPIRICAL MEASURES) *Let  $P \in \mathcal{B}(\mathcal{X})$  be an arbitrary Borel probability measure, and let  $\hat{P}_0^n$  denotes the empirical measure associated with the i.i.d. samples  $\mathbf{X}_1, \dots, \mathbf{X}_n \sim_{i.i.d.} P$ . Then,*

(i)  $\hat{P}_0^n \xrightarrow{\text{weakly}} P$ .

DRAFT

(ii) For  $f$ -divergences, the following inequality holds with the probability of at least  $1 - \rho$

$$(A.5) \quad \sup_{P: D_f(P||Q) \leq \alpha} D_f(P||\hat{P}_0^n) \leq \sup_{P: D_f(P||Q) \leq \alpha} \mathbb{E}_P \left[ D_f \left( P \left\| \frac{1}{n} \sum_{i=1}^n \delta_{X_i} \right. \right) \right] + \left( \frac{\beta^2}{2n} \log \frac{1}{\rho} \right)^{\frac{1}{2}}.$$

provided that the Fenchel conjugate  $f^*(y) = \sup_{x \in \mathbb{R}} [xy - f(y)]$  satisfies  $|f^*(y)| < \beta$  for all  $y \in \text{dom}(f^*)$  for some constant  $\beta < +\infty$ .

(iii) For the special case of the TV distance, with the probability of at least  $1 - \rho$ , we have

$$(A.6) \quad \sup_{P: D_{\text{TV}}(P||Q) \leq \alpha} D_{\text{TV}}(P||\hat{P}_0^n) \leq \sqrt{\frac{6 \log(en/3)}{n}} + \sqrt{\frac{1}{2n} \log \frac{1}{\rho}}.$$

*Proof.* The proof is presented in Section B.1 of Appendix.  $\square$

We make some comments on the interpretation of Proposition A.1. Note that  $\hat{P}^n$  defines a (sequence of) random probability measure(s), while  $P \in \mathcal{B}(\mathcal{X})$  is a deterministic Borel probability measure. In the first part of the theorem, we use terminology that is standard in the theory of random matrices to say that the sequence of random measures  $\hat{P}_0^n$  converges weakly to the deterministic measure  $P$ , denoted by  $\hat{P}^n \xrightarrow{\text{weakly}} P$ , if for every continuous compactly supported test function  $e : \mathcal{X} \rightarrow \mathbb{R}$  we have  $\int_{\mathcal{X}} e(\mathbf{x}) \hat{P}^n(d\mathbf{x}) \rightarrow \int_{\mathcal{X}} e(\mathbf{x}) P(d\mathbf{x})$ ; see, e.g., [64].

Part (ii) provides a non-asymptotic convergence bound for general  $f$ -divergences satisfying the condition (A.1). Lastly, in part (iii), we establish an explicit convergence rate of  $\mathcal{O}(1/\sqrt{n})$  for the special case of the total variation distance via its variational form.

We now leverage Inequality (A.6) of Proposition A.1 to upper bound the TV distance in the right hand side of Eq. (B.11). Applying the union bound, we obtain that with the probability of at least  $1 - \rho$

$$\sup_{P: D_f(P||Q) \leq \alpha} |D_{k_{\mathcal{X}}}^{\text{MMD}}[P, Q] - D_{k_{\mathcal{X}}}^{\text{MMD}}[\hat{P}^n, \hat{Q}^n]| \leq 2\sqrt{\frac{M}{n}} + 2\sqrt{\frac{M}{2n} \log \left( \frac{2}{\rho} \right)}.$$

A.1.2. *The Lower Bound.* To prove the lower bound, we use the Fano's method which is a standard technique in computing the minimax lower bound. The main essence of Fano's method is to reduce the estimation problem to a multiple hypothesis testing [65]. We first review some preliminary results about Fano's method based on the lecture notes in [65].

Let  $\mathcal{P}$  denote a class of distributions on a sample space  $\mathcal{X}$ , and let  $\theta : \mathcal{P} \rightarrow \Theta$  denote a function defined on  $\mathcal{P}$ , that is, a mapping  $P \mapsto \theta(P)$ . Let  $d_{\Theta} : \Theta \times \Theta \rightarrow \mathbb{R}_+$  denotes a (semi)metric on  $\Theta$ , and let  $\Phi : \mathbb{R}_+ \rightarrow \mathbb{R}_+$  be a non-decreasing function with  $\Phi(0) = 0$ . Given the samples  $X_1, \dots, X_n \sim_{\text{i.i.d.}} P$ , we define the *minimax* risk as follows

$$(A.7) \quad \mathfrak{R}_n(\theta(\mathcal{P}); \Phi \circ d_{\Theta}) \stackrel{\text{def}}{=} \inf_{\hat{\theta}} \sup_{P \in \mathcal{P}} \mathbb{E}_P[\Phi(d_{\Theta}(\hat{\theta}(X_1, \dots, X_n), \theta(P)))],$$

where the infimum is taken over all estimators  $\hat{\theta} = \hat{\theta}(X_1, \dots, X_n)$ , and the supremum is over the worst case distribution  $P \in \mathcal{P}$

Given an index set  $\mathcal{V}$  of finite cardinality, consider a family of distributions  $\{P_v\}_{v \in \mathcal{V}}$  contained within  $\mathcal{P}$ . This family induces a collection of parameters  $\{\theta(P_v)\}_{v \in \mathcal{V}}$ ; we call the family a  $2\delta$ -packing in the  $d_{\Theta}$ -semimetric if

$$(A.8) \quad d_{\Theta}(\theta(P_{v_1}), \theta(P_{v_2})) \geq 2\delta, \quad \text{for all } v_1 \neq v_2.$$

Now, we leverage the following proposition regarding the lower bound on the minimax risk defined in (A.7):

**Proposition A.2.** (FANO'S MINIMAX LOWER BOUND [65]) *Let  $\{\theta(P_v)\}_{v \in \mathcal{V}}$  be a  $2\delta$  packing in the  $d$ -semimetric norm. Assume that  $V$  is uniform on the set  $\mathcal{V}$ , and conditional on  $V = v$ , we draw a sample  $v \sim P_v$ . Then, the minimax risk has the following lower bound*

$$(A.9) \quad \mathfrak{R}_n(\theta(\mathcal{P}); \Phi \circ d_\Theta) \geq \Phi(\delta) \left( 1 - \frac{I(V; X) + \log 2}{\log |\mathcal{V}|} \right),$$

where  $I(V; X) = D_{\text{KL}}(P_{V,X} \| P_V P_X)$  is the mutual information between the random variables  $V$  and  $X$  with the joint distribution  $P_{V,X}$ .  $\square$

We endow the probability distributions with the KL divergence, *i.e.*, let  $f(x) = x \log(x)$ . To apply the Fano's method, we consider the class of distributions

$$(A.10) \quad \{(\mathbf{N}(v\mathbf{n}, \sigma^2 \mathbf{I}_{d \times d}), \mathbf{N}(\mathbf{0}, \sigma^2 \mathbf{I}_{d \times d}))\}_{v \in \mathcal{V}},$$

where the set is defined as follows  $\mathcal{V} = \{\delta, 2\delta, \dots, N\delta\}$ , for some  $\delta$  to be determined, and  $\mathbf{n} \in \mathbb{R}^d$  is a fixed vector of the unit norm  $\|\mathbf{n}\|_2 = 1$ . Clearly, to attain a non-trivial lower bound from Inequality (A.9), we require that  $|\mathcal{V}| > 2$ . The case of  $|\mathcal{V}| = 2$  will be discussed separately (cf. Remark A.1).

The TV divergence between two multivariate Gaussian distributions  $P = \mathbf{N}(\boldsymbol{\mu}_P, \sigma^2 \mathbf{I}_{d \times d})$  and  $Q = \mathbf{N}(\boldsymbol{\mu}_Q, \sigma^2 \mathbf{I}_{d \times d})$  with  $\boldsymbol{\mu}_0, \boldsymbol{\mu}_1 \in \mathbb{R}^d$  is given by

$$\begin{aligned} D_{\text{KL}}(\mathbf{N}(\boldsymbol{\mu}_P, \sigma^2 \mathbf{I}_{d \times d}) \| \mathbf{N}(\boldsymbol{\mu}_Q, \sigma^2 \mathbf{I}_{d \times d})) &= \int \log(P/Q) \, dP \\ &= \int_{\mathbb{R}^d} \log \left( \frac{\exp(-\frac{1}{2\sigma^2}(\mathbf{x} - \boldsymbol{\mu}_P)(\mathbf{x} - \boldsymbol{\mu}_P)^T)}{\exp(-\frac{1}{2\sigma^2}(\mathbf{x} - \boldsymbol{\mu}_Q)(\mathbf{x} - \boldsymbol{\mu}_Q)^T)} \right) P(d\mathbf{x}) \\ &= \frac{1}{2\sigma^2} \|\boldsymbol{\mu}_P - \boldsymbol{\mu}_Q\|_2^2. \end{aligned}$$

Therefore, the KL divergence between the parametric distributions parameterized by  $v \in \mathcal{V}$  are given by

$$(A.11) \quad D_{\text{KL}}(\mathbf{N}(v\mathbf{n}, \sigma^2 \mathbf{I}_{d \times d}) \| \mathbf{N}(\mathbf{0}, \sigma^2 \mathbf{I}_{d \times d})) = \frac{\delta^2}{2\sigma^2}.$$

Equation (A.11) yields the following upper bound on the total variation distance via Pinsker's inequality [66],

$$(A.12) \quad D_{\text{TV}}(\mathbf{N}(v\mathbf{n}, \sigma^2 \mathbf{I}_{d \times d}) \| \mathbf{N}(\mathbf{0}, \sigma^2 \mathbf{I}_{d \times d})) \leq \sqrt{\frac{1}{2} D_{\text{KL}}(\mathbf{N}(v\mathbf{n}, \sigma^2 \mathbf{I}_{d \times d}) \| \mathbf{N}(\mathbf{0}, \sigma^2 \mathbf{I}_{d \times d}))} = \frac{\delta}{2\sigma}.$$

Therefore, by letting  $\delta = 2\sigma\alpha$ , the set of distributions  $\{(\mathbf{N}(v\mathbf{n}, \sigma^2 \mathbf{I}_{d \times d}), \mathbf{N}(\mathbf{0}, \sigma^2 \mathbf{I}_{d \times d}))\}_{v \in \mathcal{V}}$  are contained in  $\mathcal{P}_\alpha = \{(P, Q) \in \mathcal{B}^{\otimes 2}(\mathcal{X}) : D_{\text{TV}}(P \| Q) \leq \alpha\}$ .

Let  $P_v \stackrel{\text{def}}{=} \mathbf{N}(v\mathbf{n}, \sigma^2 \mathbf{I}_{d \times d})$  and  $Q = \mathbf{N}(\mathbf{0}, \sigma^2 \mathbf{I}_{d \times d})$ . Furthermore, define the mixture  $\bar{P} \stackrel{\text{def}}{=} \frac{1}{|\mathcal{V}|} \sum_{v \in \mathcal{V}} P_v$ . We compute an upper bound the mutual information  $I(X; V)$  on the r.h.s.

of Eq. (A.9) as follows

$$\begin{aligned}
I(X; V) &\leq \frac{1}{|\mathcal{V}|} \sum_{v \in \mathcal{V}} D_{\text{KL}}(P_v \otimes Q \| \bar{P} \otimes Q) \\
&\stackrel{\text{(a)}}{=} \frac{1}{|\mathcal{V}|} \sum_{v \in \mathcal{V}} D_{\text{KL}}(P_v \| \bar{P}) \\
&\stackrel{\text{(b)}}{\leq} \frac{1}{|\mathcal{V}|^2} \sum_{v \in \mathcal{V}} D_{\text{KL}}(P_v \| P_{v'}) \\
&= \frac{1}{|\mathcal{V}|^2} \sum_{v, v' \in \mathcal{V}} D_{\text{KL}}(\mathbf{N}(v\mathbf{n}, \sigma^2 \mathbf{I}_{d \times d}) \| \mathbf{N}(v'\mathbf{n}, \sigma^2 \mathbf{I}_{d \times d})) \\
&= \frac{\alpha}{N^2} \sum_{i, j=1}^N |i - j|^2 \\
\text{(A.13)} \quad &\leq \alpha N^2.
\end{aligned}$$

where (a) follows from the tensorization property of the KL divergence, *i.e.*,

$$\begin{aligned}
D_{\text{KL}}(P_0 \otimes Q \| P_1 \otimes Q) &= D_{\text{KL}}(P_0 \| P_1) + D_{\text{KL}}(Q \| Q) \\
\text{(A.14)} \quad &= D_{\text{KL}}(P_0 \| P_1).
\end{aligned}$$

Furthermore, (b) follows from the convexity of the KL divergence  $D_{\text{KL}}(P_v \| \cdot)$ .

To obtain a non-trivial lower bound via Fano's inequality (A.9), we additionally require that

$$\text{(A.15)} \quad 1 - \frac{I(V; X) + \log(2)}{\log |\mathcal{V}|} \geq 1 - \frac{\alpha N^2 + \log(2)}{\log N} \geq \varsigma > 0.$$

The preceding inequality can be achieved if we choose  $2^{\frac{1}{1-\varsigma}} \leq N \leq \lfloor 0.628 \times (1/\sqrt{\alpha}) \rfloor$ , for  $\alpha \leq 0.04$ .

In addition, the squared MMD between two multivariate Gaussian distributions can be computed as follows (cf. Lemma 14 of [67])

$$(D_{k_{\mathcal{X}}}^{\text{MMD}}(\mathbf{N}(\boldsymbol{\mu}_P, \sigma^2 \mathbf{I}_{d \times d}), \mathbf{N}(\boldsymbol{\mu}_Q, \sigma^2 \mathbf{I}_{d \times d})))^2 = \frac{2}{(2\pi)^{d/2}} \int_{\mathbb{R}^d} e^{-\sigma^2 \|\boldsymbol{\xi}\|_2^2} (1 - \cos(\langle \boldsymbol{\mu}_P - \boldsymbol{\mu}_Q, \boldsymbol{\xi} \rangle)) \mu_{\Xi}(\mathrm{d}\boldsymbol{\xi}).$$

In the case of the Gaussian RBF kernel  $k_{\mathcal{X}}(\mathbf{x}, \mathbf{y}) = \exp(-\|\mathbf{x} - \mathbf{y}\|_2^2 / 2\varrho^2)$ , the squared MMD admits a closed form expression as follows

$$(D_{k_{\mathcal{X}}}^{\text{MMD}}(\mathbf{N}(\boldsymbol{\mu}_P, \sigma^2 \mathbf{I}_{d \times d}), \mathbf{N}(\boldsymbol{\mu}_Q, \sigma^2 \mathbf{I}_{d \times d})))^2 = 2 \left( \frac{\varrho^2}{\varrho^2 + \sigma^2} \right)^{\frac{d}{2}} \left( 1 - \exp\left(-\frac{\|\boldsymbol{\mu}_P - \boldsymbol{\mu}_Q\|_2^2}{2\varrho^2 + \sigma^2}\right) \right),$$

The preceding formula yields the following packing number for  $v_0, v_1 \in \mathcal{V} : v_0 \neq v_1$ ,

$$\begin{aligned}
& |(D_{k_{\mathcal{X}}}^{\text{MMD}}(P_{v_0}, Q))^2 - (D_{k_{\mathcal{X}}}^{\text{MMD}}(P_{v_1}, Q))^2| \\
& \geq 2 \left( \frac{\varrho^2}{\varrho^2 + \sigma^2} \right)^{\frac{d}{2}} \left| \exp\left(-\frac{v_0^2}{2\varrho^2 + \sigma^2}\right) - \exp\left(-\frac{v_1^2}{2\varrho^2 + \sigma^2}\right) \right|^{1/2} \\
& \geq 2 \left( \frac{\varrho^2}{\varrho^2 + \sigma^2} \right)^{\frac{d}{2}} \left| \exp\left(-\frac{4N^2\sigma^2\alpha}{2\varrho^2 + \sigma^2}\right) - \exp\left(-\frac{4(N-1)^2\sigma^2\alpha}{2\varrho^2 + \sigma^2}\right) \right|^{1/2} \\
& \geq 2 \left( \frac{\varrho^2}{\varrho^2 + \sigma^2} \right)^{\frac{d}{2}} \exp\left(-\frac{2(N-1)^2\sigma^2\alpha}{2\varrho^2 + \sigma^2}\right) \left| 1 - \exp\left(-\frac{4(2N-1)\sigma^2\alpha}{2\varrho^2 + \sigma^2}\right) \right|^{1/2} \\
& \geq (2/e) \left( \frac{\varrho^2}{\varrho^2 + \sigma^2} \right)^{\frac{d}{4}} \left| 1 - \exp\left(-\frac{20\sigma^2\alpha}{2\varrho^2 + \sigma^2}\right) \right|^{1/2}.
\end{aligned}$$

Since the choice of the variance  $\sigma^2 > 0$  in the Gaussian distributions is arbitrary, we let  $\sigma^2 = \varrho^2(n^2 - 1)$ . Then, using Fano's inequality in Proposition 5.1 in conjunction with the function  $\Phi(\delta) = \delta$  results in

$$(A.16) \quad \sup_{(P, Q) \in \mathcal{P}} \left| D_{k_{\mathcal{X}}}^{\text{MMD}}[P, Q] - D_{k_{\mathcal{X}}}^{\text{MMD}}[\hat{P}^{n+}, \hat{Q}^{n-}] \right| \geq \frac{1}{8\sqrt{d+1}} \frac{1}{\sqrt{n}}.$$

Due to the fact that the kernel is Hilbert-Schmidt (cf. (A.2)), the following inequality holds

$$(A.17) \quad \left| (D_{k_{\mathcal{X}}}^{\text{MMD}}[P, Q])^2 - (D_{k_{\mathcal{X}}}^{\text{MMD}}[\hat{P}^{n+}, \hat{Q}^{n-}])^2 \right| \leq 2\sqrt{3M} \left| D_{k_{\mathcal{X}}}^{\text{MMD}}[P, Q] - D_{k_{\mathcal{X}}}^{\text{MMD}}[\hat{P}^{n+}, \hat{Q}^{n-}] \right|$$

Combining Eqs. (A.16) and (A.17) yields

$$(A.18) \quad \left| D_{k_{\mathcal{X}}}^{\text{MMD}}[P, Q] - D_{k_{\mathcal{X}}}^{\text{MMD}}[\hat{P}^{n+}, \hat{Q}^{n-}] \right| \geq \frac{1}{2\sqrt{3M}}$$

*Remark A.1.* When  $|\mathcal{V}| = 2$ , the minimax lower bound in Eq. (5.3) is trivial since  $I(V; X) + \log(2)/\log|\mathcal{V}| \geq 1$ . In such case, the Le Cam's two point method provide a non-trivial lower bound, see, *e.g.*, [33]. However, the minimax we presented yields a tighter lower bound than that of Le Cam's two point method.

**A.2. Proof of Proposition 5.1.** Recall the definition of the function class  $\mathcal{F}_m(R)$  from Eq. (4.9). We prove Part (i) by writing the empirical Rademacher complexity for the class of functions in  $\mathcal{F}_m(R)$  as follows

$$\begin{aligned}
\hat{\mathfrak{R}}_S^n(\mathcal{F}_m(R)) &= \frac{1}{n} \mathbb{E}_{P_\epsilon} \left[ \sup_{f \in \mathcal{F}_m(R)} \sum_{i=1}^n \epsilon_i f(\mathbf{X}_i) \middle| \mathbf{X}_1, \dots, \mathbf{X}_n \right] \\
&= \frac{1}{n\sqrt{D}} \mathbb{E}_{P_\epsilon} \left[ \sup_{\beta \in \mathcal{A}} \sum_{i=1}^n \sum_{j=1}^D \epsilon_i \beta_{j,m} \sqrt{w_m} \phi_m(\mathbf{x}_i; \boldsymbol{\xi}_j) \middle| \mathbf{X}_1, \dots, \mathbf{X}_n \right] \\
(A.19) \quad &= \frac{1}{n\sqrt{D}} \mathbb{E}_{P_\epsilon} \left[ \sup_{\beta \in \mathcal{A}} \boldsymbol{\epsilon}^T \boldsymbol{\Phi} \boldsymbol{\beta} \middle| \mathbf{X}_1, \dots, \mathbf{X}_n \right],
\end{aligned}$$

where in the last equality,  $\boldsymbol{\Phi} \stackrel{\text{def}}{=} [\phi^{\mathbf{w}}(\mathbf{X}_i; \boldsymbol{\xi}_j)]_{(i,j) \in [n] \times [mD]}$  is the feature matrix with with and  $\mathcal{A} \stackrel{\text{def}}{=} \{\boldsymbol{\beta} \in \mathbb{R}^{mD} : \|\boldsymbol{\beta}\|_2 \leq R/\sqrt{mD}\}$ .

From the Cauchy-Schwarz inequality, it is easy to see that the supremum in Eq. (A.19) is attained when  $\beta$  and  $\varepsilon^T \Phi$  are co-linear, i.e.,  $\beta = R \cdot \Phi \varepsilon / (\sqrt{mD} \|\Phi \varepsilon\|_2)$ . Therefore, from Eq. (A.19) we obtain that

$$(A.20) \quad \widehat{\mathfrak{R}}_S^n(\mathcal{F}_m(R)) = \frac{R}{nD\sqrt{m}} \mathbb{E}_{P_\varepsilon} \left[ \|\varepsilon \Phi\|_2 \middle| \mathbf{X}_1, \dots, \mathbf{X}_n \right].$$

We now compute the expectation (A.28) via the following concentration inequality for quadratic forms of independent random variables satisfying the moment assumption:

**Theorem A.2.** (CONCENTRATION INEQUALITY FOR QUADRATIC MATRIX FORMS, [68, Thm. 3]) *Let  $\mathbf{Z} = (Z_1, \dots, Z_n) \in \mathbb{R}^n$  be a random vector satisfying the following moment conditions for some  $K > 0$ :*

$$(A.21) \quad \mathbb{E}|Z_i|^{2p} \leq \frac{1}{2} p! b_i^2 K^{2(p-1)}, \quad p \geq 1.$$

Let  $\mathbf{A} \in \mathbb{R}^{n \times n}$  be a real matrix. Then, for every  $t \geq 0$ ,

$$(A.22) \quad \mathbb{P}\{|\mathbf{Z}^T \mathbf{A} \mathbf{Z} - \mathbb{E}[\mathbf{Z}^T \mathbf{A} \mathbf{Z}]| > t\} \leq \exp\left(-\min\left(\frac{t^2}{192K^2 \|\mathbf{A} \mathbf{D}_b\|_F^2}, \frac{t}{256K^2 \|\mathbf{A}\|_2}\right)\right),$$

where  $\mathbf{D}_b = \text{diag}(b_1, \dots, b_n)$ ,  $\|\mathbf{A}\|_F = \sum_{i,j=1}^n |A_{ij}|^2$ .  $\square$

*Remark A.3.* Despite resemblance of Inequality (A.22) to the Hanson-Wright (HW) Inequality [69], it differs from the HW Inequality in that it does not have an implicit universal constant in the upper bound. Indeed, the concentration inequality in Eq. (A.22) is sharper than the HW Inequality, albeit with the strong conditions on the moments of the random variables in Eq. (A.21).

Now, let us apply the concentration inequality (A.22) in Theorem A.2 to compute the expectation in Eq. (A.20). First, we show that Rademacher random variable  $\varepsilon \sim P_\varepsilon = \text{Uni}\{-1, 1\}$  satisfies the moment conditions (A.21). In particular, for all  $p \geq 1$ , we have

$$\mathbb{E}|\varepsilon_i|^{2p} = (1/2)|-1|^{2p} + (1/2)|1|^{2p} = 1.$$

Therefore, the moment condition in Eq. (A.21) is satisfied with  $b_i = 1$  for all  $i = 1, 2, \dots, n$ , and  $K = 1$ .

Let  $\mathbf{A} = \Phi \Phi^T$  and  $\mathbf{Z} = \varepsilon^T$ . Then,  $\mathbf{Z}^T \mathbf{A} \mathbf{Z} = \varepsilon \Phi \Phi^T \varepsilon^T = \|\Phi \varepsilon\|_2^2$ ,  $\mathbb{E}[\mathbf{Z}^T \mathbf{A} \mathbf{Z}] = \mathbb{E}[\varepsilon \Phi \Phi^T \varepsilon^T] = \|\Phi\|_F^2$ . Furthermore,  $\mathbf{D}_b = \mathbf{I}_n$ .

The concentration inequality in Eq. (A.22) turns into

$$(A.23) \quad \mathbb{P}\{|\|\Phi \varepsilon\|_2^2 - \|\Phi\|_F^2| > t \mid \mathbf{X}_1, \dots, \mathbf{X}_n\} \leq \exp\left(-\min\left(\frac{t^2}{192\|\Phi \Phi^T\|_F^2}, \frac{t}{256\|\Phi\|_2}\right)\right).$$

Also, note that since all Rademacher random variables  $\varepsilon_i$  have unit variance, we have  $K \geq 2^{-1/2}$ . Thus we obtain for any  $u \geq 0$  that

$$\mathbb{P}\{|\|\Phi \varepsilon\|_2^2 - \|\Phi\|_F^2| > u \mid \mathbf{X}_1, \dots, \mathbf{X}_n\} \leq \exp\left(-\min\left(\frac{u^2}{192\|\Phi \Phi^T\|_F^2}, \frac{u}{256\|\Phi\|_2}\right)\right).$$

Let  $\delta \geq 0$  be arbitrary, and let us use this estimate for  $u = \delta \|\Phi\|_F^2$ . Since  $\|\Phi^T \Phi\|_F^2 \leq \|\Phi^T\|_2^2 \|\Phi\|_F^2 = \|\Phi\|_2^2 \|\Phi\|_F^2$ , it follows that

$$\begin{aligned} \mathbb{P}\{\|\Phi \varepsilon\|_2^2 - \|\Phi\|_F^2 \geq \delta \|\Phi\|_F^2 | \mathbf{X}_1, \dots, \mathbf{X}_n\} &\leq \exp\left(-\min\left(\frac{\delta}{192}, \frac{\delta^2}{256}\right) \frac{\|\Phi\|_F^2}{\|\Phi\|_2^2}\right) \\ \text{(A.24)} \qquad \qquad \qquad &\leq \exp\left(-\frac{1}{192} \min(\delta, \delta^2) \frac{\|\Phi\|_F^2}{\|\Phi\|_2^2}\right). \end{aligned}$$

Now let  $\epsilon \geq 0$  be arbitrary; we shall use this inequality for  $\delta = \max(\epsilon, \epsilon^2)$ . Observe that the (likely) event  $\|\Phi \varepsilon\|_2^2 - \|\Phi\|_F^2 \leq \delta \|\Phi\|_F^2$  implies the event  $\|\Phi \varepsilon\|_2 - \|\Phi\|_F \leq \epsilon \|\Phi\|_F$ . This can be seen by dividing both sides of the inequalities by  $\|\Phi\|_F^2$  and  $\|\Phi\|_F$  respectively, and using the numeric bound  $\max(|z-1|, |z-1|^2) \leq |z^2-1|$ , which is valid for all  $z \geq 0$ . Using this observation along with the identity  $\min(\delta, \delta^2) = \epsilon^2$ , we deduce from Eq. (A.24) that

$$\text{(A.25)} \qquad \mathbb{P}\{\|\Phi \varepsilon\|_2 - \|\Phi\|_F \geq \epsilon \|\Phi\|_F | \mathbf{X}_1, \dots, \mathbf{X}_n\} \leq \exp\left(-\frac{1}{192} \epsilon^2 \frac{\|\Phi\|_F^2}{\|\Phi\|_2^2}\right).$$

Using  $\epsilon = \varrho / \|\Phi\|_F$  yields

$$\text{(A.26)} \qquad \mathbb{P}\{\|\Phi \varepsilon\|_2 - \|\Phi\|_F \geq \varrho | \mathbf{X}_1, \dots, \mathbf{X}_n\} \leq \exp\left(-\frac{1}{192} \frac{\varrho^2}{\|\Phi\|_2^2}\right).$$

Now, we return to computing the expectation in Eq. (A.20). For the positive random variable  $\|\varepsilon \Phi\|_2$ , its expectation can be computed as follows

$$\begin{aligned} \widehat{\mathfrak{R}}_S^n(\mathcal{F}_m(R)) &= \frac{R}{nD\sqrt{m}} \mathbb{E}_{P_\varepsilon} \left[ \|\varepsilon \Phi\|_2 \mid \mathbf{X}_1, \dots, \mathbf{X}_n \right] \\ &= \frac{R}{nD\sqrt{m}} \int_{-\|\Phi\|_F}^{\infty} \mathbb{P}[\|\varepsilon \Phi\|_2 - \|\Phi\|_F > t | \mathbf{X}_1, \dots, \mathbf{X}_n] dt \\ &\stackrel{\text{(a)}}{\leq} \frac{R}{nD\sqrt{m}} \int_{-\|\Phi\|_F}^{\infty} \exp\left(-\frac{1}{192} \frac{t^2}{\|\Phi\|_2^2}\right) dt \\ \text{(A.27)} \qquad \qquad \qquad &= \frac{R}{nD\sqrt{m}} \sqrt{\frac{\pi}{192}} \|\Phi\|_2 \cdot \operatorname{erfc}\left(\sqrt{192} \frac{\|\Phi\|_F}{\|\Phi\|_2}\right), \end{aligned}$$

where (a) follows from the concentration inequality in Eq. (A.26). Recall that  $D \ll n$ . Using the basic inequality  $\|\Phi\|_F \leq \sqrt{\operatorname{Rank}(\Phi)} \|\Phi\|_2$  in conjunction with the fact that  $\operatorname{Rank}(\Phi) = \min\{D, n\} = D$  yields the upper bound (5.6) on the Rademacher complexity.

We remark that the upper bound we derived here is sharper than that of Lemma 1 of [10] which is based on the Khintchine-Kahane type inequality. More specifically, the Khintchine inequality yields the following upper bound

$$\begin{aligned} \widehat{\mathfrak{R}}_S^n(\mathcal{F}_m(R)) &= \frac{R}{nD\sqrt{m}} \mathbb{E}_{P_\varepsilon} \left[ \sqrt{\|\varepsilon \Phi \Phi^T \varepsilon^T\|} \mid \mathbf{X}_1, \dots, \mathbf{X}_n \right] \\ &\leq \frac{R}{nD\sqrt{m}} \left( \frac{23}{44} \operatorname{Tr}(\Phi \Phi^T) \right)^{\frac{1}{2}} \\ \text{(A.28)} \qquad \qquad \qquad &= \frac{R}{nD\sqrt{m}} \sqrt{\frac{23}{44}} \|\Phi\|_F. \end{aligned}$$

Since  $0 < \operatorname{erfc}(x) \leq 1$  for  $0 < x$ , and  $\|\Phi\|_2 \leq \|\Phi\|_F$  for any matrix  $\Phi \in \mathbb{R}^{n \times D}$ , the upper bound we established in Eq. (A.27) is sharper than that of Eq. (A.28) using techniques of Lemma 1 in [10].

We now prove Part (ii) of Proposition 5.1. Similar to the derivation in Eq. (A.19), we have that

$$\begin{aligned} \widehat{\mathfrak{G}}_S^n(\mathcal{F}_m(R)) &= \frac{1}{n} \mathbb{E}_{P_\sigma} \left[ \sup_{f \in \mathcal{F}_m(R)} \sum_{i=1}^n \sigma_i f(\mathbf{X}_i) \middle| \mathbf{X}_1, \dots, \mathbf{X}_n \right] \\ &= \frac{R}{nD\sqrt{m}} \mathbb{E}_{P_\sigma} \left[ \|\sigma^T \Phi\|_2 \middle| \mathbf{X}_1, \dots, \mathbf{X}_n \right]. \end{aligned}$$

Now, recall that  $\sigma_i \sim \mathbf{N}(0, 1)$ , and  $\Phi \stackrel{\text{def}}{=} [\cos(\langle (\mathbf{X}_i, 1), \boldsymbol{\xi}_j \rangle)]_{i \in [n], j \in [D]}$ , where  $\boldsymbol{\xi}_j = (\mathbf{v}_j, w_j) \sim \mathbf{N}(0, 1) \times [0, 2\pi]$ , where  $\sigma_i$  and  $\mathbf{X}_i$  are independent. A direct calculation of the expectation yields that

$$(A.29) \quad \widehat{\mathfrak{G}}_S^n(\mathcal{F}_m(R)) = \frac{1}{nD\sqrt{m}} \mathbb{E}_{P_\sigma} \left[ \|\sigma^T \Phi\|_2 \middle| \mathbf{X}_1, \dots, \mathbf{X}_n \right].$$

To compute the expectation, we use the following standard tail bound for the sum of  $\chi^2$  random variables due to Laurent and Massart [70]:

**Theorem A.4.** (TAIL BOUND FOR  $\chi^2$  R.V.'S [70]) *Let  $Z_1, \dots, Z_n$  be independent  $\chi^2$  random variables, each with one degree of freedom. For any vector  $\mathbf{a} \stackrel{\text{def}}{=} (a_1, \dots, a_n) \in \mathbb{R}_+^n$  with non-negative entries, and any  $t > 0$ ,*

$$(A.30) \quad \mathbb{P} \left\{ \sum_{i=1}^n a_i Z_i \geq \|\mathbf{a}\|_1 + 2\|\mathbf{a}\|_2 \sqrt{t} + 2\|\mathbf{a}\|_\infty t \right\} \leq e^{-t}.$$

□

Now, consider the eigenvalue decomposition  $\Phi\Phi^T = \mathbf{V}\boldsymbol{\Lambda}\mathbf{V}$ , where  $\mathbf{V}$  is a matrix of orthonormal eigenvectors, and  $\boldsymbol{\Lambda} \stackrel{\text{def}}{=} \operatorname{diag}(\lambda_1, \dots, \lambda_n)$  is the diagonal matrix of corresponding eigenvalues  $\boldsymbol{\lambda} \stackrel{\text{def}}{=} (\lambda_1, \dots, \lambda_n)$ . Due to the rotational invariance of the Gaussian distribution,  $\mathbf{z} \stackrel{\text{def}}{=} \sigma\mathbf{V}$  is an isotropic multi-variate Gaussian random vector with mean zero. Thus,  $\|\sigma^T \Phi\|_2 = \mathbf{z}^T \boldsymbol{\Lambda} \mathbf{z} = \lambda_1 z_1^2 + \dots + \lambda_n z_n^2$ , and the  $z_i^2$ 's are independent  $\chi^2$  random variables, each with one degree of freedom. Therefore, using the concentration inequality in Eq. (A.30) with  $\|\boldsymbol{\lambda}\|_2 = (\operatorname{Tr}((\Phi\Phi^T)^2))^{1/2}$ ,  $\|\boldsymbol{\lambda}\|_1 = \operatorname{Tr}(\Phi\Phi^T) = \|\Phi\|_F^2$ , and  $\|\boldsymbol{\lambda}\|_\infty = \|\Phi\|_2^2$  yields for all  $t > 0$ ,

$$(A.31) \quad \mathbb{P} \left\{ \|\sigma^T \Phi\|_2^2 - \|\Phi\|_F^2 \geq 2\sqrt{\operatorname{Tr}((\Phi\Phi^T)^2)t} + 2\|\Phi\|_2^2 t \middle| \mathbf{X}_1, \dots, \mathbf{X}_n \right\} \leq e^{-t}.$$

Alternatively, by letting

$$(A.32) \quad t = \left( \sqrt{\frac{\varepsilon \|\Phi\|_F^2}{2\|\Phi\|_2^2} + \frac{\operatorname{Tr}((\Phi\Phi^T)^2)}{4\|\Phi\|_2^4}} - \frac{\sqrt{\operatorname{Tr}((\Phi\Phi^T)^2)}}{2\|\Phi\|_2^2} \right)^2,$$

the concentration bound in Eq. (A.31) can be rewritten as follows

$$\mathbb{P} \left\{ \|\sigma^T \Phi\|_2^2 - \|\Phi\|_F^2 \geq \varepsilon \|\Phi\|_F^2 \right\} \leq e^{-\left( \sqrt{\frac{\varepsilon \|\Phi\|_F^2}{2\|\Phi\|_2^2} + \frac{\operatorname{Tr}((\Phi\Phi^T)^2)}{4\|\Phi\|_2^4}} - \frac{\sqrt{\operatorname{Tr}((\Phi\Phi^T)^2)}}{2\|\Phi\|_2^2} \right)^2}.$$



Due to the inequality  $\max\{|z - 1|, |z + 1|^2\} \leq |z^2 - 1|, z > 0$ , the preceding inequality in turn implies that

$$\mathbb{P} \left\{ \|\sigma^T \Phi\|_2 - \|\Phi\|_F \geq \varepsilon \|\Phi\|_F \right\} \leq e^{-\left( \sqrt{\frac{\varepsilon \|\Phi\|_F^2}{2\|\Phi\|_2^2} + \frac{\text{Tr}((\Phi\Phi^T)^2)}{4\|\Phi\|_2^4}} - \frac{\sqrt{\text{Tr}((\Phi\Phi^T)^2)}}{2\|\Phi\|_2^2} \right)^2}.$$

Letting  $\varrho = \varepsilon \|\Phi\|_F$  yields

$$(A.33) \quad \mathbb{P} \left\{ \|\sigma^T \Phi\|_2 - \|\Phi\|_F \geq \varrho \right\} \leq e^{-\left( \sqrt{\frac{\varrho \|\Phi\|_F}{2\|\Phi\|_2^2} + \frac{\text{Tr}((\Phi\Phi^T)^2)}{4\|\Phi\|_2^4}} - \frac{\sqrt{\text{Tr}((\Phi\Phi^T)^2)}}{2\|\Phi\|_2^2} \right)^2}.$$

Using Inequality (A.33) and similar to our derivation in Eq. (A.27), we have that

$$(A.34) \quad \begin{aligned} \widehat{\mathfrak{G}}_S^n(\mathcal{F}_m(R)) &= \frac{R}{nD\sqrt{m}} \int_0^\infty \mathbb{P}[\|\sigma^T \Phi\|_2 > t | \mathbf{X}_1, \dots, \mathbf{X}_n] dt \\ &\leq \frac{R}{nD\sqrt{m}} \int_{-\|\Phi\|_F}^\infty e^{-\left( \sqrt{\frac{t\|\Phi\|_F}{2\|\Phi\|_2^2} + \frac{\text{Tr}((\Phi\Phi^T)^2)}{4\|\Phi\|_2^4}} - \frac{\sqrt{\text{Tr}((\Phi\Phi^T)^2)}}{2\|\Phi\|_2^2} \right)^2} dt \\ &= \frac{R}{nD\sqrt{m}} \sqrt{\pi} \frac{\sqrt{\text{Tr}((\Phi\Phi^T)^2)}}{\|\Phi\|_F} \left( 1 + \text{erf} \left( \frac{\sqrt{\text{Tr}((\Phi\Phi^T)^2)}}{2\|\Phi\|_2^2} - \sqrt{-\frac{\|\Phi\|_F^2}{2\|\Phi\|_2^2} + \frac{\text{Tr}((\Phi\Phi^T)^2)}{4\|\Phi\|_2^4}} \right) \right) \\ &+ \frac{R}{nD\sqrt{m}} \frac{\|\Phi\|_F}{2\|\Phi\|_2^2} e^{-\left( \sqrt{-\frac{\|\Phi\|_F^2}{2\|\Phi\|_2^2} + \frac{\text{Tr}((\Phi\Phi^T)^2)}{4\|\Phi\|_2^4}} - \frac{\sqrt{\text{Tr}((\Phi\Phi^T)^2)}}{2\|\Phi\|_2^2} \right)^2}. \end{aligned}$$

Since  $\text{erf}(x) \leq 1$  for all  $x \in \mathbb{R}$ , and  $e^{-(\sqrt{-a+b^2}-b)^2} \leq e^{-\frac{a^2}{4b^2}}$  for all  $a, b > 0$ , we can simplify the preceding bound as follows

$$\widehat{\mathfrak{G}}_S^n(\mathcal{F}_m(R)) \leq \frac{R}{nD\sqrt{m}} \left( 2\sqrt{\pi} \frac{\sqrt{\text{Tr}((\Phi\Phi^T)^2)}}{\|\Phi\|_F} + \frac{\|\Phi\|_F}{2\|\Phi\|_2^2} e^{-\frac{\|\Phi\|_F^4}{4\text{Tr}((\Phi\Phi^T)^2)}} \right).$$

**A.3. Proof of Lemma 5.3.** We first compute an upper bound on the Frobenius norm of the feature matrix  $\Phi$ . We have that

$$(A.35) \quad \begin{aligned} \|\Phi\|_F^2 - D \cdot \text{Tr}(\mathbf{K}_n^w) &= |\text{Tr}(\Phi\Phi^T) - D \cdot \text{Tr}(\mathbf{K}_n^w)| \\ &= \left| \sum_{i=1}^n \left[ \sum_{j=1}^D \sum_{\ell=1}^m w_\ell \phi^\ell(\mathbf{x}_i; \boldsymbol{\xi}_j) \phi^\ell(\mathbf{x}_i; \boldsymbol{\xi}_j) - D \cdot k_{\mathcal{X}}^w(\mathbf{x}_i, \mathbf{x}_j) \right] \right| \\ &\stackrel{(a)}{\leq} D \sum_{i=1}^n \left| \frac{1}{D} \sum_{j=1}^D \sum_{\ell=1}^m w_\ell \phi^\ell(\mathbf{x}_i; \boldsymbol{\xi}_j) \phi^\ell(\mathbf{x}_i; \boldsymbol{\xi}_j) - \sum_{\ell=1}^m w_\ell k_{\mathcal{X}}^\ell(\mathbf{x}_i, \mathbf{x}_i) \right| \\ &\stackrel{(b)}{\leq} D \cdot n \sup_{\mathbf{x}, \mathbf{y} \in \mathcal{X}} \sum_{\ell=1}^m w_\ell \left| \frac{1}{D} \sum_{j=1}^D \phi^\ell(\mathbf{x}; \boldsymbol{\xi}_j) \phi^\ell(\mathbf{y}; \boldsymbol{\xi}_j) - k_{\mathcal{X}}^\ell(\mathbf{x}, \mathbf{y}) \right|, \\ &\stackrel{(c)}{\leq} D \cdot n \left( \sup_{\mathbf{x}, \mathbf{y} \in \mathcal{X}} \left| \frac{1}{D} \sum_{j=1}^D \phi^\ell(\mathbf{x}; \boldsymbol{\xi}_j) \phi^\ell(\mathbf{y}; \boldsymbol{\xi}_j) - k_{\mathcal{X}}^\ell(\mathbf{x}, \mathbf{y}) \right|^2 \right)^{1/2} \cdot \|\mathbf{w}\|_2 \\ &\stackrel{(d)}{\leq} D \cdot n \sup_{\mathbf{x}, \mathbf{y} \in \mathcal{X}} \sum_{\ell=1}^m \left| \frac{1}{D} \sum_{j=1}^D \phi^\ell(\mathbf{x}; \boldsymbol{\xi}_j) \phi^\ell(\mathbf{y}; \boldsymbol{\xi}_j) - k_{\mathcal{X}}^\ell(\mathbf{x}, \mathbf{y}) \right| \|\mathbf{w}\|_2, \end{aligned}$$

where (a) and (b) follows by the triangle inequality, (c) follows by the Cauchy-Schwarz inequality, and (d) is due to the fact that  $\ell_1$ -norm is larger than  $\ell_2$ -norm. From the point-wise estimate in Eq. (2.17) and the union bound, we have that

$$\mathbb{P} [|\|\Phi\|_F^2 - D \cdot \text{Tr}(\mathbf{K}_n^{\mathbf{w}})| \geq \delta] \leq 2^8 m \left( \frac{\sigma_p D n \|\mathbf{w}\|_2 \text{diam}(\mathcal{X})}{\delta} \right)^2 \exp \left( - \frac{\delta^2}{4 D n^2 \|\mathbf{w}\|_2 (d+2)} \right).$$

Next, we compute a concentration result for the spectral norm  $\|\Phi\|_2$  of the feature matrix. To achieve this goal, we define the estimation error matrix  $\Delta_n \stackrel{\text{def}}{=} \mathbf{K}_n^{\mathbf{w}} - (1/D)\Phi\Phi^T$ . We now use the standard  $\varepsilon$ -net argument in [38] and the following lemma:

**Lemma A.5.** (SPECTRAL NORM ON A NET, [38, Lemma 5.4.]) *Let  $\mathbf{A}$  be a symmetric  $n \times n$  matrix, and let  $N_\varepsilon$  be an  $\varepsilon$ -net of  $S^{n-1}$  for some  $\varepsilon \in [0, 1)$ . Then*

$$(A.36) \quad \|\mathbf{A}\|_2 = \sup_{\mathbf{y} \in S^{n-1}} |\langle \mathbf{A}\mathbf{y}, \mathbf{y} \rangle| \leq (1 - 2\varepsilon)^{-1} \sup_{\mathbf{y} \in N_\varepsilon} |\langle \mathbf{A}\mathbf{y}, \mathbf{y} \rangle|.$$

□

Let  $N_\varepsilon$  be  $\varepsilon$ -covering of the sphere  $S^{n-1}$ . It is shown in [38] that  $\log N_\varepsilon \leq n \log(1 + \frac{2}{\varepsilon})$ . From Inequality (A.36), we obtain that

$$(A.37) \quad \|\Delta_n\|_2 \leq (1 - 2\varepsilon)^{-1} \sup_{\mathbf{y} \in N_\varepsilon} |\langle \Delta_n \mathbf{y}, \mathbf{y} \rangle|.$$

For each point in the cover  $\mathbf{y} \in N_\varepsilon$ , the inner product in Eq. (A.37) has the following upper bound

$$\begin{aligned}
|\langle \Delta_n \mathbf{y}, \mathbf{y} \rangle| &= \left| \langle \mathbf{K}_n^w - \frac{1}{D} \Phi \Phi^T \mathbf{y}, \mathbf{y} \rangle \right| \\
&= \left| \sum_{i,j=1}^n \left( [\mathbf{K}_n^w]_{ij} - \frac{1}{D} [\Phi \Phi^T]_{ij} \right) y_i y_j \right| \\
&= \left| \sum_{i,j=1}^n \left( \sum_{\ell=1}^m w_\ell k_{\mathcal{X}}^\ell(\mathbf{x}_i, \mathbf{x}_j) - \frac{1}{D} \sum_{k=1}^D \sum_{\ell=1}^m w_\ell \phi^\ell(\mathbf{x}_i; \boldsymbol{\xi}_k) \phi^\ell(\mathbf{x}_j; \boldsymbol{\xi}_k) \right) y_i y_j \right| \\
&\leq \sum_{i,j=1}^n \sum_{\ell=1}^m w_\ell \left| k_{\mathcal{X}}^\ell(\mathbf{x}_i, \mathbf{x}_j) - \frac{1}{D} \sum_{k=1}^D \phi^\ell(\mathbf{x}_i; \boldsymbol{\xi}_k) \phi^\ell(\mathbf{x}_j; \boldsymbol{\xi}_k) \right| |y_i y_j| \\
&\stackrel{(a)}{\leq} \sum_{\ell=1}^m w_\ell \left( \sum_{i,j=1}^n \left| k_{\mathcal{X}}^\ell(\mathbf{x}_i, \mathbf{x}_j) - \frac{1}{D} \sum_{k=1}^D \phi^\ell(\mathbf{x}_i; \boldsymbol{\xi}_k) \phi^\ell(\mathbf{x}_j; \boldsymbol{\xi}_k) \right|^2 \right)^{1/2} \left( \sum_{i,j=1}^n |y_i y_j|^2 \right)^{1/2} \\
&= \sum_{\ell=1}^m w_\ell \left( \sum_{i,j=1}^n \left| k_{\mathcal{X}}^\ell(\mathbf{x}_i, \mathbf{x}_j) - \frac{1}{D} \sum_{k=1}^D \phi^\ell(\mathbf{x}_i; \boldsymbol{\xi}_k) \phi^\ell(\mathbf{x}_j; \boldsymbol{\xi}_k) \right|^2 \right)^{1/2} \|\mathbf{y}\|_2^2 \\
&\stackrel{(b)}{=} \sum_{\ell=1}^m w_\ell \left( \sum_{i,j=1}^n \left| k_{\mathcal{X}}^\ell(\mathbf{x}_i, \mathbf{x}_j) - \frac{1}{D} \sum_{k=1}^D \phi^\ell(\mathbf{x}_i; \boldsymbol{\xi}_k) \phi^\ell(\mathbf{x}_j; \boldsymbol{\xi}_k) \right|^2 \right)^{1/2} \\
&\stackrel{(c)}{\leq} \sum_{i,j=1}^n \sum_{\ell=1}^m w_\ell \left| k_{\mathcal{X}}^\ell(\mathbf{x}_i, \mathbf{x}_j) - \frac{1}{D} \sum_{k=1}^D \phi^\ell(\mathbf{x}_i; \boldsymbol{\xi}_k) \phi^\ell(\mathbf{x}_j; \boldsymbol{\xi}_k) \right| \\
&\stackrel{(d)}{\leq} \left( \sum_{i,j=1}^n \sum_{\ell=1}^m \left| k_{\mathcal{X}}^\ell(\mathbf{x}_i, \mathbf{x}_j) - \frac{1}{D} \sum_{k=1}^D \phi^\ell(\mathbf{x}_i; \boldsymbol{\xi}_k) \phi^\ell(\mathbf{x}_j; \boldsymbol{\xi}_k) \right|^2 \right)^{1/2} \|\mathbf{w}\|_2 \\
&\leq \|\mathbf{w}\|_2 \sum_{i,j=1}^n \left| k_{\mathcal{X}}^\ell(\mathbf{x}_i, \mathbf{x}_j) - \frac{1}{D} \sum_{k=1}^D \phi^\ell(\mathbf{x}_i; \boldsymbol{\xi}_k) \phi^\ell(\mathbf{x}_j; \boldsymbol{\xi}_k) \right| \\
\text{(A.38)} \quad &\leq n^2 \|\mathbf{w}\|_2 \cdot \sup_{\mathbf{x}, \mathbf{y} \in \mathcal{X}} \left| k_{\mathcal{X}}^\ell(\mathbf{x}_i, \mathbf{x}_j) - \frac{1}{D} \sum_{k=1}^D \phi^\ell(\mathbf{x}_i; \boldsymbol{\xi}_k) \phi^\ell(\mathbf{x}_j; \boldsymbol{\xi}_k) \right|,
\end{aligned}$$

where (a) is due to the Cauchy-Schwarz inequality, (b) is due to the fact that  $\mathbf{y} \in \mathbb{S}^{n-1}$  and thus  $\|\mathbf{y}\|_2 = 1$ , (c) is due to the fact that  $\ell_2$ -norm of a matrix is smaller than its  $\ell_1$ -norm, and (d) is due the Cauchy-Schwarz inequality.

Taking the union bound over  $N_\varepsilon$  with  $\varepsilon = 1/4$  as well as over  $\ell = 1, 2, \dots, m$ , and using the inequality Eq. (A.37) as well as the point-wise estimate in Eq. (2.17) results in

$$\begin{aligned}
\mathbb{P} \{ \|\Delta_n\|_2 \geq \delta/D \} &\leq \mathbb{P} \left\{ \sup_{\mathbf{y} \in N_{1/4}} |\langle \Delta_n \mathbf{y}, \mathbf{y} \rangle| \geq \delta/2D \right\} \\
&\leq e^{3n \log 3} \sup_{\mathbf{y} \in N_{1/4}} \mathbb{P} \{ |\langle \Delta_n \mathbf{y}, \mathbf{y} \rangle| \geq \delta/2D \} \\
&\leq e^{3n \log 3} m \mathbb{P} \left\{ \sup_{\mathbf{x}, \mathbf{y} \in \mathcal{R}} \left| k_{\mathcal{X}}(\mathbf{x}, \mathbf{y}) - \frac{1}{D} \sum_{k=1}^D \phi(\mathbf{x}; \boldsymbol{\xi}_k) \phi(\mathbf{y}; \boldsymbol{\xi}_k) \right| \geq \delta/2D \|\mathbf{w}\|_2 n^2 \right\} \\
\text{(A.39)} \quad &\leq e^{3n \log 3} 2^8 m \left( \frac{2Dn^2 \|\mathbf{w}\|_2 \sigma_P \text{diam}(\mathcal{X})}{\delta} \right)^2 \exp \left( - \frac{\delta^2}{16n^2 \|\mathbf{w}\|_2 D(d+2)} \right).
\end{aligned}$$

We now use the following theorem:

**Theorem A.6.** (WEYL'S INEQUALITY, e.g., [71, Corollary III.2.6 ]) *Let  $\mathbf{A}$  and  $\mathbf{B}$  be  $n \times n$  Hermitian matrices with eigenvalues ordered as  $\lambda_1(\mathbf{A}) \geq \lambda_2(\mathbf{A}) \geq \dots \geq \lambda_n(\mathbf{A})$  and  $\lambda_1(\mathbf{B}) \geq \lambda_2(\mathbf{B}) \geq \dots \geq \lambda_n(\mathbf{B})$ . Then,*

$$\text{(A.40)} \quad \sup_{1 \leq j \leq n} |\lambda_j(\mathbf{A}) - \lambda_j(\mathbf{B})| \leq \|\mathbf{A} - \mathbf{B}\|_2.$$

Moreover, for given matrix  $\mathbf{A}$ , this value is attained by some such  $\mathbf{B}$ . □

The Weyl's inequality (A.40) implies that

$$\text{(A.41)} \quad |\lambda_i(\mathbf{K}_n^{\mathbf{w}}) - (1/D)\lambda_i(\boldsymbol{\Phi}\boldsymbol{\Phi}^T)| \leq \|\Delta_n\|_2,$$

for all  $i = 1, 2, \dots, n$ . Thus in particular,

$$\text{(A.42)} \quad \left| \|\mathbf{K}_n^{\mathbf{w}}\|_2 - (1/D)\|\boldsymbol{\Phi}\|_2^2 \right| \leq \|\Delta_n\|_2,$$

and hence

$$\text{(A.43)} \quad \mathbb{P} \left\{ \left| \|\mathbf{K}_n^{\mathbf{w}}\|_2 - (1/D)\|\boldsymbol{\Phi}\|_2^2 \right| \geq \delta/D \right\} \leq \mathbb{P} \{ \|\Delta_n\|_2 \geq \delta/D \}$$

where we used the fact that  $\|\boldsymbol{\Phi}\boldsymbol{\Phi}^T\|_2 = \|\boldsymbol{\Phi}\|_2^2$ . Combining this inequality with the concentration bound in Eq. (A.39) completes the proof.

**A.4. Proof of Lemma 5.4.** Recall the notions of the sub-Gaussian and sub-exponential norms from Definition 2.1. In the sequel we collect several useful lemmas regarding the properties of the sub-Gaussian and sub-exponential r.v.s's:

**Lemma A.7.** (NORM OF DIFFERENCE OF SUB-GAUSSIAN R.V.'S) *Suppose  $\mathbf{X} \in \mathbb{R}^d$  and  $\mathbf{Y} \in \mathbb{R}^d$  are two sub-Gaussian random variables such that  $\|\mathbf{X}\|_{\psi_2} = K_1$  and  $\|\mathbf{Y}\|_{\psi_2} = K_2$ . Then,  $Z = \|\mathbf{X} - \mathbf{Y}\|_2$  is also sub-Gaussian random variables, and*

$$\text{(A.44)} \quad \|Z\|_{\psi_2} \leq \|\mathbf{X}\|_{\psi_2} + \|\mathbf{Y}\|_{\psi_2} \leq K_1 + K_2.$$

Furthermore, the random variable  $W = |\langle \mathbf{X}, \mathbf{Y} \rangle|$  is sub-exponential, and

$$\text{(A.45)} \quad \|W\|_{\psi_1} \leq \|\mathbf{X}\|_{\psi_2} \cdot \|\mathbf{Y}\|_{\psi_2} = K_1 K_2.$$

□

*Proof.* See Section B.2. □

**Lemma A.8.** (SUM OF SUB-GAUSSIAN AND SUB-EXPONENTIAL R.V.'S) *There exists a universal constant  $C_s$ , such that the sum of two dependent sub-Gaussian random variables with parameters  $K_1$  and  $K_2$  is  $C_s(K_1 + K_2)$ -sub-Gaussian, and the sum of two dependent sub-exponential random variables with parameters  $K_1$  and  $K_2$  is  $C_s(K_1 + K_2)$ -sub-exponential.*  $\square$

The proof of lemma A.8 follows directly from the equivalent form of definition of sub-Gaussian and sub-exponential random variables using Orlicz norms.

**Lemma A.9.** (BERNSTEIN INEQUALITY FOR SUB-EXPONENTIAL RANDOM VARIABLES) *Let  $X_1, \dots, X_n$  be independent sub-exponential random variables with  $\|X_i\|_{\psi_1} \leq b$ , and define  $S_n = \sum_{i=1}^n X_i - \mathbb{E}[X_i]$ . Then there exists a universal constant  $c > 0$  such that, for all  $t > 0$ ,*

$$(A.46) \quad \mathbb{P}(S_n \geq \delta) \leq \exp \left\{ -c \cdot \min \left( \frac{\delta^2}{nb^2}, \frac{\delta}{b} \right) \right\}.$$

$\square$

In the following lemma, we prove that under suitable conditions, random features are sub-exponential r.v.'s:

**Lemma A.10.** (SUB-EXPONENTIAL RANDOM FEATURES) *Consider the shift invariant kernel  $k_{\mathcal{X}}(\mathbf{x}, \mathbf{y}) = k_{\mathcal{X}}(\mathbf{x} - \mathbf{y})$  with the associated feature maps  $\varphi(\mathbf{x}; \boldsymbol{\xi}) = \sqrt{2} \cos(\langle \mathbf{x}, \boldsymbol{\xi} \rangle + b)$ , where  $\boldsymbol{\xi} \sim \mu_{\Xi}$  and  $b \sim \text{Uniform}(-\pi, \pi)$ . Then, the following two claims hold:*

- *If  $\mathbf{X} \sim \text{N}(0, \mathbf{I}_{d \times d})$ ,  $\varphi(\mathbf{X}, \boldsymbol{\xi})$  is a sub-exponential random variable with the Orlicz norm of*

$$(A.47) \quad \|\varphi(\mathbf{X}; \boldsymbol{\xi})\|_{\psi_1} \leq 16/\|\boldsymbol{\xi}\|_2.$$

- *If  $\mathbf{X} = (X_1, \dots, X_d)$  has bounded independent components  $|X_i| \leq K, i = 1, 2, \dots, d$ , then  $\varphi(\mathbf{X}, \boldsymbol{\xi})$  is a sub-exponential random variable with the Orlicz norm of*

$$(A.48) \quad \|\varphi(\mathbf{X}; \boldsymbol{\xi})\|_{\psi_1} \leq 32/K\|\boldsymbol{\xi}\|_2.$$

*Proof.* See Section B.2.  $\square$

We also need the decoupling technique from the probability theory. To state this result, consider independent  $\{0, 1\}$  valued random variables  $\delta_1, \dots, \delta_n$  with  $\mathbb{E}[\delta_i] = m/n$ , often known as *independent selectors*. Then, we define the subset  $T = \{i \in [n] : \delta_i = 1\}$ . Its average size is  $\mathbb{E}[|T|] = m$ . Now, we are in position to state the following lemma:

**Lemma A.11.** (DECOUPLING, [38, Lemma 5.60]) *Consider a double array of real numbers  $\{a_{ij}\}_{i,j=1}^n$  such that  $a_{ii} = 0$  for all  $i = 1, 2, \dots, n$ . Then,*

$$(A.49) \quad \sum_{i,j \in [n]} a_{ij} = 4\mathbb{E} \sum_{i \in [T], j \in [T]^c} a_{ij}$$

where  $T$  is a random subset of  $[n]$  with average size  $\mathbb{E}[|T|] = n/2$ . In particular,

$$(A.50) \quad 4 \min_{T \subseteq [n]} \sum_{i \in T, j \in T^c} a_{ij} \leq \sum_{i,j \in [n]} a_{ij} \leq 4 \max_{T \subseteq [n]} \sum_{i \in T, j \in T^c} a_{ij},$$

where the maximum and the minimum are over all subsets  $T$  of  $[n]$ .  $\square$

Let  $N_{1/4}$  be a  $(1/4)$ -net of the unit sphere  $S^{n-1}$  such that  $|N_{1/4}| \leq 9^n$ . By Lemma A.5, we then have

$$\begin{aligned} \|\mathbf{K}_n\|_2 &= \sup_{\mathbf{z} \in S^{n-1}} \langle \mathbf{z}, \mathbf{K}_n \mathbf{z} \rangle \leq 2 \max_{\mathbf{z} \in N_{1/4}} \langle \mathbf{z}, \mathbf{K}_n \mathbf{z} \rangle \\ (A.51) \quad &= 2 \max_{\mathbf{z} \in N_{1/4}} \sum_{i=1}^n z_i^2 k_{\mathcal{X}}(\mathbf{X}_i, \mathbf{X}_i) + \sum_{i,j \in [n]} z_i z_j k_{\mathcal{X}}(\mathbf{X}_i, \mathbf{X}_j). \end{aligned}$$

We note that for the shift invariant kernels, the identity  $k_{\mathcal{X}}(\mathbf{X}_i, \mathbf{X}_i) = k_{\mathcal{X}}(\mathbf{X}_i - \mathbf{X}_i) = k_{\mathcal{X}}(0)$  for all  $i \in [n]$ . Leveraging the decoupling technique in Lemma A.11 then yields

$$(A.52) \quad \|\mathbf{K}_n\|_2 \leq 2k_{\mathcal{X}}(0) + 4 \max_{\mathbf{y} \in N_{1/4}} \mathbb{E}_T \sum_{i \in T, j \in T^c} z_i z_j k_{\mathcal{X}}(\mathbf{X}_i, \mathbf{X}_j)$$

$$(A.53) \quad \leq 2k_{\mathcal{X}}(0) + 4 \max_{\mathbf{z} \in N_{1/4}} \mathbb{E}_T \sum_{i \in T, j \in T^c} y_i y_j \mathbb{E}_{\mu_{\Xi}}[\varphi(\mathbf{X}_i; \boldsymbol{\xi}) \varphi(\mathbf{X}_j; \boldsymbol{\xi})]$$

$$(A.54) \quad \leq 2k_{\mathcal{X}}(0) + 4 \mathbb{E}_{\mu_{\Xi}, T} \left[ \max_{\mathbf{z} \in N_{1/4}} \sum_{i \in T, j \in T^c} z_i z_j \varphi(\mathbf{X}_i; \boldsymbol{\xi}) \varphi(\mathbf{X}_j; \boldsymbol{\xi}) \right].$$

Conditioned on the random variables  $T$ ,  $(\mathbf{X}_j)_{j \in T^c}$  as well  $\boldsymbol{\xi} \sim \mu_{\Xi}$ , the right hand side of Eq. (B.11) is the sum of  $T$  independent random variables. Let  $g \stackrel{\text{def}}{=} \sum_{j \in T^c} z_j \varphi(\mathbf{X}_j; \boldsymbol{\xi})$ . Note that  $g$  has the following upper bound

$$\begin{aligned} |g| &\leq \left| \sum_{j \in T^c} z_j \varphi(\mathbf{X}_j; \boldsymbol{\xi}) \right| \\ &\stackrel{(a)}{\leq} \sum_{j \in T^c} |z_j| \cdot |\varphi(\mathbf{X}_j; \boldsymbol{\xi})| \\ &\leq \sqrt{2} \sum_{j \in T^c} |z_j| \\ &\leq \sqrt{2|T^c|} \left( \sum_{j \in T^c} |z_j|^2 \right)^{1/2} \\ &\leq \sqrt{2|T^c|} \cdot \|\mathbf{z}\|_2 \\ (A.55) \quad &\stackrel{(b)}{\leq} \sqrt{2|T^c|}, \end{aligned}$$

where (a) follows from the triangle inequality, and (b) follows from the fact that  $\mathbf{z} \in N_{1/4}$  and thus  $\mathbf{z} \in S^{n-1}$ . Using the inequality (A.55), we proceed from Eq. (A.54) as follows

$$\begin{aligned} (A.56) \quad &\mathbb{P} \left( \max_{\mathbf{z} \in N_{1/4}} g \cdot \sum_{i \in T} z_i \varphi(\mathbf{X}_i; \boldsymbol{\xi}) \geq \delta \left| (\mathbf{X}_j)_{j \in T^c}, \boldsymbol{\xi}, T \right. \right) \\ &\leq e^{2n \log 3} \max_{\mathbf{z} \in N_{1/4}} \mathbb{P} \left( |g| \cdot \sum_{i \in T} z_i \varphi(\mathbf{X}_i; \boldsymbol{\xi}) \geq \delta \left| (\mathbf{X}_j)_{j \in T^c}, \boldsymbol{\xi}, T \right. \right) \\ (A.57) \quad &\leq e^{2n \log 3} \max_{\mathbf{z} \in N_{1/4}} \mathbb{P} \left( \sum_{i \in T} z_i \varphi(\mathbf{X}_i; \boldsymbol{\xi}) \geq \delta / \sqrt{2|T^c|} \left| (\mathbf{X}_j)_{j \in T^c}, \boldsymbol{\xi}, T \right. \right). \end{aligned}$$

Due to Lemma A.10, the expression on the right hand side is the sum of sub-exponential random variables. We thus apply the Bernstein inequality (A.46) to attain

$$(A.58) \quad \mathbb{P} \left( \sum_{i \in T} z_i \varphi(\mathbf{X}_i; \boldsymbol{\xi}) \geq \delta / \sqrt{2|T^c|} \middle| (\mathbf{X}_j)_{j \in T^c}, \boldsymbol{\xi}, T \right) \leq e^{-c \cdot \min \left\{ \frac{\delta^2 \|\boldsymbol{\xi}\|_2^2}{1024|T| \cdot |T^c|}, \frac{\delta \|\boldsymbol{\xi}\|_2}{64\sqrt{|T^c|}} \right\}}.$$

Let  $\delta = n$ . Conditioned on  $T$ ,  $(\mathbf{X}_j)_{j \in T^c}$  as well  $\boldsymbol{\xi} \sim \mu_{\Xi}$ , with the probability of at least  $1 - \rho$ , we have

(A.59)

$$\max_{z \in N_{1/4}} g \cdot \sum_{i \in T} z_i \varphi(\mathbf{X}_i; \boldsymbol{\xi}) \leq e^{2n \log 3} \cdot \max \left\{ 2^{10} \frac{|T| \cdot |T^c|}{c \|\boldsymbol{\xi}\|_2^2} \sqrt{\ln \left( \frac{1}{\rho} \right)}, 2^6 \frac{\sqrt{|T^c|}}{c \|\boldsymbol{\xi}\|_2} \ln \left( \frac{1}{\rho} \right) \right\}.$$

We take the expectation with respect to the random variable  $T$  and then  $\boldsymbol{\xi}$  and note that due to the construction of Lemma A.11, we have  $\mathbb{E}[|T| |T^c|] = n - \mathbb{E}[|T|^2] = n - \mathbb{E}[(\sum_{i=1}^n \delta_i)^2] = n - \frac{1}{2}(1 - \frac{1}{2})n = 3n/4$ , where we used the fact that  $\sum_{i=1}^n \delta_i$  is a binomial distribution with the parameters  $n$  and  $p = 1/2$  and the variance  $np(1 - p)$ . Similarly,  $\mathbb{E}[\sqrt{|T^c|}] \leq \sqrt{\mathbb{E}[|T^c|]} = \sqrt{n - \mathbb{E}[|T|]} = \sqrt{n/2}$ . The following inequality then follows from Eq. (A.59) by substituting the values of the expectations  $\mathbb{E}[|T| |T^c|]$  and  $\mathbb{E}[|T^c|]$ ,

$$(A.60) \quad 4\mathbb{E}_{\mu_{\Xi}, T} \left[ \max_{z \in N_{1/4}} \sum_{i \in T, j \in T^c} z_i z_j \varphi(\mathbf{X}_i; \boldsymbol{\xi}) \varphi(\mathbf{X}_j; \boldsymbol{\xi}) \right] \leq \frac{e^{2n \log 3}}{c\sqrt{2}} \max \left\{ 3n \times 2^{10} \mathbb{E}_{\mu_{\Xi}} \left[ \frac{1}{\|\boldsymbol{\xi}\|_2^2} \right] \sqrt{\ln \left( \frac{1}{\rho} \right)}, 2^8 \sqrt{\frac{n}{2}} \mathbb{E}_{\mu_{\Xi}} \left[ \frac{1}{\|\boldsymbol{\xi}\|_2} \right] \ln \left( \frac{1}{\rho} \right) \right\}.$$

Plugging the inequality (A.60) into Eq. (B.11) yields the following upper bound on the spectral norm of the random matrix  $\mathbf{K}_n$ :

(A.61)

$$\|\mathbf{K}_n\|_2 \leq 2k_{\mathcal{X}}(0) + \frac{e^{2n \log 3}}{c\sqrt{2}} \max \left\{ 3n \times 2^{10} \mathbb{E}_{\mu_{\Xi}} \left[ \frac{1}{\|\boldsymbol{\xi}\|_2^2} \right] \sqrt{\ln \left( \frac{1}{\rho} \right)}, 2^8 \sqrt{\frac{n}{2}} \mathbb{E}_{\mu_{\Xi}} \left[ \frac{1}{\|\boldsymbol{\xi}\|_2} \right] \ln \left( \frac{1}{\rho} \right) \right\},$$

with the probability of (at least)  $1 - \rho$ .

Now, consider the mixture kernel model  $k_{\mathcal{X}}^w(\mathbf{x}, \mathbf{y}) = \sum_{\ell=1}^m w_{\ell} k_{\mathcal{X}}^{\ell}(\mathbf{x}, \mathbf{y})$ . Let  $\mu_{\Xi}^{\ell}$  denotes the generative distribution of the random features associated with the kernel  $k_{\mathcal{X}}^{\ell}(\mathbf{x}, \mathbf{y}) = k_{\mathcal{X}}^{\ell}(\mathbf{x} - \mathbf{y})$ , given by the Fourier transform of  $k_{\mathcal{X}}^{\ell}(x)$ . We note that the spectral norm is convex as it satisfies the triangle inequality. Therefore, by Jensen's inequality, we have

$$(A.62) \quad \|\mathbf{K}_n^w\|_2 = \left\| \sum_{\ell=1}^m w_{\ell} \mathbf{K}_n^{\ell} \right\|_2 \leq \sum_{\ell=1}^m w_{\ell} \|\mathbf{K}_n^{\ell}\|_2.$$

Applying the upper bound in Inequality (A.61) to each kernel on the right hand side of Eq. (A.62) completes the proof of Inequality (5.14).

The proof of Inequality (5.15) is based on the same argument leading to (A.61), except that the Orlicz norm in Eq. (A.48) is used in place of Eq. (A.47).

## APPENDIX B.

**B.1. Proof of Proposition A.1.** The weak convergence of the empirical measure  $\hat{P}^n$  to its population measure  $P$  is a straightforward consequence of Glivenko-Cantelli theorem and is omitted, see, *e.g.* [72].

Before we embark with the proof of the rest of the theorem, we recall the result of Sanov's theorem stating that

$$(B.1) \quad \limsup_{n \rightarrow \infty} \frac{1}{n} \log \mathbb{P} \left[ d(P, \widehat{P}^n) \geq \varepsilon \right] \leq -\alpha(\varepsilon),$$

where  $\alpha(\varepsilon) \stackrel{\text{def}}{=} \inf_{P: d(P, Q) \leq \varepsilon} D_{\text{KL}}(P||Q)$ , and  $d(\cdot, \cdot)$  is any distance function that is continuous with respect to the weak\* topology, see, *e.g.*, [73]. However, Sanov's theorem is an asymptotic result and does not provide explicit estimate given  $n$ .

To prove the inequality Eq. (A.5), consider a convex lower semicontinuous function  $f$  with  $f(1) = 0$ . The Fenchel conjugate  $f^*$  of  $f$  is defined as follows

$$(B.2) \quad f^*(y) = \sup_{x \in \mathbb{R}} [xy - f(y)].$$

Using the notion of convex conjugate, a variational representation of  $f$ -divergence in terms of the convex conjugate of  $f$  is given by (see [74])

$$(B.3) \quad \begin{aligned} D_f(P||Q) &= \mathbb{E}_Q \left[ f \left( \frac{P}{Q} \right) \right] \\ &= \sup_{g \in \mathcal{G}} \mathbb{E}_P[g(X)] - \mathbb{E}_Q[f^*(g(X))], \end{aligned}$$

where  $\mathcal{G}$  is an arbitrary function class of functions mapping  $\mathcal{X}$  to  $\mathbb{R}$  that satisfies two conditions: (i) for all  $g \in \mathcal{G}$  the right hand side of Eq. (B.3) is finite, and (ii) there exists a function  $g \in \mathcal{G}$  such that  $g(\mathbf{x}) \in \partial f(dP(\mathbf{x})/dQ(\mathbf{x})) \neq \emptyset$  for all  $\mathbf{x} \in \mathcal{X}$ , cf. [74]. Here,  $\partial f$  is the sub-differential set of function  $f$  defined as follows

$$(B.4) \quad \partial f \stackrel{\text{def}}{=} \{g \in \mathbb{R} : f(y) \geq f(x) + g(y - x), \forall x, y \in \mathbb{R}\}.$$

Let  $\widehat{P}_0^n$  denotes the empirical measure associated with the *i.i.d.* samples  $\mathbf{X}_1, \dots, \mathbf{X}_n \sim_{\text{i.i.d.}} P$ :

$$(B.5) \quad \widehat{P}_0^n = \frac{1}{n} \sum_{i=1}^n \delta_{\mathbf{X}_i}(\mathbf{x}).$$

Using the variational form of the  $f$ -divergence in Eq. (B.3), we obtain that

$$(B.6) \quad D_f(P||\widehat{P}_0^n) = \sup_{g \in \mathcal{G}} \mathbb{E}_P[g(\mathbf{X})] - \mathbb{E}_{\widehat{P}_0^n}[f^*(g(\mathbf{X}))]$$

$$(B.7) \quad = \sup_{g \in \mathcal{G}} \mathbb{E}_P[g(\mathbf{X})] - \frac{1}{n} \sum_{i=1}^n f^*(g(\mathbf{X}_i)),$$

where the supremum is taken with respect to all functions  $g$  such that the expectations are finite.

We now use the martingale method of McDiarmid [75]:

**Proposition B.1.** (MARTINGALE INEQUALITY [75]) *Consider independent random variables  $\mathbf{X}_1, \dots, \mathbf{X}_n \in \mathcal{X}$  and a mapping  $\phi : \mathcal{X}^n \rightarrow \mathbb{R}$ . If, for all  $i \in \{1, 2, \dots, n\}$  and for all  $\mathbf{x}_1, \dots, \mathbf{x}_n, \mathbf{x}'_i \in \mathcal{X}$ , the function  $\phi$  satisfies*

$$(B.8) \quad \begin{aligned} &|\phi(\mathbf{x}_1, \dots, \mathbf{x}_{i-1}, \mathbf{x}_i, \mathbf{x}_{i+1}, \dots, \mathbf{x}_n) \\ &\quad - \phi(\mathbf{x}_1, \dots, \mathbf{x}_{i-1}, \mathbf{x}'_i, \mathbf{x}_{i+1}, \dots, \mathbf{x}_n)| \leq c_i, \end{aligned}$$



Then, the following concentration inequality holds,

$$(B.9) \quad \mathbb{P}(\phi(\mathbf{X}_1, \dots, \mathbf{X}_n) - \mathbb{E}[\phi] \geq t) \geq \exp\left(-\frac{2t^2}{\sum_{i=1}^n c_i^2}\right).$$

□

We now define the function

$$(B.10) \quad \phi(\mathbf{x}_1, \dots, \mathbf{x}_n) = \mathbb{E}_P[g(\mathbf{X})] - \sup_{g \in \mathcal{G}} \frac{1}{n} \sum_{i=1}^n f^*(g(\mathbf{x}_i)).$$

Then, we have that

$$(B.11) \quad |\phi(\mathbf{x}_1, \dots, \mathbf{x}_{i-1}, \mathbf{x}_i, \mathbf{x}_{i+1}, \dots, \mathbf{x}_n) - \phi(\mathbf{x}_1, \dots, \mathbf{x}_{i-1}, \mathbf{x}'_i, \mathbf{x}_{i+1}, \dots, \mathbf{x}_n)| \\ \leq \sup_{g \in \mathcal{G}} \frac{1}{n} \sum_{k=1}^n f^*(g(\mathbf{x}_k)) - \sup_{\hat{g} \in \mathcal{G}} \frac{1}{n} \sum_{\substack{k=1 \\ k \neq i}}^n f^*(\hat{g}(x_k)) - f^*(\hat{g}(x'_i))$$

$$(B.12) \quad \leq \frac{1}{n} \left( \sup_{g \in \mathcal{G}} f^*(g(x_i)) - f^*(g(x'_i)) \right)$$

$$(B.13) \quad \leq \frac{\beta}{n},$$

where the last inequality is due to assumption stated in Lemma A.1.

From the concentration inequality in Eq. (B.9), we obtain that

$$(B.14) \quad \mathbb{P}\left(D_f(P||\hat{P}_0^n) - \mathbb{E}_P[D_f(P||\hat{P}_0^n)] \geq t\right) \leq \exp\left(-\frac{2nt^2}{\beta^2}\right),$$

where the expectation in  $\mathbb{E}_P[D_f(P||\hat{P}_0^n)]$  is taken with respect to the distribution of random samples  $\mathbf{X}_1^n \stackrel{\text{def}}{=} (\mathbf{X}_1, \dots, \mathbf{X}_n)$ . Therefore, with the probability of at least  $1 - \rho$ , we have

$$(B.15) \quad D_f(P||\hat{P}_0^n) \leq \mathbb{E}_P \left[ D_f(P||\hat{P}_0^n) \right] + \left( \frac{\beta^2}{2n} \log \frac{1}{\rho} \right)^{\frac{1}{2}}.$$

Now, take the supremum on the both sides of the inequality and substitute the definition of the empirical measure  $\hat{P}_0^n$ , as follows

$$(B.16) \quad \sup_{P: D_f(P||Q) \leq \alpha} D_f(P||\hat{P}_0^n) \leq \sup_{P: D_f(P||Q) \leq \alpha} \mathbb{E}_{\mathbf{X}_1^n \sim P^{\otimes n}} \left[ D_f\left(P \left\| \frac{1}{n} \sum_{i=1}^n \delta_{\mathbf{X}_i}\right.\right) \right] + \left( \frac{\beta^2}{2n} \log \frac{1}{\rho} \right)^{\frac{1}{2}}.$$

In the sequel, we focus on the special case of the total variation distance. To compute an upper bound on the expectation on the right hand side of Eq. (B.16), we once again leverage the variational form of the total variation divergence

$$(B.17) \quad D_{\text{TV}}(P||Q) = \sup_{g \in \mathcal{G}} \mathbb{E}_P[g(\mathbf{X})] - \mathbb{E}_Q[g(\mathbf{X})],$$

where  $\mathcal{G}_\infty \subset \mathcal{G}$  is an arbitrary class of functions  $g: \mathcal{X} \rightarrow \mathbb{R}$  satisfying two conditions:

- (i) For every  $g \in \mathcal{G}_\infty$  we have  $\|g\|_\infty \leq 1/2$ , and
- (ii) there exists  $g \in \mathcal{G}_\infty$  such that  $g(\mathbf{x}) \in \partial f(dP(\mathbf{x})/dQ(\mathbf{x})) \neq \emptyset$  for any  $\mathbf{x} \in \mathcal{X}$ .

The first condition is due to the fact that the convex conjugate of  $f(x) = \frac{1}{2}|x - 1|$  defined by

$$(B.18) \quad f^*(y) = \begin{cases} 1 & |y| \leq 1 \\ +\infty & |y| \geq 1. \end{cases}$$

is unbounded for  $|x| > 1/2$ . To leverage the variational form, we also need the following symmetrisation approach of van der Vaart and Wellner [76]: We reproduce it here for the sake of readability:

**Theorem B.1.** (SYMMETRIZATION, [76, Lemma 2.3.1]) *Let  $X_1, \dots, X_n$  be independent random variables with values in  $\mathcal{X}$  and  $\mathcal{F}$  is a class of real valued functions on  $\mathcal{X}$ . Then*

$$(B.19) \quad \mathbb{E} \left[ \sup_{f \in \mathcal{F}} |\mathbb{E}_{\hat{\mu}_X^n} [f(X)] - \mathbb{E}_{\mu_X} [f(X)]| \right] \leq 2 \mathbb{E} \left[ \sup_{f \in \mathcal{F}} \left| \frac{1}{n} \sum_{i=1}^n \varepsilon_i f(X_i) \right| \right],$$

where  $\varepsilon_1, \dots, \varepsilon_n$  is a Rademacher sequence, independent of  $X_1, \dots, X_n$ .  $\square$

Using symmetrisation approach of van der Vaart and Wellner [76], yields

$$(B.20) \quad \begin{aligned} \mathbb{E}_{\mathbf{X}_1^n \sim P^{\otimes n}} \left[ D_{\text{TV}} \left( P \middle| \frac{1}{n} \sum_{i=1}^n \delta_{\mathbf{X}_i} \right) \right] &= \mathbb{E}_{\mathbf{X}_1^n \sim P^{\otimes n}} \left[ \sup_{g \in \mathcal{G}_\infty} \mathbb{E}_P [g(X)] - \frac{1}{n} \sum_{i=1}^n g(X_i) \right] \\ &= \mathbb{E}_{\mathbf{X}_1^n \sim P^{\otimes n}} \left[ \sup_{g \in \mathcal{G}_\infty} \mathbb{E}_{\mathbf{Y}_1^n \sim P} \left[ \frac{1}{n} \sum_{i=1}^n g(Y_i) \right] - \frac{1}{n} \sum_{i=1}^n g(X_i) \right] \\ &\leq \mathbb{E}_{\mathbf{X}_1^n, \mathbf{Y}_1^n \sim P^{\otimes n}} \left[ \sup_{g \in \mathcal{G}_\infty} \frac{1}{n} \sum_{i=1}^n g(Y_i) - \frac{1}{n} \sum_{i=1}^n g(X_i) \right] \\ &\stackrel{(a)}{\leq} 2 \mathbb{E}_{\boldsymbol{\varepsilon} \sim P_\varepsilon^{\otimes n}, \mathbf{X}_1^n \sim P^{\otimes n}} \left[ \sup_{g \in \mathcal{G}_\infty} \frac{1}{n} \sum_{i=1}^n \varepsilon_i g(X_i) \right] \\ &\leq 2 \mathbb{E}_{\boldsymbol{\varepsilon} \sim P_\varepsilon^{\otimes n}, \mathbf{X}_1^n \sim P^{\otimes n}} \left[ \sup_{g \in \mathcal{G}_\infty} \left| \frac{1}{n} \sum_{i=1}^n \varepsilon_i g(X_i) \right| \right], \end{aligned}$$

where in (a) we used Inequality (B.20) in Theorem B.1, and  $\boldsymbol{\varepsilon} \stackrel{\text{def}}{=} (\varepsilon_1, \dots, \varepsilon_n) \in \{-1, 1\}^n$  is the Rademacher sequence (cf. Definition 5.2), and  $P_\varepsilon^{\otimes n}$  where  $P_\varepsilon = \text{Uniform}\{-1, 1\}$  is the uniform distribution.

Now, we leverage the following lemma whose proof is due to Ben-Tal *et al.* [77]. The proof of the following lemma can also be found in Duchi *et al.* [7]:

**Lemma B.2.** (DISTRIBUTIONALLY ROBUST OPTIMIZATION, [77]) *Let  $f$  be any closed convex function with the domain  $\text{dom } f \subset [0, \infty)$ , and the conjugate function  $f^*$ . Then, for any distribution  $P$  and any function  $h : \mathcal{X}^{\otimes n} \rightarrow \mathbb{R}$  we have*

$$(B.21) \quad \sup_{P: D_f(P||Q) \leq \alpha} \mathbb{E}_{\mathbf{X}_1^n \sim P^{\otimes n}} [h(X_1, \dots, X_n)] = \inf_{(\lambda, \rho) \in \mathbb{R}_+ \times \mathbb{R}} \left\{ \lambda \mathbb{E}_{\mathbf{X}_1^n \sim Q^{\otimes n}} \left[ f^* \left( \frac{h(X_1, \dots, X_n) - \rho}{\lambda} \right) \right] + \lambda \alpha + \rho \right\}.$$

$\square$

We apply the upper bound in Eq. (B.21) to the expectation in Eq. (B.20). Letting  $h(X_1, \dots, X_n) = \sup_{g \in \mathcal{G}_\infty} \left| \frac{1}{n} \sum_{i=1}^n \varepsilon_i g(X_i) \right|$  yields

$$\begin{aligned}
& \sup_{P: D_f(P||Q) \leq \alpha} \mathbb{E}_{\mathbf{X}_1^n \sim P^{\otimes n}} \left[ D_{\text{TV}} \left( P \middle| \middle| \frac{1}{n} \sum_{i=1}^n \delta_{\mathbf{X}_i} \right) \right] \\
& \leq \sup_{P: D_f(P||Q) \leq \alpha} 2 \mathbb{E}_{\boldsymbol{\varepsilon} \sim P_\varepsilon^{\otimes n}, \mathbf{X}_1^n \sim P^{\otimes n}} \left[ \sup_{g \in \mathcal{G}_\infty} \left| \frac{1}{n} \sum_{i=1}^n \varepsilon_i g(X_i) \right| \right] \\
& \leq 2 \mathbb{E}_{\boldsymbol{\varepsilon} \sim P_\varepsilon^{\otimes n}} \left[ \sup_{P: D_f(P||Q) \leq \alpha} \mathbb{E}_{\mathbf{X}_1^n \sim P^{\otimes n}} \left[ \sup_{g \in \mathcal{G}_\infty} \left| \frac{1}{n} \sum_{i=1}^n \varepsilon_i g(X_i) \right| \right] \right] \\
& \leq 2 \mathbb{E}_{\boldsymbol{\varepsilon} \sim P_\varepsilon^{\otimes n}} \left[ \inf_{(\lambda, \rho) \in \mathbb{R}_+ \times \mathbb{R}} \lambda \mathbb{E}_{\mathbf{X}_1^n \sim Q^{\otimes n}} \left[ f^* \left( \frac{1}{\lambda} \sup_{g \in \mathcal{G}_\infty} \left| \frac{1}{n} \sum_{i=1}^n \varepsilon_i g(X_i) \right| - \rho \right) \right] + \lambda \alpha + \rho \right].
\end{aligned}$$

Now, consider the special case of TV divergence, *i.e.*,  $D_{\text{TV}}(P||Q) \leq \alpha$ . Then, it is easy to see that due to the definition of the convex conjugate  $f^*$  Eq. (B.18), the upper bound in Eq. (B.22) becomes

$$\begin{aligned}
& \sup_{P: D_{\text{TV}}(P||Q) \leq \alpha} \mathbb{E}_{\mathbf{X}_1^n \sim P^{\otimes n}} \left[ D_{\text{TV}} \left( P \middle| \middle| \frac{1}{n} \sum_{i=1}^n \delta_{\mathbf{X}_i} \right) \right] \\
\text{(B.22)} \quad & \leq 2 \inf_{(\lambda, \rho) \in \mathbb{R}_+ \times \mathbb{R}} \mathbb{E}_{\boldsymbol{\varepsilon} \sim P_\varepsilon^{\otimes n}, \mathbf{X}_1^n \sim Q^{\otimes n}} \left[ \sup_{g \in \mathcal{G}_\infty} \left| \frac{1}{n} \sum_{i=1}^n \varepsilon_i g(X_i) \right| \right] + \lambda \alpha
\end{aligned}$$

$$\text{(B.23)} \quad = \mathbb{E}_{\boldsymbol{\varepsilon} \sim P_\varepsilon^{\otimes n}, \mathbf{X}_1^n \sim Q^{\otimes n}} \left[ \sup_{g \in \mathcal{G}_\infty} \left| \frac{1}{n} \sum_{i=1}^n \varepsilon_i g(X_i) \right| \right]$$

$$\text{(B.24)} \quad = \mathfrak{R}_n(\mathcal{G}_\infty).$$

It now remains to compute the Rademacher complexity of the class of functions  $\mathcal{G}_\infty$ . The total variation norm correspond to the  $f$ -divergence with  $f(x) = \frac{1}{2}|x - 1|$ . Therefore, the sub-differential set  $\partial f$  is given by

$$\text{(B.25)} \quad \partial f = \begin{cases} \frac{1}{2} & \text{if } x > 1 \\ -\frac{1}{2} & \text{if } x < 1 \\ [-\frac{1}{2}, \frac{1}{2}] & \text{if } x = 1 \end{cases}$$

Therefore, the sub-differential set include piece-wise constant functions. Hence, the function class

$$\text{(B.26)} \quad \mathcal{G}_\infty \stackrel{\text{def}}{=} \left\{ x \mapsto \frac{1}{4} \text{sgn}(ax + b) + \frac{1}{4}, a, b \in \mathbb{R} \right\}.$$

is an admissible choice, where  $\text{sgn}(\cdot)$  denotes the sign function.

**Definition B.3.** (GROWTH FUNCTION, VC DIMENSION, SHATTERING,[78]) Let  $\mathcal{F}$  denote a class of functions from  $\mathcal{X}$  to  $\{0, 1\}$  (the hypotheses, or the classification rules). For any non-negative integer  $m$ , we define the growth function of  $\mathcal{H}$  as

$$\text{(B.27)} \quad \Pi_{\mathcal{F}}(n) \stackrel{\text{def}}{=} \max |(f(x_1), \dots, f(x_m)) : f \in \mathcal{F}|, x_1, \dots, x_n \in \mathcal{X}.$$

If  $|(f(x_1), \dots, f(x_n)) : f \in \mathcal{F}| = 2^n$ , we say  $\mathcal{F}$  shatters the set  $\{x_1, \dots, x_n\}$ . The Vapnik-Chervonenkis dimension of  $\mathcal{F}$ , denoted  $\text{dim}_{\text{VC}}(\mathcal{F})$ , is the size of the largest shattered set, *i.e.*, the largest  $n$  such that  $\Pi_{\mathcal{F}}(n) = 2^n$ . If there is no largest  $n$ , we define  $\text{dim}_{\text{VC}}(\mathcal{F}) = \infty$ .

We also define the following generalization of VC dimension:

**Definition B.4.** (POLLARD'S PSEUDO-DIMENSION, [79]) Let  $\mathcal{F}$  denote a class of real-valued functions mapping  $\mathcal{X}$  to  $[0, B]$ . Consider the function class  $\mathcal{G}$  defined as follows

$$(B.28) \quad \mathcal{G} \stackrel{\text{def}}{=} \{g : \mathcal{X} \times \mathbb{R} \rightarrow \{0, 1\} : x \mapsto \mathbb{I}_{\{f(x) \geq c\}}, f \in \mathcal{F}\}.$$

Then, the Pollard's pseudo-dimension is defined as follows

$$(B.29) \quad \dim_P(\mathcal{F}) \stackrel{\text{def}}{=} \dim_{VC}(\mathcal{G}).$$

*Remark B.5.* For any class  $\mathcal{F}$ , clearly  $\dim_{VC}(\mathcal{F}) \leq \dim_P(\mathcal{F})$ .

In the sequel, we establish the Pollard's pseudo-dimension for a more general class of functions that subsumes  $\mathcal{G}_\infty$  as a special case. More formally, define the  $\mathcal{F}$  to be the set of functions  $f : \mathbb{R}^d \times \mathbb{R} \mapsto [0, B]$ , where, for all  $\mathbf{a} \in \mathbb{R}^d$  and  $b \in \mathbb{R}$ ,

$$(B.30) \quad f(\mathbf{x}) = [\mathbf{a}^T \mathbf{x} + b]_B.$$

Here,  $[u]_B \stackrel{\text{def}}{=} \max(\min(u, B), 0)$ , and  $\mathbf{a} \in \mathbb{R}^d, b \in \mathbb{R}$  is a vector and a scalar, respectively, that parameterizes  $f$ . Clearly, for the special case of  $d = 1$ , we have  $\mathcal{F} = \mathcal{G}_\infty$ .

We use contradiction to prove that  $\dim_P(\mathcal{F}) \leq d + 2$ . Suppose  $\dim_P(\mathcal{F}) > d + 2$ . It must be that there exists a shattered set

$$(B.31) \quad \{(\mathbf{a}_1, b_1, c_1), (\mathbf{a}_2, b_2, c_2), \dots, (\mathbf{a}_{(d+3)}, b_{(d+3)}, c_{(d+3)})\} \subset \mathbb{R}^d \times \mathbb{R} \times \mathbb{R}.$$

such that, for all  $\mathbf{e} \in \{0, 1\}^{d+3}$ , there exists a vector  $\mathbf{x} \in \mathbb{R}^d$  satisfying

$$(B.32) \quad [\mathbf{a}_i^T \mathbf{x} + b_i]_B \geq c_i, \text{ iff } e_i = 1, \quad \forall 1 \leq i \leq d + 3.$$

Observe that we must have  $c_i \in (0, B]$  for all  $i = 1, 2, \dots, d$ , since if  $c_i \leq 0$  or  $c_i > B$ , then no such shattered set can be demonstrated. But if  $c_i \in (0, B]$ , for all  $\mathbf{x} \in \mathbb{R}^d$ , then

$$(B.33a) \quad [\mathbf{a}_i^T \mathbf{x} + b_i]_B \geq c_i \Rightarrow \mathbf{a}_i^T \mathbf{x} \geq c_i - b_i$$

$$(B.33b) \quad [\mathbf{a}_i^T \mathbf{x} + b_i]_B < c_i \Rightarrow \mathbf{a}_i^T \mathbf{x} \leq c_i - b_i.$$

For each  $1 \leq i \leq d + 3$ , define the vector  $\mathbf{y}_i = (y_i^1, \dots, y_i^{d+1}) \in \mathbb{R}^{d+1}$  component-wise according to

$$(B.34) \quad y_i^j \stackrel{\text{def}}{=} \begin{cases} a_i^j & \text{if } j < d + 1 \\ c_i - b_i & \text{if } j = d + 1 \end{cases}$$

Let  $\mathcal{A} = \{\mathbf{y}_1, \mathbf{y}_2, \dots, \mathbf{y}_{(d+3)}\} \subset \mathbb{R}^{d+1}$ , and let  $\mathcal{A}_1$  and  $\mathcal{A}_2$  be subsets of  $\mathcal{A}$  satisfying the conditions of Radon's lemma (cf. Lemma ??). Define a vector  $\mathbf{e} \in \{0, 1\}^{d+3}$  component-wise according to

$$(B.35) \quad e_i = \mathbb{I}_{\{\mathbf{y}_i \in \mathcal{A}_1\}}.$$

Then, for the corresponding pair  $(\mathbf{a}, b)$ , we have,

$$(B.36a) \quad \sum_{j=1}^d a_j y_j \geq y_{d+1}, \quad \forall \mathbf{y} \in \mathcal{A}_1$$

$$(B.36b) \quad \sum_{j=1}^d a_j y_j < y_{d+1}, \quad \forall \mathbf{y} \in \mathcal{A}_2.$$

Now, let  $\mathbf{y}_0 \in \mathbb{R}^{d+1}$  be a point contained in both the convex hull of  $\text{Conv}(\mathcal{A}_1)$  and the convex hull of  $\text{Conv}(\mathcal{A}_2)$ . Such a point must exist by Radons lemma (cf. Lemma ??). Since  $\mathbf{y}_0$  satisfies both inequalities in Eqs. (B.36a)-(B.36b) simultaneously, this yields a

contradiction. Therefore,  $\dim_P(\mathcal{F}) \leq d + 2$ . For the particular case of  $F = \mathcal{G}_\infty$ , we obtain  $\dim_P(\mathcal{G}_\infty) \leq 3$ . Based on Remark B.5, we then have  $\dim_{VC}(\mathcal{G}_\infty) < 3$ .

Now, using Sauer's lemma [80], we have the following upper bound on the Rademacher complexity

$$(B.37) \quad \mathfrak{R}^n(\mathcal{G}_\infty) \leq \sqrt{\frac{2 \log(\Pi_{\mathcal{F}}(n))}{n}} \leq \sqrt{\frac{2 \log\left(\sum_{i=0}^{VC(\mathcal{G}_\infty)} \binom{n}{i}\right)}{n}} \leq \sqrt{\frac{2 \log\left(\sum_{i=0}^3 \binom{n}{i}\right)}{n}} \leq \sqrt{\frac{6 \log(en/3)}{n}}.$$

**B.2. Proof of Lemmata A.7 and A.10.** We first present the proof of Lemma A.7. Taking square from both sides yields

$$(B.38) \quad Z^2 = \|\mathbf{X} - \mathbf{Y}\|_2^2 = \|\mathbf{X}\|_2^2 + \|\mathbf{Y}\|_2^2 - 2\langle \mathbf{X}, \mathbf{Y} \rangle.$$

Since  $\mathbf{X} \in \mathbb{R}^d$  is a  $K_1$ -sub-Gaussian vector, we have that

$$(B.39) \quad \|\mathbf{X}\|_{\psi_2} \leq \sup_{\mathbf{v} \in \mathbb{S}^{d-1}} \|\langle \mathbf{X}, \mathbf{v} \rangle\|_{\psi_2} = K_1.$$

and thus  $\sup_{\mathbf{v} \in \mathbb{S}^{d-1}} \mathbb{E}[\|\langle \mathbf{v}, \mathbf{X} \rangle\|^2 / K_1^2] \leq 2$ . Letting  $\mathbf{v} = \mathbf{X} / \|\mathbf{X}\|_2$ , it follows that  $\mathbb{E}[\|\mathbf{X}\|^2 / K_1^2] \leq 2$ . Therefore,  $\|\mathbf{X}\|_2^2$  is sub-exponential and  $\|\|\mathbf{X}\|_2^2\|_{\psi_1} \leq K_1^2$ . Similarly,  $\|\|\mathbf{Y}\|_2^2\|_{\psi_1} \leq K_1^2$ . Now, consider  $\langle \mathbf{X}, \mathbf{Y} \rangle$ . Then,

$$(B.40) \quad \begin{aligned} \mathbb{E}[\exp(\|\langle \mathbf{X}, \mathbf{Y} \rangle\| / K_1 K_2)] &\stackrel{(a)}{\leq} \mathbb{E}[\exp(\|\mathbf{X}\|_2 \|\mathbf{Y}\|_2 / K_1 K_2)] \\ &\stackrel{(b)}{\leq} \mathbb{E}[\exp(\|\mathbf{X}\|_2^2 / 2K_1^2 + \|\mathbf{Y}\|_2^2 / 2K_2^2)] \\ &\leq \mathbb{E}[\exp(\|\mathbf{X}\|_2^2 / 2K_1^2) \exp(\|\mathbf{Y}\|_2^2 / 2K_2^2)] \\ &\stackrel{(c)}{\leq} \frac{1}{2} (\mathbb{E}[\exp(\|\mathbf{X}\|_2^2 / K_1^2)] + \mathbb{E}[\exp(\|\mathbf{X}\|_2^2 / K_2^2)]) \end{aligned}$$

$$(B.41) \quad \leq 2,$$

where (b) and (c) is due to Young's inequality  $ab \leq (a^2 + b^2)/2$ , and (a) is due to the Cauchy-Schwarz inequality. From Inequality Eq. (B.40), we conclude that  $\|\langle \mathbf{X}, \mathbf{Y} \rangle\|_{\psi_1} \leq K_1 K_2$ .

For the random variable  $Z^2$  defined in Eq. (B.38), we have that

$$\begin{aligned} \|Z^2\|_{\psi_1} &\leq \|\|\mathbf{X}\|_2^2 + \|\mathbf{Y}\|_2^2 - 2\langle \mathbf{X}, \mathbf{Y} \rangle\|_{\psi_1} \\ &\leq \|\|\mathbf{X}\|_2^2\|_{\psi_1} + \|\|\mathbf{Y}\|_2^2\|_{\psi_1} + 2\|\langle \mathbf{X}, \mathbf{Y} \rangle\|_{\psi_1} = K_1^2 + K_2^2 + 2K_1 K_2 \\ &= (K_1 + K_2)^2. \end{aligned}$$

Since  $\|Z^2\|_{\psi_1} = \|Z\|_{\psi_2}^2$ , it follows that  $\|Z\|_{\psi_2} \leq K_1 + K_2$ .

We now prove Lemma A.10. To this end, it is easier to expand the cosine function as follows

$$(B.42) \quad \varphi(\mathbf{X}; \boldsymbol{\xi}) = \sqrt{2} \cos(\langle \mathbf{X}, \boldsymbol{\xi} \rangle + B) = \sqrt{2} \cos(B) \cos(\langle \mathbf{X}, \boldsymbol{\xi} \rangle) - \sqrt{2} \sin(B) \sin(\langle \mathbf{X}, \boldsymbol{\xi} \rangle).$$

Recall that  $B \sim \text{Uniform}[-\pi, \pi]$ . We prove that  $\cos(B)$  and  $\sin(B)$  are sub-Gaussian r.v.'s with  $\|\cos(B)\|_{\psi_2} \leq 4$  and  $\|\sin(B)\|_{\psi_2} \leq 4$ . In particular, for any  $\lambda > 0$ , we have

$$(B.43) \quad \mathbb{E}[\exp(\lambda \cos(B))] = \frac{1}{2\pi} \int_{-\pi}^{\pi} \exp(\lambda \cos(x)) dx$$

$$(B.44) \quad \stackrel{(a)}{=} I_0(\lambda)$$

$$(B.45) \quad = \sum_{n \in \mathbb{N}} \frac{(\lambda/2)^{2n}}{(n!)^2}$$

$$(B.46) \quad \leq \exp(\lambda^2/2),$$

where in (a),  $I_0(\lambda)$  is the modified Bessel function of the first kind. Consequently, by Markov's inequality we have

$$(B.47) \quad \mathbb{P}(\cos(B) \geq t) \leq \frac{\mathbb{E}[\exp(\lambda B)]}{\exp(\lambda t)} \leq \exp(\lambda^2/2 - \lambda t) \leq \exp(-t^2/2),$$

where the last step follows by letting  $\lambda = t > 0$ . It can be shown that a similar inequality holds for  $\mathbb{P}(\cos(B) \leq -t)$  and thus by union bound we have

$$(B.48) \quad \mathbb{P}\{|\cos(B)| \geq t\} \leq 2 \exp(-t^2/2).$$

Hence,

$$(B.49) \quad \begin{aligned} \mathbb{E}[\exp(\cos^2(B)/4)] &= \int_1^{\infty} \mathbb{P}\{\exp(\cos^2(B)/4) \geq t\} dt \\ &= \int_0^{\infty} \mathbb{P}\{|\cos(B)| \geq 2\sqrt{t}\} e^t dt \\ &\stackrel{(a)}{=} \int_0^{\infty} 2e^{t-2t} dt = 2, \end{aligned}$$

where (a) follows from concentration inequality in Eq. (B.48). A similar analysis for  $\sin(B)$  proves that  $\|\sin(B)\|_{\psi_2} \leq 4$ .

We now consider the function  $\cos(\langle \mathbf{X}, \boldsymbol{\xi} \rangle)$ . Our proof is based on the Gaussian log-Sobolev argument of Herbst appeared in [?]. To present the proof, we first need the following definition:

**Theorem B.6.** (GAUSSIAN LOG-SOBOLEV INEQUALITY) *Let  $(\mathcal{X}, d_{\mathcal{X}}, \mu_{\mathcal{X}})$  denotes a metric measure space  $\mathcal{X} \stackrel{\text{def}}{=} \mathcal{X}_1 \times \mathcal{X}_2 \times \dots \times \mathcal{X}_d$ , with the metric  $d_{\mathcal{X}} : \mathcal{X} \times \mathcal{X} \rightarrow \mathbb{R}$ , and the canonical Gaussian measure  $\mu_{\mathcal{X}}$ . Let  $f : \mathcal{X} \rightarrow \mathbb{R}$  denotes a function from the space  $f \in L_2(\mu)$ . The modulus of the gradient of  $f$  is defined as follows:*

$$(B.50) \quad |\nabla f(\mathbf{x})| \stackrel{\text{def}}{=} \limsup_{\mathbf{y} \rightarrow \mathbf{x}} \frac{|f(\mathbf{y}) - f(\mathbf{x})|}{d(\mathbf{y}, \mathbf{x})}.$$

When  $\mathbf{x}$  is not an accumulation point of  $\mathcal{X}$ , we define  $|\nabla f(\mathbf{x})| = 0$ .

Then, the following log-Sobolev inequality holds for all  $f \in L_2(\mu)$ ,

$$(B.51) \quad \int_{\mathcal{X}} f^2(\mathbf{x}) \log(f^2(\mathbf{x})) d\mu(\mathbf{x}) - \left( \int_{\mathcal{X}} f(\mathbf{x}) d\mu(\mathbf{x}) \right) \log \left( \int_{\mathcal{X}} f(\mathbf{x}) d\mu(\mathbf{x}) \right) \leq 2 \int_{\mathcal{X}} |\nabla f(\mathbf{x})|^2 d\mu_{\mathcal{X}}(\mathbf{x}).$$

□

We apply the log-Sobolev inequality in Eq. (B.51) with  $f^2 = e^{\lambda F}$ , where  $F(\mathbf{X}) = \cos(\langle \mathbf{X}, \boldsymbol{\xi} \rangle)$ . Now,  $\|\nabla F(\mathbf{X})\|_2 = \|\boldsymbol{\xi} \sin(\langle \mathbf{X}, \boldsymbol{\xi} \rangle)\| \leq |\sin(\langle \mathbf{X}, \boldsymbol{\xi} \rangle)| \cdot \|\boldsymbol{\xi}\|_2 \leq \|\boldsymbol{\xi}\|_2$ . Therefore, the right hand side of Eq. (B.51) becomes

$$(B.52) \quad \int_{\mathcal{X}} |\nabla f(\mathbf{x})|^2 d\mu(\mathbf{x}) = \frac{\lambda^2}{4} \int_{\mathcal{X}} \|\nabla F(\mathbf{x})\|_2^2 e^{\lambda F(\mathbf{x})} d\mu(\mathbf{x})$$

$$(B.53) \quad \leq 2 \frac{\lambda^2}{2} \|\boldsymbol{\xi}\|_2 \int_{\mathcal{X}} e^{\lambda F(\mathbf{x})} d\mu_{\mathcal{X}}(\mathbf{x}).$$

Defining the function  $H(\lambda) \stackrel{\text{def}}{=} \mathbb{E}_{\mu}[e^{\lambda F(\mathbf{x})}] = \int_{\mathcal{X}} (e^{\lambda F(\mathbf{x})}) d\mu(\mathbf{x})$ ,  $\lambda \in \mathbb{R}$ , we obtain from log-Sobolev inequality (B.51) as well as (B.53) that

$$(B.54) \quad \lambda H'(\lambda) - H(\lambda) \log(H(\lambda)) \leq 2\lambda^2 \|\boldsymbol{\xi}\|_2 H(\lambda).$$

Dividing both sides by  $(1/\lambda^2)H(\lambda)$ , yields

$$(B.55) \quad \frac{1}{\lambda} \frac{H'(\lambda)}{H(\lambda)} - \frac{1}{\lambda^2} \log(H(\lambda)) \leq 2\|\boldsymbol{\xi}\|_2.$$

Alternatively,

$$(B.56) \quad \frac{d}{d\lambda} \left( \frac{1}{\lambda} \log(H(\lambda)) \right) \leq \|\boldsymbol{\xi}\|_2.$$

Due to L'Hospital's Rule, the initial condition is  $\lim_{\lambda \rightarrow 0} \frac{\lambda}{\log(H(\lambda))} = H'(0)/H(0) = \mathbb{E}_{\mu_{\mathcal{X}}}[F]$ .

Hence, the differential equation in Eq. (B.56) has the following solution

$$(B.57) \quad \frac{1}{\lambda} \log(H(\lambda)) = \lim_{\lambda \rightarrow 0} \frac{1}{\lambda} \log(H(\lambda)) + \int_0^{\lambda} (H'(\gamma)/H(\gamma)) d\gamma$$

$$(B.58) \quad = \mathbb{E}_{\mu_{\mathcal{X}}}[F(\mathbf{x})] + 2\lambda \|\boldsymbol{\xi}\|_2.$$

Alternatively,

$$(B.59) \quad H(\lambda) = \mathbb{E}_{\mu_{\mathcal{X}}}[e^{\lambda F(\mathbf{x})}] \leq e^{\lambda \mathbb{E}_{\mu_{\mathcal{X}}}[F(\mathbf{x})] + 2\|\boldsymbol{\xi}\|_2 \lambda^2}$$

Using Chebyshev's inequality, and recalling that  $F(\mathbf{X}) = \cos(\langle \mathbf{X}, \boldsymbol{\xi} \rangle)$ , we derive the following inequality

$$(B.60) \quad \mathbb{P}(\cos(\langle \mathbf{X}, \boldsymbol{\xi} \rangle) - \mathbb{E}_{\mu_{\mathcal{X}}}[\cos(\langle \mathbf{X}, \boldsymbol{\xi} \rangle)] \geq t) \leq e^{-\lambda t + 2\lambda^2 \|\boldsymbol{\xi}\|_2^2},$$

for every  $\lambda, t \geq 0$ . Letting  $\lambda = t/\|\boldsymbol{\xi}\|_2^2$ , we compute from Eq. (B.60) that

$$(B.61) \quad \mathbb{P}(\cos(\langle \mathbf{X}, \boldsymbol{\xi} \rangle) - \mathbb{E}_{\mu_{\mathcal{X}}}[\cos(\langle \mathbf{X}, \boldsymbol{\xi} \rangle)] \geq t) \leq e^{-t^2/\|\boldsymbol{\xi}\|_2^2}.$$

Due to the symmetry, and identical inequality holds by replacing  $\cos$  with  $-\cos$ . Therefore, taking the union bound, we derive

$$(B.62) \quad \mathbb{P}(|\cos(\langle \mathbf{X}, \boldsymbol{\xi} \rangle) - \mathbb{E}_{\mu_{\mathcal{X}}}[\cos(\langle \mathbf{X}, \boldsymbol{\xi} \rangle)]| \geq t) \leq 2e^{-t^2/\|\boldsymbol{\xi}\|_2^2}.$$

An argument identical to that we used in Eqs. (B.47)-(B.49) proves that  $\|\cos(\langle \mathbf{X}, \boldsymbol{\xi} \rangle)\|_{\psi_2} \leq 2/\|\boldsymbol{\xi}\|_2$ . The proof of  $\|\sin(\langle \mathbf{X}, \boldsymbol{\xi} \rangle)\|_{\psi_2} \leq 2/\|\boldsymbol{\xi}\|_2$  is similar and is thus omitted.